MARSHALL ISLANDS FILE TRACKING DOCUMENT

Record Number: 204

File Name (TITLE): Damage Survey and Analysis of Structures

Document Number (ID): WT-611

DATE: 11/1954

Previous Location (FROM): CIC

AUTHOR: J. S. Archer, et al.

Addditional Information:

OrMIbox: 13

CyMIbox: 8

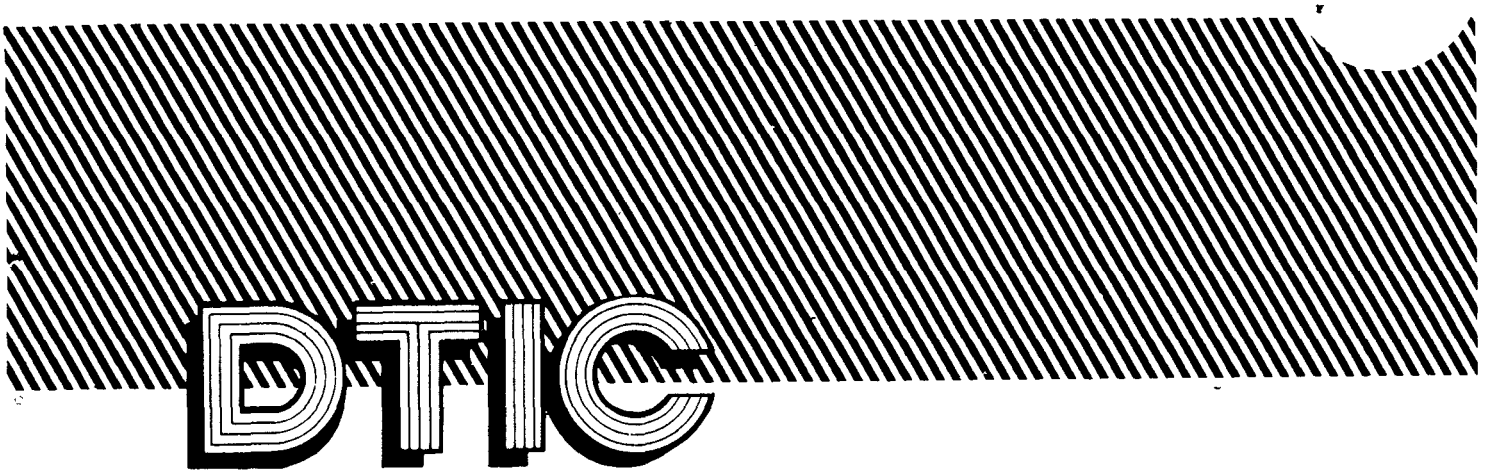

Technical Report

NOTICE

We are pleased to supply this document in response to your request.

The acquisition of technical reports, notes, memorandums, etc., is an active, ongoing program at the Defense Technical Information Center (DTIC) that depends, in part, on the efforts and interests of users and contributors.

Therefore, if you know of the existence of any significant reports, etc., that are not in the DTIC collection, we would appreciate receiving copies or information related to their sources and availability.

The appropriate regulations are Department of Defense Directive 5100.36, Defense Scientific and Technical Information Program; Department of Defense Directive 5200.20, Distribution Statements on Technical Documents; Military Standard (MIL-STD) 847-A, Format Requirements for Scientific and Technical Reports Prepared by or for the Department of Defense; Department of Defense Regulation 5200.1-R, Information Security Program Regulation.

Our Acquisition Section, DTIC-DDA-1, will assist in resolving any questions you may have. Telephone numbers of that office are: (202) 274-6847, 274-6874 or Autovon 284-6847, 284-6874

June 1982

[illegible] (UNLIMITED)

[illegible] PUBLIC RELEASE

[illegible] 5200 20 ANT

[illegible] JPON

AD 356270L

UNCLASSIFIED

NOTICE: When government or other drawings, specifications or other data are used for any purpose other than in connection with a definitely related government procurement operation, the U. S. Government thereby incurs no responsibility, nor any obligation whatsoever; and the fact that the Government may have formulated, furnished, or in any way supplied the said drawings, specifications, or other data is not to be regarded by implication or otherwise as in any manner licensing the holder or any other person or corporation, or conveying any rights or permission to manufacture, use or sell any patented invention that may in any way be related thereto.

NOTICE:

THIS DOCUMENT CONTAINS INFORMATION AFFECTING THE NATIONAL DEFENSE OF THE UNITED STATES WITHIN THE MEANING OF THE ESPIONAGE LAWS, TITLE 18, U.S.C., SECTIONS 793 and 794. THE TRANSMISSION OR THE REVELATION OF ITS CONTENTS IN ANY MANNER TO AN UNAUTHORIZED PERSON IS PROHIBITED BY LAW.

WT-611

This document consists of 176 pages
No. 150 of 230 copies, Series A

Report to the Scientific Director

DAMAGE SURVEY AND ANALYSIS OF STRUCTURES

By

John S. Archer

and

Edward A. Lawlor

[redacted]
Massachusetts Institute of Technology
Cambridge, [redacted]

Nov 54

05864

ABSTRACT

The purpose of this study, "Damage Survey and Analysis of Structures," is to determine the damage and blast loading on Operation Greenhouse Army Test Structure 3.1.1 and to survey the damage done to Greenhouse Structure 3.1.3 and other miscellaneous structures. These structures, located on the Eniwetok Atoll, were exposed to the effects of the two atomic bursts (Mike and King) of Operation Ivy in the late fall of 1952. A damage survey was conducted by the Office of the Chief of Engineers and the Massachusetts Institute of Technology in August 1953 to obtain data upon which to base a correlation of the damage incurred with the measured air-blast overpressures caused by the two shots.

The damage caused to Structure 3.1.1 by shot Mike was comparable to that caused by shot Easy of Operation Greenhouse. It is probable that no damage occurred to Structure 3.1.1 from shot King. Only the final permanent deflections were recorded of Structure 3.1.1 for shot Mike. The lack of transient response records for this shot increased the difficulty of correlating the loading with the deformations sustained.

Analyses were performed on Buildings 2 and 3 of Structure 3.1.1. The effect of varying overpressure and the shape of the load-time curve were investigated. The structural parameters of Buildings 2 and 3 were obtained by correlation of the measured overpressure with the recorded response for shot Easy of Operation Greenhouse. The results of the various analyses for Operation Ivy indicate that the free-air overpressure in the vicinity of Structure 3.1.1 was between 12 and 14 psi for shot Mike, which compares reasonably well with pressures predicted at Structure 3.1.1 based on actual measurements made at other locations near the structure.

The observations made in the gross-damage survey may be summarized as follows:

1. The damage sustained by the various buildings of Structure 3.1.1 due to shot Mike was as follows: The test panels of Buildings 1 and 7 sustained only slight additional damage due to air blast. The steel frames of Building 2 suffered moderate plastic deformation, and the steel sheeting of the rear face was distorted inward between girts. The steel frame and siding of Building 6 received no apparent additional damage. The concrete frames of Buildings 3 and 5 suffered moderate plastic deformation. The rear wall of Building 5 was blown out by the air blast. The shear walls of Building 4 were undamaged. However, large cracks were opened in the roof slabs adjacent to the shear walls and roof girders. The overpressure was approximately 14 psi.

2. Structure 3.1.3 suffered no major structural damage. The blast doors were removed prior to the test. The wood-frame air lock, which was left in place, was destroyed by the air blast. The painted surface of the vent pipe was charred on the side facing Ground Zero. The gage overpressure was approximately 18 psi.

3. All reinforced-concrete semiburied instrumentation shelters appeared to have performed their function satisfactorily without exhibiting any primary structural failures.

4. Of the many one story reinforced-concrete surface and semiburied structures observed, none were badly damaged. The only serious structural failures observed were confined to wing walls designed to retain portions of the fill on the semiburied structures. Exposed

steel beams and pipes attached to these structures were damaged and destroyed by overpressures of 11 psi and greater.

5. Small buildings covered with thin sheet metal over diagonal wood sheathing generally withstood overpressures up to 5 and 6 psi. However, one structure of this type was observed badly damaged by an overpressure of 4.5 psi.

6. Lightly constructed wood-frame shacks apparently sheathed with corrugated metal and located in regions with overpressures greater than 4 psi were completely destroyed. No structures of this type were observed in regions subjected to less than 4 psi overpressure.

7. Palm trees were destroyed by air-blast overpressures of 4 to 5 psi and greater, but none were destroyed by overpressures less than 4 psi.

CONTENTS

CONTENTS (Continued)

ILLUSTRATIONS

ILLUSTRATIONS (Continued)

CHAPTER 3 DAMAGE SURVEY OF MISCELLANEOUS STRUCTURES

ILLUSTRATIONS (Continued)

ILLUSTRATIONS (Continued)

ILLUSTRATIONS (Continued)

TABLES

CHAPTER 1

INTRODUCTION

1.1 PURPOSE

The purpose of this report is to (1) record and interpret the results of the damage resulting from shots King and Mike of Operation Ivy at Eniwetok on a number of miscellaneous structures including the Greenhouse Army Test Structure 3.1.1 and (2) to present a dynamic analysis of Structure 3.1.1 to determine the probable loading and establish correlation with measured blast pressures in the region near Structure 3.1.1.

1.2 SCOPE

A general damage survey of all structures of interest at Eniwetok was made in August 1953 by T. O. Stark of the Office of the Chief of Engineers and John S. Archer of the Massachusetts Institute of Technology. Excerpts from a letter report on this field trip written by Stark are included as Appendix A of this report.

The pertinent data and photographs obtained in the field survey are included in Chap. 2 and Appendix B for Structure 3.1.1 and in Chap. 3 for all other structures.

A general damage survey of all structures other than 3.1.1 at the site was made with the intention of correlating overpressures with observed structural damage. Photographic evidence of the damage was obtained whenever possible, and detailed measurements were made of the damage where an analysis of the structural behavior appeared practical.

1.3 HISTORY

With the exception of Structures 3.1.1 and 3.1.3, practically all buildings observed at the site were constructed for the support of Operation Ivy. Structures 3.1.1 and 3.1.3 were completed in 1951 as test structures under the sponsorship of the Office of the Chief of Engineers, Department of the Army, for Operation Greenhouse. During the Greenhouse operation Structure 3.1.1 was subjected to a peak reflected air-blast overpressure of about 30 psi as a result of shot Easy, the structures test shot. Following an extensive damage survey the structure was again subjected to an air blast from shot Item but from a different direction. A less extensive damage survey was made after this shot since the orientation of the blast wave was such that the air blast caused less damage than shot Easy to the frames of the test structure.

A program of electronic instrumentation of Structure 3.1.1 was proposed by the Office of the Chief of Engineers for Operation Ivy but was not approved on the basis that this operation

was primarily a weapons development test. As a result only two electronic pressure gages were mounted on Structure 3.1.1. A program of transient displacement instrumentation would have materially assisted in correlating the analysis with the measured results.

Prior to Operation Ivy in the fall of 1952, a representative of the Office of the Chief of Engineers, Department of the Army, visited the site and supervised extensive photography of Structure 3.1.1 as well as other structures of interest. Following the completion of Operation Ivy the damage survey by Stark and Archer was undertaken.

CHAPTER 2

DAMAGE SURVEY AND ANALYSIS OF STRUCTURE 3.1.1

2.1 GENERAL

Structure 3.1.1, the Greenhouse Army Test Building, was the only structure examined at the site of Operation Ivy which had been constructed for the exclusive purpose of measuring the effect of air blast from nuclear weapons on surface structures. This structure happened to be located at a range from Ground Zero of shot Mike* of Operation Ivy such that the damage caused by the air blast was within limits suitable for a dynamic analysis. In addition, complete plans were available for the structure, and damage survey notes were available for the previous nuclear shots which had damaged the structure.

The magnitude of the air-blast wave for shot Mike of Operation Ivy at the location of Structure 3.1.1 was not known reliably, although a number of measurements of air-blast overpressures were made at various distances from Ground Zero.[1] Therefore an estimate of the actual air-blast pressure at Structure 3.1.1 can best be obtained by dynamic analyses of Buildings 2 and 3 of this structure. Various levels of air-blast overpressure are assumed, and the response is computed using methods of analysis which have been developed.[1,3-7] A comparison of the computed response for the various assumed levels of air-blast overpressure with the actual values of permanent deflection measured in the field survey leads to an estimate of the probable air-blast overpressure at the location of Structure 3.1.1.

The field survey measurements and photographs of Structure 3.1.1 are presented in Sec. 2.2. The dynamic analyses of Buildings 2 and 3 are presented in Sec. 3.2.

2.2 SURVEY MEASUREMENTS AND RESULTS

The damage survey measurements made after Operation Ivy consisted of exterior-wall-offset measurements, column-offset measurements, and roof-elevation measurements. In addition, general observations and photographs were made of the structure which is shown diagrammatically in Fig. 2.1. Since no bench marks or fixed points were available upon which to base the measurements, only relative horizontal and vertical displacements of the structure were obtained.

The pre-Ivy condition of Structure 3.1.1 was determined from survey notes and photographs obtained following shots Easy and Item of Operation Greenhouse[8-10] and from the pretest visit made by a representative of the Office of the Chief of Engineers in the fall of 1952.

A description of the post-Ivy damage survey and results is presented in the following sections.

---

*Shot King of Operation Ivy produced air-blast overpressures at Structure 3.1.1 of such a low magnitude that no measurable damage occurred from this shot.

2.2.1 Exterior-wall-offset Measurements

The exterior-wall-offset measurements were made by establishing lines of sight approximately parallel with the walls of Structure 3.1.1, using a surveyor's transit. Each line of sight defined a vertical plane located about 1 ft from the face of a wall. Offset measurements were made perpendicular from each vertical plane to the survey points located in the walls (Fig. 2.2). The location of the survey points is shown in Fig. 2.3. The position of each point relative to a vertical plane through the base point was then determined by the difference in the offset

Table 2.1—SUMMARY OF EXTERIOR-WALL-OFFSET AND COLUMN-OFFSET MEASUREMENTS

Bldg. No.	Floor level	Average horizontal displacement relative to base, ft			Column-offset measurements, ft	
		Ivy*	Greenhouse†	Total	Per story	Total
1	Second	0.00	0.00	0.00		
	Third	0.00	0.01	0.01		
	Roof	−0.01§	0.02	0.01		
2	Second	0.08	0.06	0.14	0.10	0.10
	Third	0.14	0.18	0.32	0.24	0.34
	Roof	0.32	0.32	0.64	0.24	0.58
3	Second	0.07	0.04	0.11	0.13	0.13
	Third	0.20	0.13	0.33	0.18	0.31
	Roof	0.34	0.26	0.60	0.21	0.52
4	Second	0.00	0.01	0.01		
	Third	0.00	0.01	0.01		
	Roof	−0.01§	0.01	0.00		
5	Second	0.14	0.09	0.23	0.22	0.22
	Third	0.20	0.14	0.34	0.11	0.33
	Roof	0.38	0.24	0.62	0.21	0.54
6	Second		0.02		0.03	0.03
	Third		0.06		0.07	0.10
	Roof		0.12		0.06	0.16
7	Second	0.03	0.01	0.04		
	Third	−0.05§	0.01	−0.04§		
	Roof	−0.06§	0.01	−0.05§		

* Average of measurements in Sec. B.1.
† Average of measurements in reference 10.
‡ Average of measurements in Sec. B.2.
§ Negative sign indicates motion toward Ground Zero.

distances to the two points. Changes in the relative positions of the survey points were obtained by comparison with earlier surveys. This information is summarized in Table 2.1, and the complete data are contained in Sec. B.1.

2.2.2 Column-offset Measurements

The column-offset measurements for Buildings 2, 3, 5, and 6 were made by hanging a plumb bob from the ceiling in each story adjacent to the front or rear of the columns on that floor. Horizontal-offset measurements were made from the plumb line to the top and bottom of the adjacent face of each column (Fig. 2.4). The relative permanent distortion of each column in a horizontal direction was determined from the difference of the offsets at the top and bottom of the column. The column deformation thus obtained is approximately the total horizontal deformation of the frame of the structure caused by all the blast tests performed in the

vicinity of Structure 3.1.1. Thus the column-offset measurements served as a check on the total lateral structural deformation obtained from the exterior-wall-survey point measurements. The results of the column-motion measurements are summarized in Table 2.1. The complete data are contained in Sec. B.2.

2.2.3 Roof-elevation Measurements

A level survey was made on the roof of Structure 3.1.1 to determine the elevation of all the roof survey points relative to a common horizontal plane. The elevations of these points were related to previous level surveys by assuming that the average elevation of the four

Table 2.2—SUMMARY OF ROOF-ELEVATION CHANGES

Bldg. No.	Total no. of usable survey point measurements*	Number of points showing indicated change in elevation						
		−0.12 ft	−0.09 ft	−0.06 ft	−0.03 ft	−0.02 ft	−0.01 ft	0 ft
1	47	0	0	0	0	0	0	19
2	35	0	0	0	1	5	6	16
3	35	0	0	0	0	0	1	0
4	49	1	1	1	2	2	7	33
5	31	0	0	0	0	0	0	0
6	35	0	0	0	1	5	11	17
7	48	0	0	0	0	2	10	24

Bldg. No.	Total no. of usable survey point measurements*	Number of points showing indicated change in elevation					
		+0.01 ft	+0.02 ft	+0.03 ft	+0.04 ft	+0.05 ft	+0.06 ft
1	47	26	2	0	0	0	0
2	35	6	1	0	0	0	0
3	35	4	8	13	6	2	1
4	49	1	0	1	0	0	0
5	31	0	8	13	9	0	1
6	35	2	0	0	0	0	0
7	48	11	1	0	0	0	0

*See Sec. B.3.

corner points of Building 4 did not change. These points were selected as the points upon which to base the elevations because of the massiveness and extreme rigidity of Building 4. The resulting elevations of other points on the roof of Structure 3.1.1 seem to verify the reasonableness of this assumption. On this basis the change in elevation of each roof survey point as a result of Operation Ivy was computed. A summary of the resulting elevation changes is given in Table 2.2. A sketch of the damage to the roof of Building 4 is given in Fig. 2.5. The complete data are contained in Sec. B.3.

2.2.4 General Observations and Photographs

The damage to Structure 3.1.1 caused by shot Mike of Operation Ivy was of the same order of magnitude as that caused by shot Easy of Operation Greenhouse. Figures 2.9 and 2.10 are posttest views of the front and back of the structure.

(a) *Building 1.* The panels of Building 1 sustained only slight damage due to air blast. A few additional haircracks were discovered in the back of some panels, but no additional major

structural damage was discerned. See Figs. 2.6 to 2.8 for pretest views and Figs. 2.9 and 2.10 for posttest views.

(b) *Building 2.* The back-wall corrugated metal sheathing on Building 2 was deflected inward between supporting beams. The large deflection of the sheathing caused the girt flanges to become distorted and twisted. This building was obviously deflected away from the blast, but the main supporting steel columns remained undamaged except for plastic rotation of their ends. The roof was undamaged. See Figs. 2.11 and 2.12 for pretest views and Figs. 2.13 and 2.14 for posttest views.

(c) *Building 3.* Building 3 was deflected away from the blast in a manner similar to Building 2. The concrete columns were cracked and spalled at the top and bottom owing to plastic hinge action. The roof was essentially undamaged. Pretest photographs are shown in Figs. 2.15 and 2.16; the only posttest views available are in Figs. 2.9, 2.10, and 2.13.

(d) *Building 4.* Building 4 was undamaged with the exception of the roof. Large cracks were opened in the roof slabs adjacent to the shear walls and roof girders. On the underside of the roof these cracks appear to be located along the ends of reinforcing bars placed in the bottom of the roof slab and terminating about 3.3 in. from walls and girders. These bars are oriented normal to the shear walls. The roof cracks originated in Operation Greenhouse following the Item shot and were widened by Operation Ivy. Several interior views of Building 4 are given in Figs. 2.18 to 2.26. Exterior views of Building 4 are shown in Figs. 2.9, 2.10, 2.17, 2.29, and 2.34.

(e) *Building 5.* The rear wall of Building 5, which had been badly damaged by the Easy shot of Operation Greenhouse, was destroyed by Operation Ivy. The wall slab was detached at the roof and floor levels and rotated about the top of the footing until it lay flat on the ground at the rear of the structure. Except for the lateral deflection of the structure, no additional damage was noted. Pretest views of Building 5 are given in Figs. 2.27 and 2.28, and posttest views are given in Figs. 2.29 to 2.31.

(f) *Buildings 6 and 7.* Buildings 6 and 7 received no apparent damage beyond that observed in previous operations. Pretest and posttest views of these buildings are contained in Figs. 2.32 to 2.38.

2.3 DYNAMIC ANALYSIS OF STRUCTURE 3.1.1

2.3.1 Introduction

Section 2.3 deals with the general features of the analysis of Buildings 2 and 3 of Structure 3.1.1. Attention is given to the over-all structural configuration, the fundamental load vs time variations, and the basic concepts used to formulate and solve the equations of motion. Methods for evaluating rebound and determining frame resistances are adopted on the basis of an investigation of data from Operation Greenhouse. The results of the various analyses are presented in graphical form.

2.3.2 Structural Properties

Building 2 is a three-story steel-frame structure, one bay wide and three bays long. The structural frame consists of two rigid frames constructed of standard rolled sections throughout. Welded connections are used to ensure continuity at all the joints of the frame. The roof and floors are one-way reinforced-concrete slabs spanning between frames. Steel V-beam sheeting is used as the covering material for the front and rear faces. The V-beam is supported on girts of standard rolled sections which span between floors. Detailed sketches of Building 2 are shown in Figs. 2.39 to 2.41.

Building 3 is a three-story reinforced-concrete frame structure, one bay wide and three bays long. The roof and floors are one-way reinforced-concrete slabs spanning between frames. The front and rear faces are one-way reinforced-concrete slabs spanning vertically

and are continuous over the entire height of the structure. Detailed sketches of Building 3 are shown in Figs. 2.42 to 2.44.

The analyses of Buildings 2 and 3 were carried out by using certain basic material properties. These properties with some modification are an average of those used by Ammann and Whitney in their study of the behavior of these structures during Operation Greenhouse.[11] The actual values of the pertinent quantities are presented in Table D.6.

2.3.3 Loading

Structure 3.1.1 was located in the region of Mach reflection for shot Mike of Operation Ivy. The following overpressure vs time variations for windowless structures located in the region of irregular reflection obtained from reference 1 were used to compute the loadings for the analysis of the structure. A more complete discussion of the theoretical and empirical basis for these methods of load determination is contained in reference 1.

The air-blast wave in the vicinity of Structure 3.1.1 may be approximated as shown in Fig. 2.45. The variations in front, rear, and roof pressures with time are shown in Figs. 2.46 to 2.48, respectively.

The nomenclature and relations used in figures are:

c_o = velocity of sound in undisturbed air

c_{refl} = velocity of sound in the reflected region
$= 422\sqrt{(16\xi^2 + 38\xi - 5)/1.6}$, where $\xi = 1 + (P_{so}/14.7)$

h' = clearing height, taken as the full height of the front face or half its width, whichever is smaller

L = length of the structure in direction of propagation of blast wave

L' = distance along the roof in direction of propagation of blast wave to point at which local roof overpressure is being calculated

P_{so} = maximum incident free-air overpressure

P_s = free-air overpressure at any time t (Fig. 2.45)

P_{refl} = reflected overpressure produced by the impingement of a plane shock on a plane surface
$= 2P_{so}[(102.9 + 4P_{so})/(102.9 + P_{so})]$

q = dynamic pressure at any time t
$= q_o[1 - (t/t_o)]e^{-3.5t/t_o}$

q_o = peak dynamic pressure generated by blast wave

t_o = duration of positive phase of blast wave

t = time, measured from instant blast wave impinges upon surface being considered

t_c = time required to clear a surface of diffraction effects
$= (3h'/c_{refl})$

U_o = velocity of propagation of shock front

The basic data for the loadings on Structure 3.1.1 are taken from reference 2. The curves of maximum free-air overpressure vs distance and duration of positive phase vs distance for shot Mike of Operation Ivy are reproduced in Figs. 2.49 and 2.50, respectively. The fact that Structure 3.1.1 was oblique to the shock from shot Mike of Operation Ivy was not considered significant and was neglected because the angle of incidence was small (see Fig. 2.51).

An alternate variation in front-face overpressure was investigated. This variation, which includes a finite time of rise, is shown in Fig. 2.52. No attempt was made to modify the rear-face and roof loads to include the rise time because its effect on the loadings would not significantly change the structural response. The magnitude of the time of rise was based on the phenomena recorded at the site during Operation Greenhouse.

2.3.4 Analysis

The idealized system used to approximate the behavior of Buildings 2 and 3 is shown in Fig. 2.53. The multi-degree-of-freedom actual system is replaced by a system having nine independent coordinates. One coordinate is used to describe the motion of each floor mass,

and one coordinate defines the motion relative to the floors of the wall slab between floors for each story of both the front and rear faces. The positive direction of motion is as shown in Fig. 2.53.

The details of construction of Building 2 make it possible to reduce the analysis of this structure to a consideration of a three-degree-of-freedom system by neglecting the effect of the front and rear faces. The basis for this approach is presented in Appendix E. The analysis of Building 3 is complicated by the continuous construction of the front and rear faces. This detail makes it necessary to include the front- and rear-wall motion because these elements significantly aid the frame in resisting the horizontal motion of the floors.

The approach employed in this report is based on the principle of conservation of energy. There are only three basic quantities to be considered in this method. These are (1) the potential energy of the external loads, (2) the strain energy stored in the various resisting elements, and (3) the kinetic energy associated with the motion of the various masses.

The evaluation of the three basic energy terms is accomplished by standard relations as shown in Appendix C. The fundamental equation which relates kinetic energy, strain energy, and the potential energy of the external load for any coordinate y_m is given in Eq. 2.1.

$$\frac{d}{dt}\left[\frac{\partial(KE)}{\partial \dot{y}_m}\right] - \frac{\partial(KE)}{\partial y_m} + \frac{\partial(PE)}{\partial y_m} = -\frac{\partial U_e}{\partial y_m} \tag{2.1}$$

where KE = total kinetic energy of the system
PE = total potential energy of the system
U_e = potential energy of all external loads
$\dot{y}_m$ = first derivative of y_m with respect to t

Equation 2.1 is written for each coordinate of the system so that an equation of motion is obtained for each independent coordinate. This relation is known as the Lagrangian form of the differential equation of motion.[17]

The detailed computations of deflections for particular loads are accomplished by a numerical method of analysis called the "Acceleration Impulse Extrapolation Method." This method is rigorously presented in reference 4. The basic recurrence formula relating three successive displacements separated by a time interval Δt is

$$y_{n+1} = 2y_n - y_{n-1} + \ddot{y}_n \Delta t^2$$

The degree of accuracy obtained with this procedure is a function of the length of the time interval.

For time intervals short in relation to the natural frequency of the element, the error is small.[4]

A detailed derivation of the equations governing the behavior of Buildings 2 and 3 is presented in Appendix C. The computations of response of these structures to the various loading conditions are presented in Appendix E.

2.3.5 Evaluation of Rebound

The maximum displacement of any element is obtained from the numerical analysis of the dynamic response. The only deflection records available for Buildings 2 and 3 for shot Mike of Operation Ivy are the permanent displacements. In order to obtain the permanent displacement of an element from the dynamic analysis, it is necessary to reduce the maximum deflection by the amount of recovery to be expected. The computed recovery (or rebound) is obtained by dividing the resistance at the time of maximum deflection by the elastic spring constant, k. The Greenhouse data and the numerical analysis for Greenhouse presented in Appendix E are examined to determine the validity of this rebound computation.

The maximum relative deflection and final relative deflection of each of the three stories of Building 2 as recorded for Operation Greenhouse are presented in Table 2.3. The computed

values of maximum relative displacement and final relative displacement from the dynamic analysis of Building 2 for the conditions of Operation Greenhouse are also presented in Table 2.3. A comparison of the recorded and computed rebound for Building 2 shows that the computed rebound is generally smaller than the actual.

Owing to the discrepancy between computed and actual rebound at Greenhouse, an empirical approach is used to evaluate the amount of recovery. The final permanent deflections for shot Mike of Operation Ivy are obtained by subtracting the actual rebound observed during

Table 2.3—COMPARISON OF RECORDED AND COMPUTED DEFLECTIONS FOR BUILDING 2 AT OPERATION GREENHOUSE

	Maximum story deflection, ft			Final story deflection, ft			Rebound, ft		
	y_1	$y_2 - y_1$	$y_3 - y_2$	y_1	$y_2 - y_1$	$y_3 - y_2$	First story	Second story	Third story
Recorded	0.135	0.403	0.262	0.060	0.129	0.140	0.075	0.203	0.122
Computed	0.133	0.417	0.256	0.059	0.289	0.152	0.074	0.128	0.104

Table 2.4—COMPUTED MAXIMUM RELATIVE DEFLECTIONS, SHOT MIKE, OPERATION IVY, BUILDING 2

	Maximum relative deflection for 0-sec time of rise, ft			Maximum relative deflection for 0.018-sec time of rise, ft		
Overpressure (P_{so}), psi	First story y_1	Second story $y_2 - y_1$	Third story $y_3 - y_2$	First story y_1	Second story $y_2 - y_1$	Third story $y_3 - y_2$
6	0.041	0.087	0.106			
10	0.064	0.193	0.252	0.065	0.196	0.246
12	0.085	0.318	0.297	0.087	0.323	0.282
13	0.113	0.387	0.316	0.115	0.397	0.291
14	0.165	0.488	0.324	0.178	0.497	0.305
15	0.256	0.526	0.361	0.260	0.533	0.323
17	0.516	0.729	0.358	0.532	0.715	0.327
19	1.170	0.721	0.428			

Operation Greenhouse (Table 2.3) from the computed maximum displacements of the various analyses. The resulting permanent deflections obtained are considered to be the most reasonable that can be estimated at the present time.

2.3.6 Results of Analysis

A series of pilot analyses was performed on Building 2 using the records obtained from Operation Greenhouse. These analyses were used to determine the resistance values for the columns of the building which would give the best approximation to the deflection records of Operation Greenhouse. The approach adopted was to vary the height of column between plastic hinges. The recorded and computed displacement vs time curves for the relative deflection of each of the three stories of Building 2 are presented in Figs. 2.54 to 2.56. The computed curves represent the best agreement obtained from the several analyses performed. The resistances were obtained using the column heights as listed on the figures. The computations for these analyses are included in Appendix E.

Fourteen loading cases were investigated for Building 2, as indicated in Tables 2.4 and 2.5, under the conditions of shot Mike of Operation Ivy. The effective column heights interpreted from the Greenhouse data were used in the determination of the resistance values for these analyses. Eight values of overpressure with an instantaneous time of rise were considered. These analyses define the variation of maximum response with overpressure for the complete range of yielding to failure. Six additional analyses were performed incorporating a time of rise of 18 msec in the front-face loading. These six analyses were used to show the

effect of rise time in the range of overpressures which bracket the pressure experienced by Building 2 during shot Mike of Operation Ivy.

The results of the various analyses for Building 2 are presented in Tables 2.4 and 2.5.

The curves of final deflection vs peak incident free-air overpressure and the recorded values of final deflection for Building 2 are shown in Figs. 2.57 to 2.59. The range of possible overpressures existing at the site for shot Mike of Operation Ivy is determined by a comparison of the computed and recorded final deflections.

Table 2.5—COMPUTED FINAL RELATIVE DEFLECTIONS, SHOT MIKE, OPERATION IVY, BUILDING 2

Overpressure (P_{so}), psi	Final relative deflection for 0-sec time of rise, ft			Final relative deflection for 0.018-sec time of rise, ft		
	First story y_1	Second story $y_2 - y_1$	Third story $y_3 - y_2$	First story y_1	Second story $y_2 - y_1$	Third story $y_3 - y_2$
6	0	0	0			
10	0	0	0.130	0	0	0.124
12	0.010	0.035	0.175	0.012	0.040	0.160
13	0.038	0.104	0.194	0.040	0.114	0.169
14	0.090	0.205	0.202	0.103	0.184	0.183
15	0.181	0.243	0.239	0.185	0.250	0.201
17	0.441	0.446	0.236	0.457	0.433	0.205
19	1.095	0.438	0.306			

Table 2.6—MAXIMUM AND FINAL DEFLECTIONS FOR BUILDING 3

P_{so}	13	14	P_{so}	13	14	P_{so}	13	14
y_1:			$y_2 - y_1$:			$y_3 - y_2$:		
Maximum	0.321	0.430	Maximum	0.403	0.411	Maximum	0.175	0.148
Rebound	0.163	0.163	Rebound	0.218	0.218	Rebound	0.210	0.210
Computed final	0.158	0.267	Computed final	0.185	0.193	Computed final	0	0
Measured final	0.070	0.070	Measured final	0.130	0.130	Measured final	0.140	0.140

The analyses of Building 3 were used merely as a check of the results obtained from Building 2. Only two overpressures with instantaneous rise time were investigated for this structure. The difficult nature of the analyses made a greater number of investigations impractical. The resistance values were obtained using column heights based on the results of the correlation of the Greenhouse analyses of Building 2. The results of the two analyses of Building 3 are presented in Table 2.6.

A study of the computed maximum relative deflections (Table 2.4), the final deflection vs overpressure curves (Figs. 2.57 to 2.59), and the final relative deflections (Table 2.5) determined for Building 2 lead to the conclusion that the maximum air-blast overpressure in the vicinity of Structure 3.1.1 was between 12 and 14 psi. Very little difference is obtained in the structural response computed with a zero time of rise and with a rise time of 18 msec. In view of the uncertainty regarding factors such as the effective mass of the superimposed dead load and other approximations used in the load computations, it is estimated that a time of rise of the magnitude used in this analysis may be neglected without greatly affecting the structural response. It may therefore be concluded that one cannot determine as a result of the analysis of this structure whether a significant time of rise was present in the air blast or not.

The comparison of the maximum and final computed deflections vs the measured final deflections for Building 3 (Table 2.6) indicates that a maximum air-blast overpressure of 12 or 13 psi would have caused the observed structural deformation. The analyses of Building 3 involve a higher degree of uncertainty than those for Building 2 because of the structural rebound assumption and the strength properties of reinforced concrete columns.

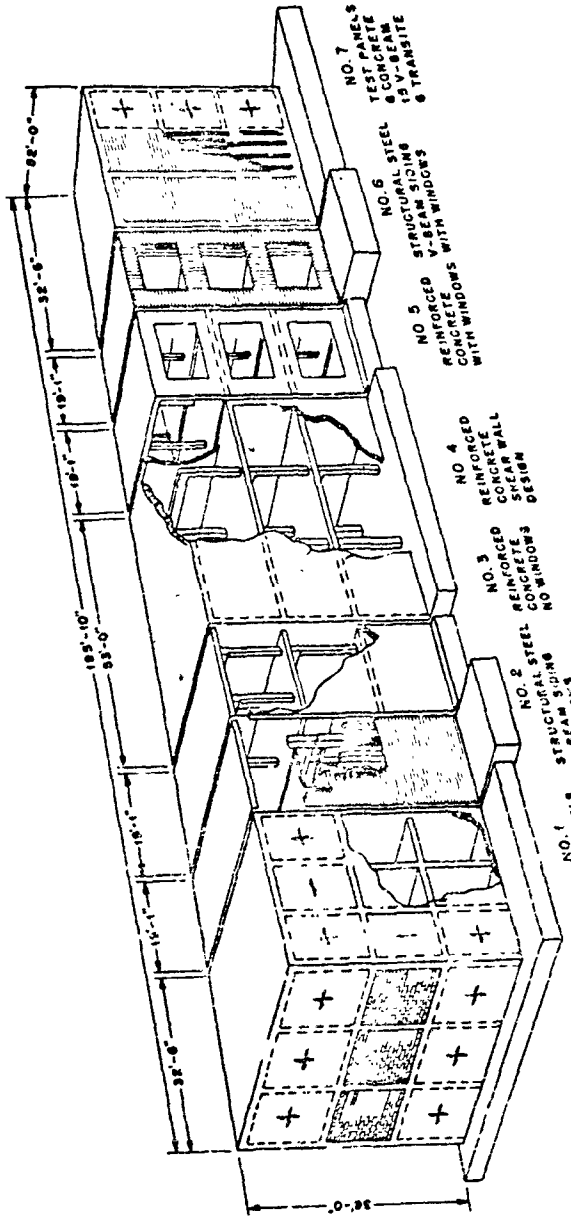

Fig. 2.1—Multistory Structure 3.1.1.

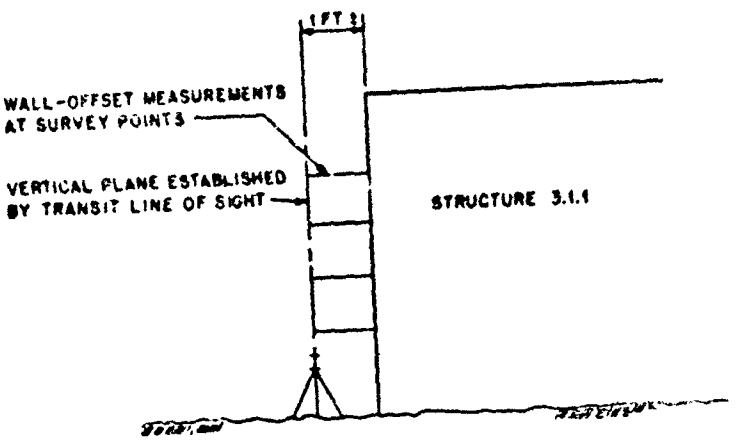

Fig. 2.2—Exterior-wall-offset measurements.

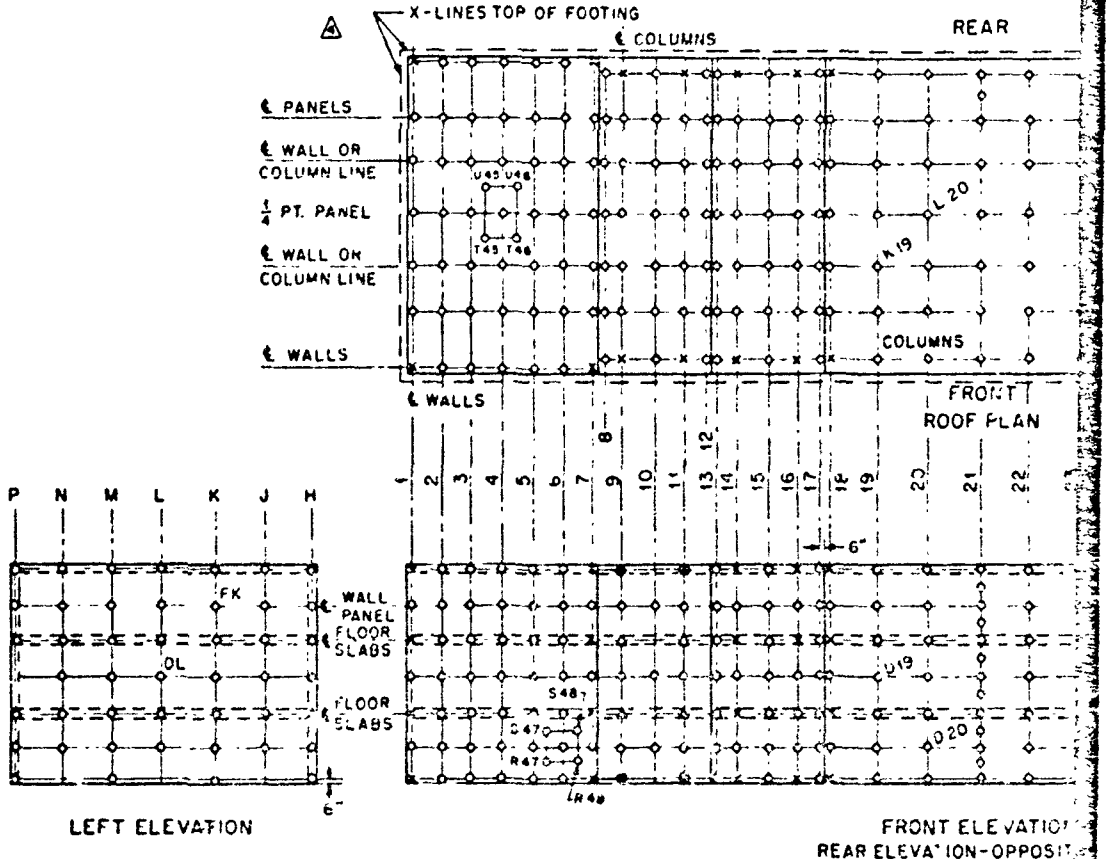

NOTES:

1. All points marked x are control points. These pins should be set as per Ammann and Whitney drawings.
2. Points marked ● are control points on Secs. 2 and 6. These may be "Drive It" pins set in main steel member at floor levels.
3. Points marked O are intermediate points. They may be "Drive It" pins. No pin shall be placed closer than 6 in. to an edge in concrete.
4. Points marked △ are heads of bolts suitably punched for identification on Secs. 2 and 6.
5. If drawing requires survey point on concrete or asbestos, do not use a "Drive It" pin. Mark with chalk.

Reference:

Location for survey points by R. C. Hall (NC 1001), dated 10 May 1950

Fig. 2.3—Location of survey points

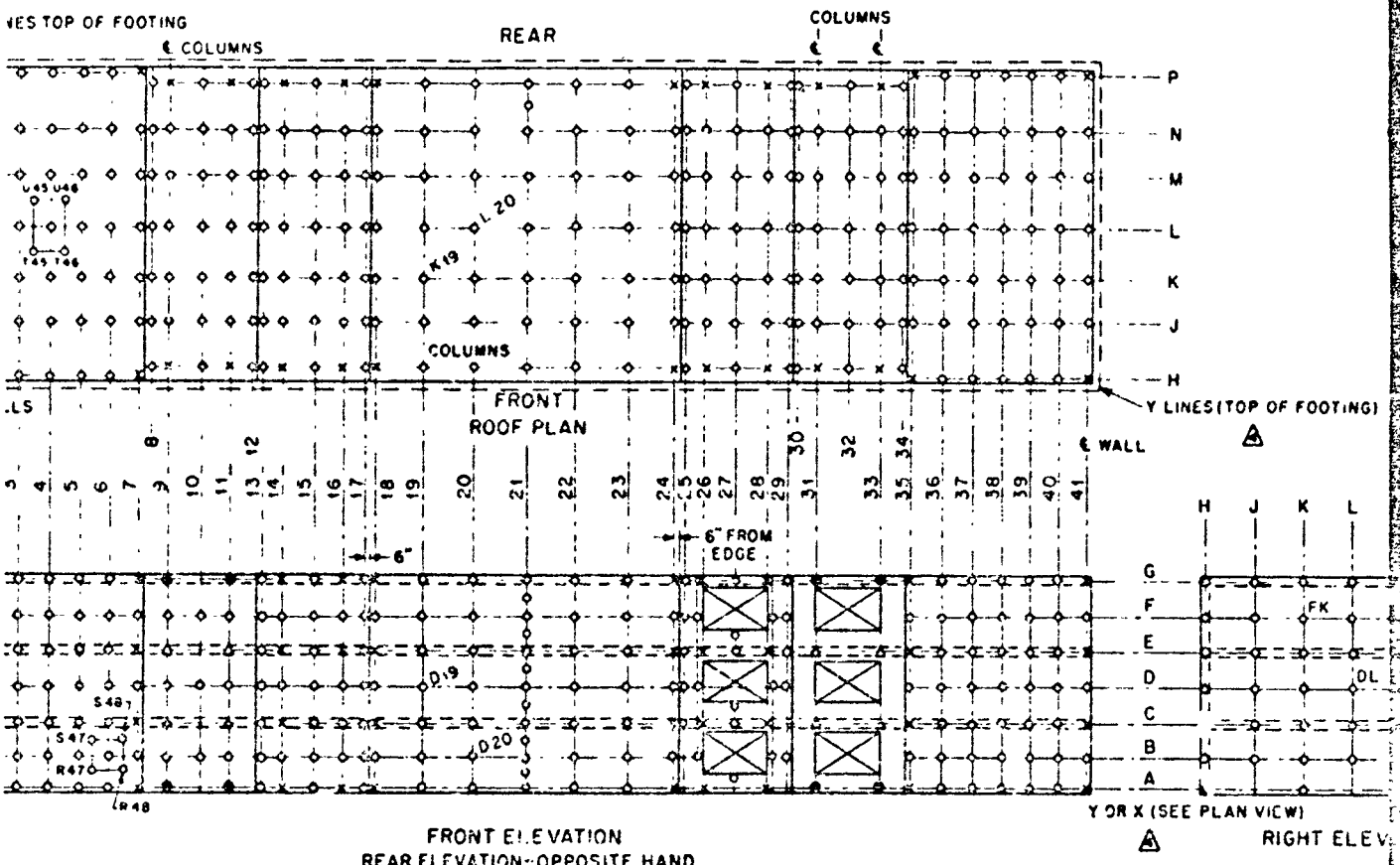

4. Points marked Δ are heads of bolts suitably center-punched for identification on Secs. 2 and 6.
5. If drawing requires survey point on corrugated asbestos, do not use a "Drive It" pin. Mark location with chalk.

Reference:

Location for survey points by R. C. Hansen, drawing NC 1000, dated 10 May 1950.

Summary of Survey Points for Army Multiple

× — 116 set in concrete		
○ — 737 "Drive It" pins	737	
● — 16 "Drive It" pins	16	
Total "Drive It" pins	753	

Δ — 16 center-punched bolts. (These may fastening bolts in V-beam siding

2

Fig. 2.3—Location of survey points on Structure 3.1.1.

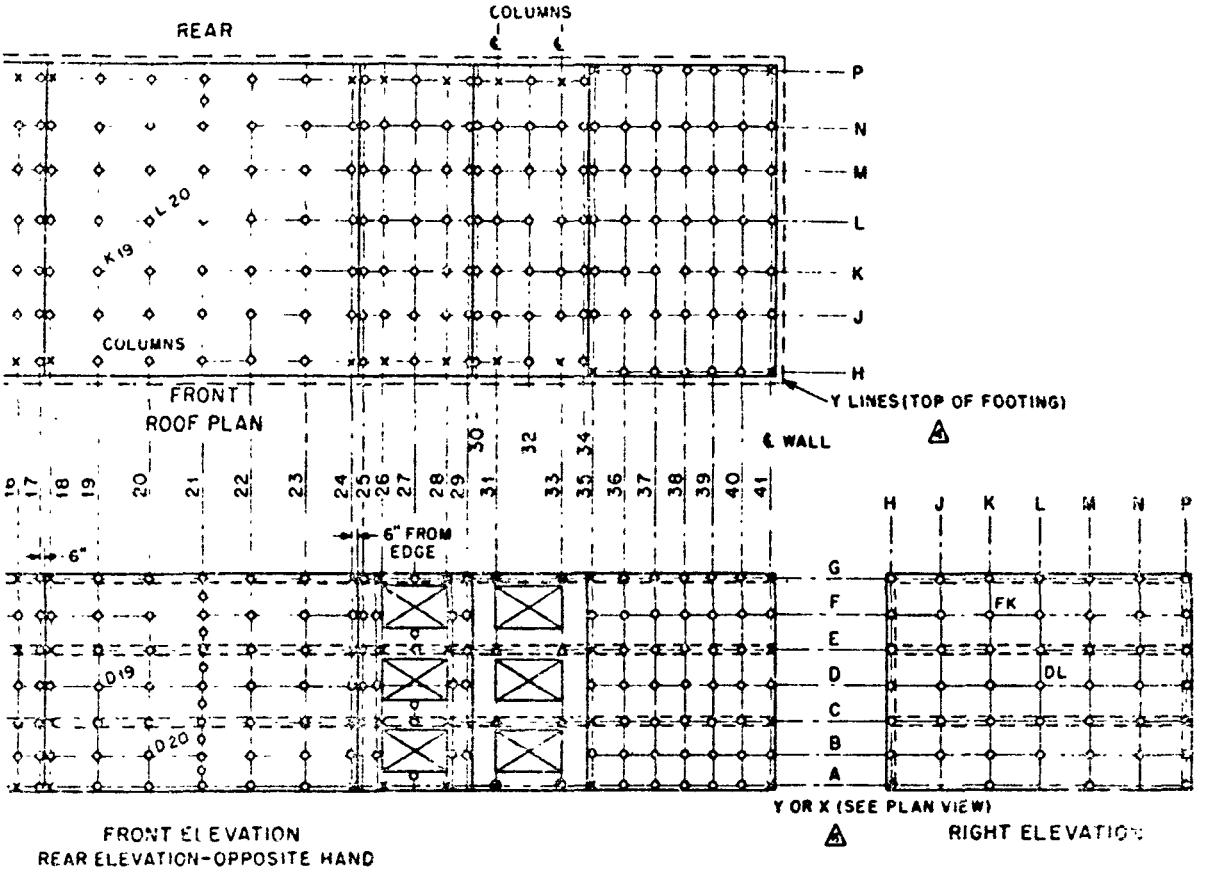

s marked Δ are heads of bolts suitably center-
hed for identification on Secs. 2 and 6
swing requires survey point on corrugated as-
s, do not use a "Drive It" pin. Mark location
chalk.

ice:

tion for survey points by R. C. Hansen, drawing
000, dated 10 May 1950.

Summary of Survey Points for Army Multiple-unit Structure

x — 116 set in concrete
O — 737 "Drive It" pins 737
● — 16 "Drive It" pins 16
Total "Drive It" pins 753
Δ — 16 center-punched bolts. (These may be fastening bolts in V-beam siding.)

. 2.3—Location of survey points on Structure 3.1.1.

3

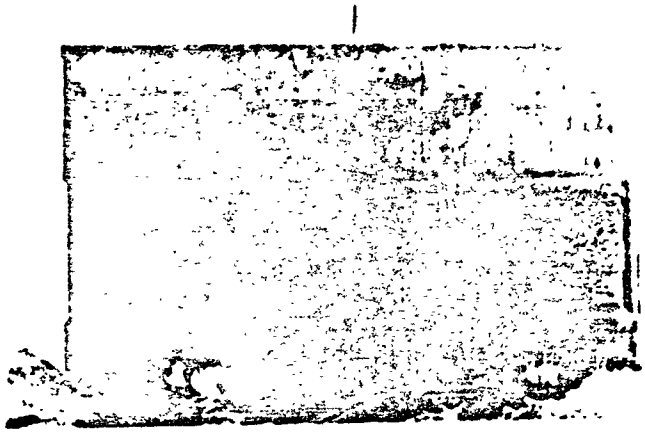

Fig. 2.7—Pretest, end of Building 1.

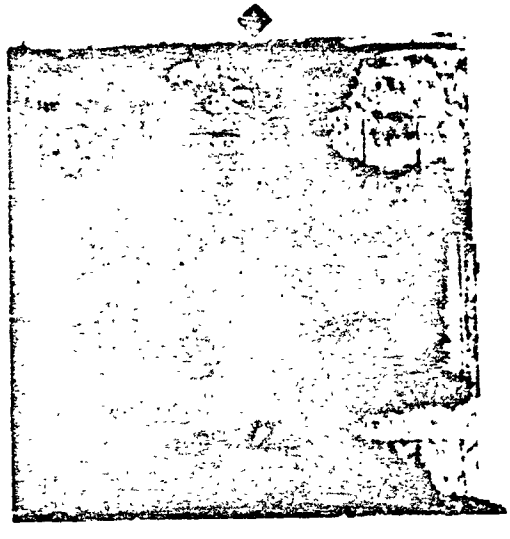

Fig. 2.8—Pretest, rear of Building 1.

Fig. 2.9—Posttest, front of Structure 3.1.1.

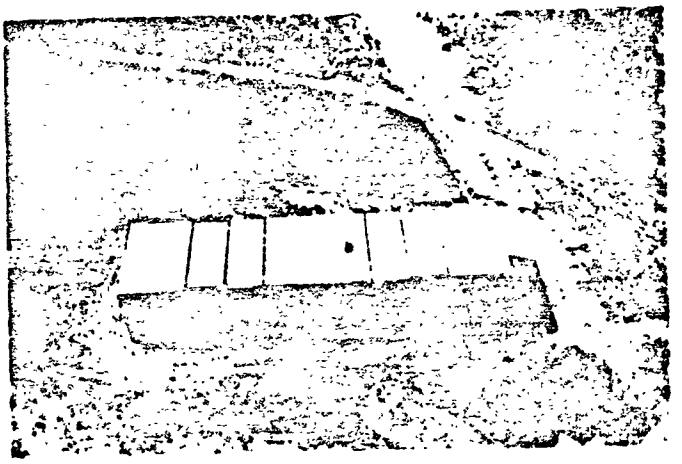

Fig. 2.10—Posttest rear of Structure 3.1.1.

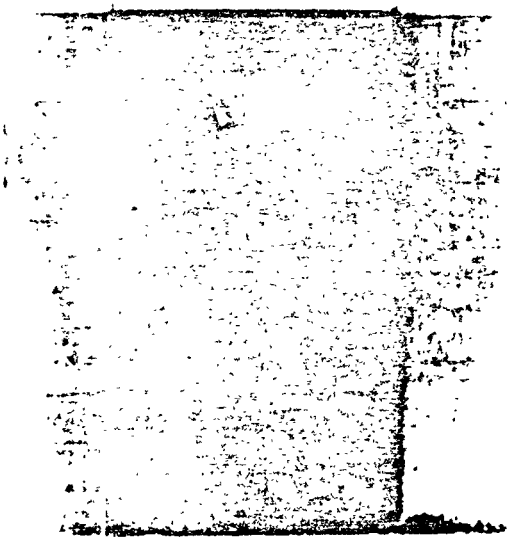

Fig. 2.11—Pretest, front of Building 2.

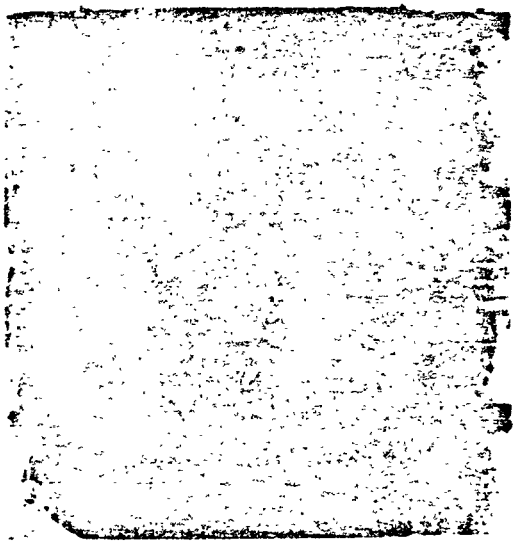

Fig. 2.12—Pretest, rear of Building 2.

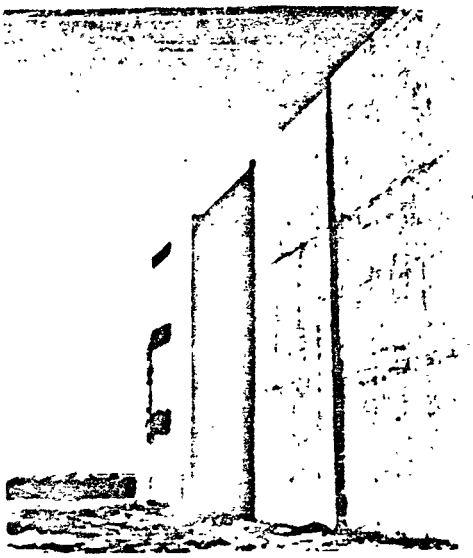

Fig. 2.13—Posttest, front of Buildings 1, 2, and 3.

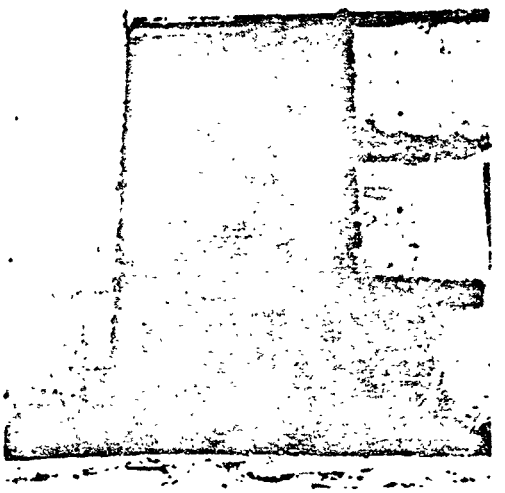

Fig. 2.14—Posttest, rear of Building 2.

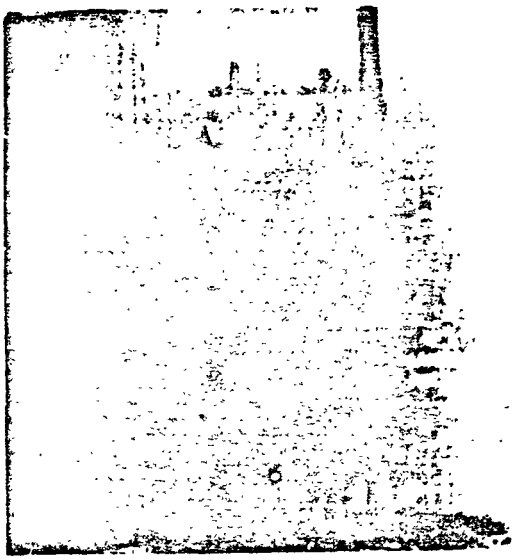

Fig. 2.15—Pretest, front of Building 3.

Fig. 2.16—Pretest, rear of Building 3.

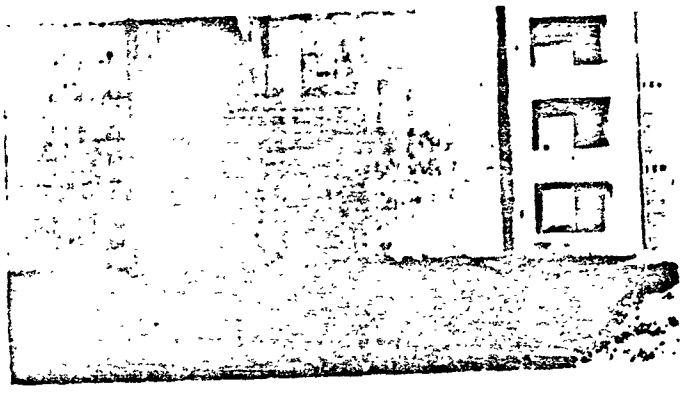

Fig. 2.17—Pretest, front of Building 4.

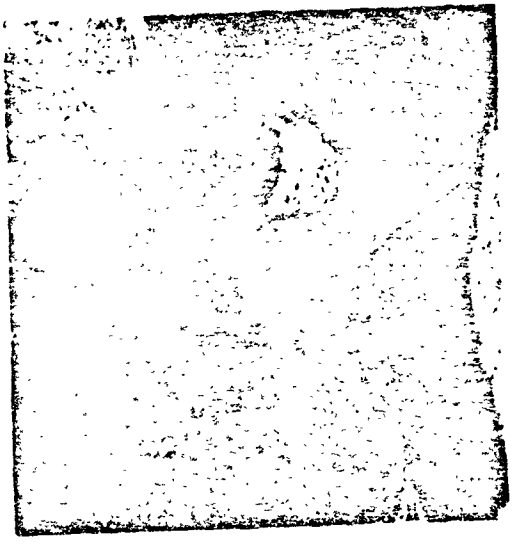

Fig. 2.18—Pretest, Building 4, interior view of roof crack adjacent to shear wall on Building 4 side (looking toward front wall).

Fig. 2.19—Posttest, Building 4, interior view of roof crack. Same location as Fig. 2.18.

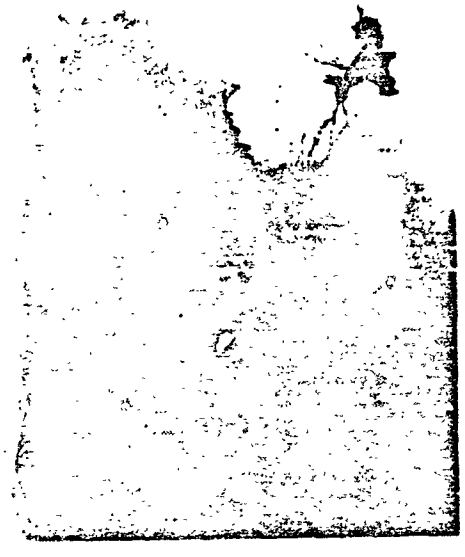

Fig. 2.20—Posttest, Building 4, interior view of roof crack. Same location as Fig. 2.18 (looking toward rear wall).

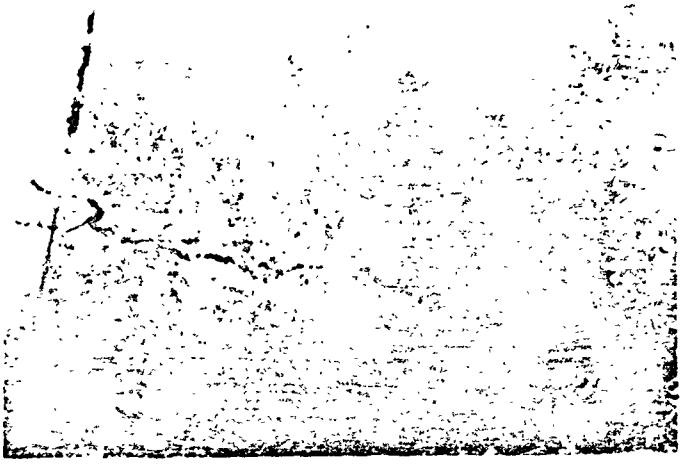

Fig. 2.21 — Pretest, Building 4, interior view of roof crack adjacent to shear wall on Building 5 side (looking toward rear wall).

Fig. 2.22 — Posttest, Building 4, interior view of roof crack. Same location as Fig. 2.21.

Fig. 2.23—Posttest, Building 4, interior view of roof crack. Same location as Fig. 2.21 (looking toward front wall).

Fig. 2.24—Posttest, Building 4, interior view of roof crack adjacent to column line on Building 3 side (looking toward front wall).

Fig. 2.25—Posttest, Building 4, interior view of roof crack. Same location as Fig. 2.24 (looking toward Building 3 side).

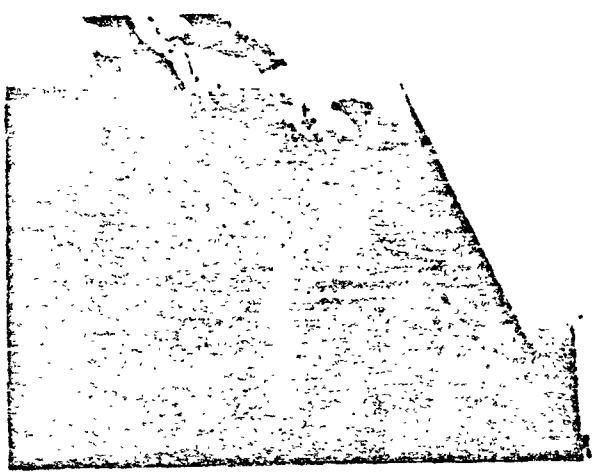

Fig. 2.26—Posttest, Building 4, interior view of roof crack. Same location as Fig. 2.24 (looking toward rear wall).

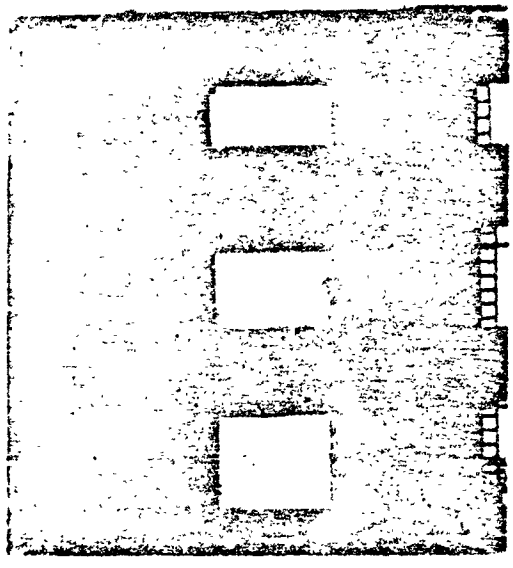

Fig. 2.27—Pretest, front of Building 5.

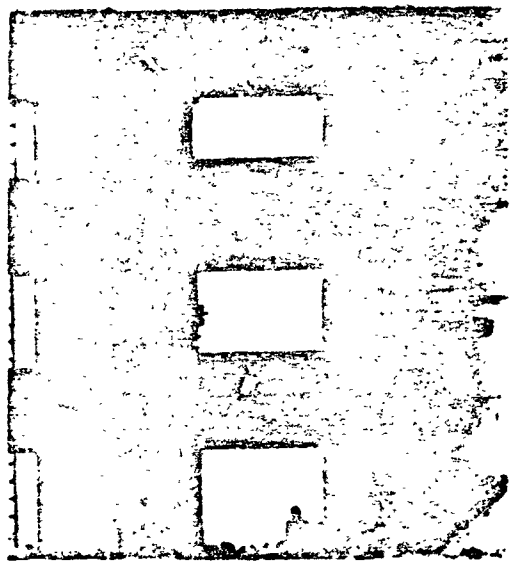

Fig. 2.28—Pretest, rear of Building 5

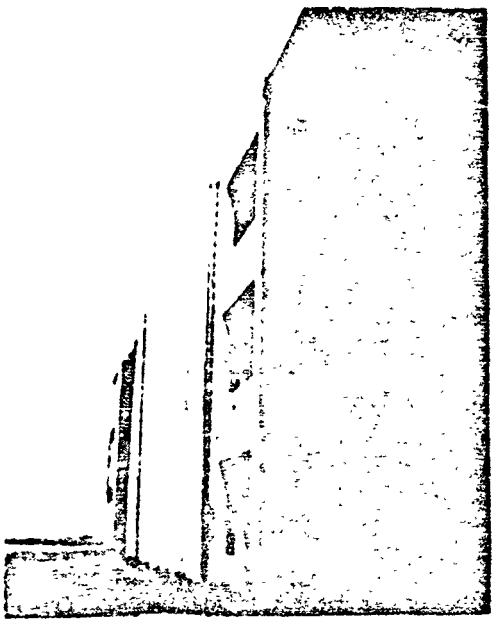

Fig. 2.29—Posttest, general view of front of Structure 3.1.1.

Fig. 2.30—Posttest, rear of Building 5.

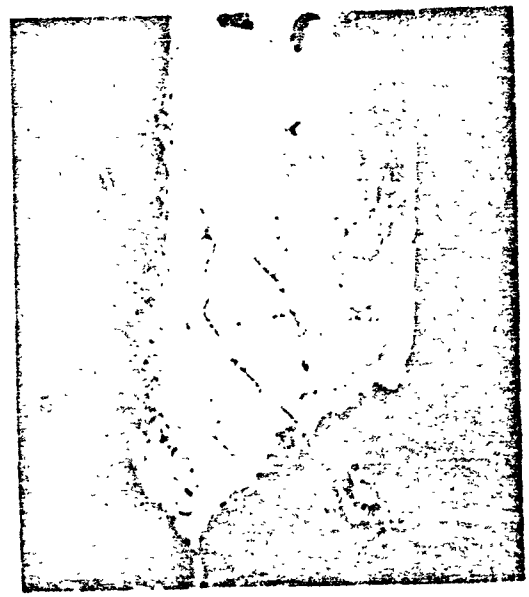

Fig. 2.31—Posttest, close-up of column base in Building 5 showing typical pattern of cracks

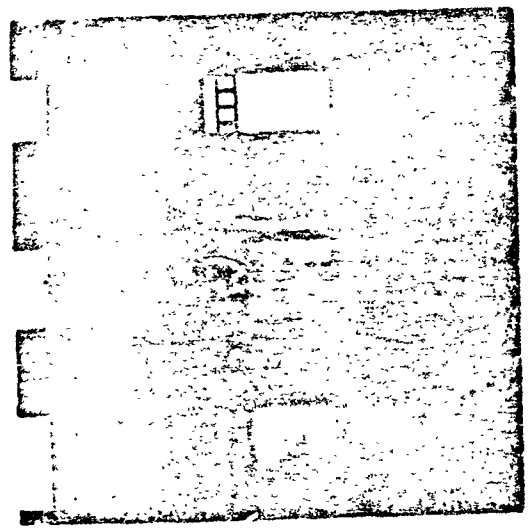

Fig. 2.32—Pretest, front of Building 6.

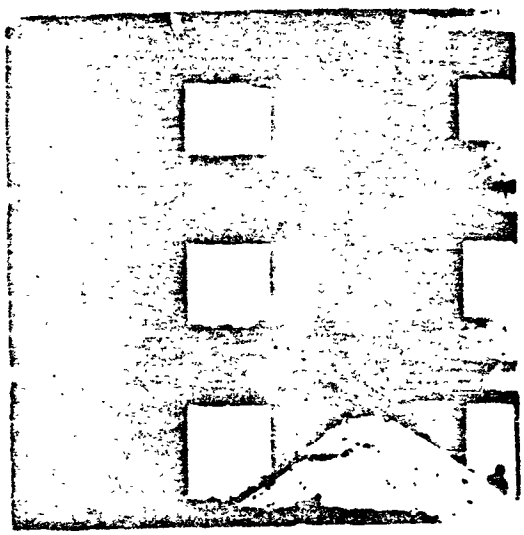

Fig. 2.33—Pretest, rear of Building 6.

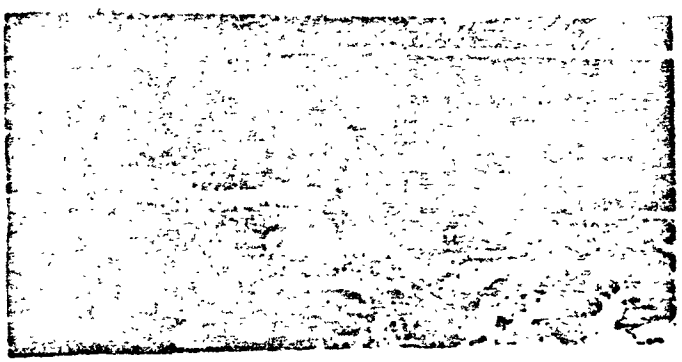

Fig. 2.34—Pretest, general view of rear of Buildings 1, 5, 6, and 7.

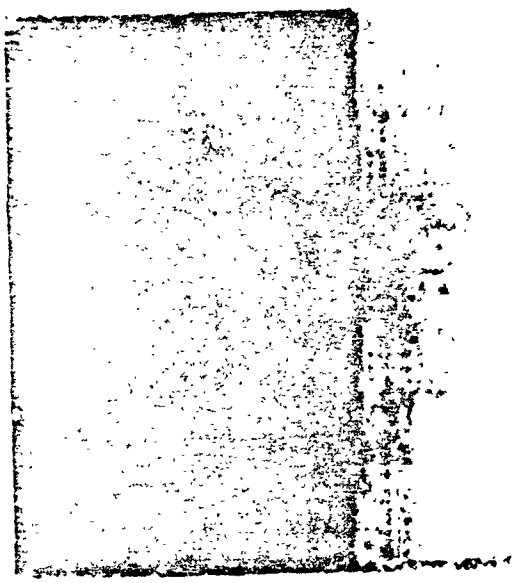

Fig. 2.35—Pretest, front of Building 7.

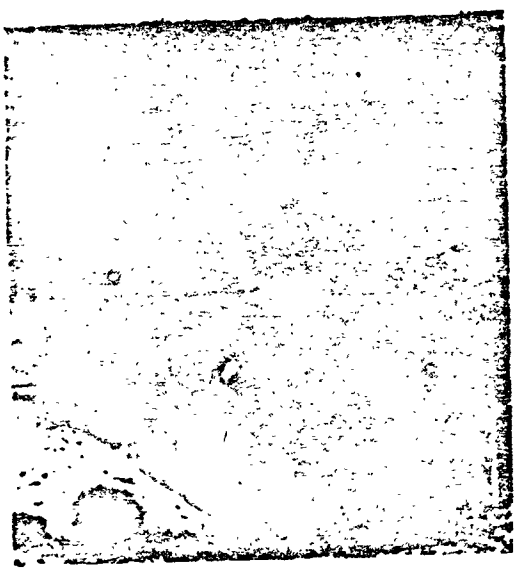

Fig. 2.36—Pretest, rear of Building 7.

Fig. 2.37—Pretest, end of Building 7.

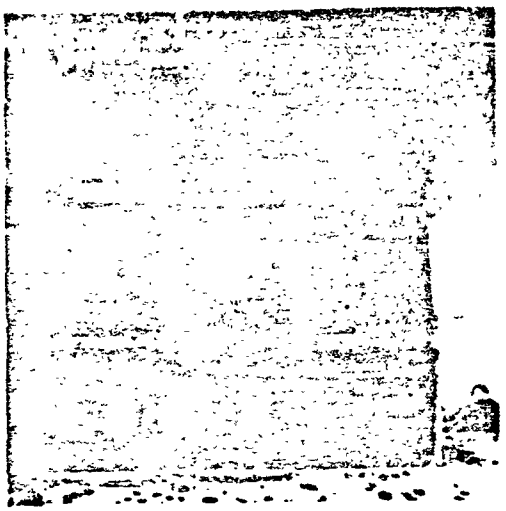

Fig. 2.38—Posttest, end of Building 7.

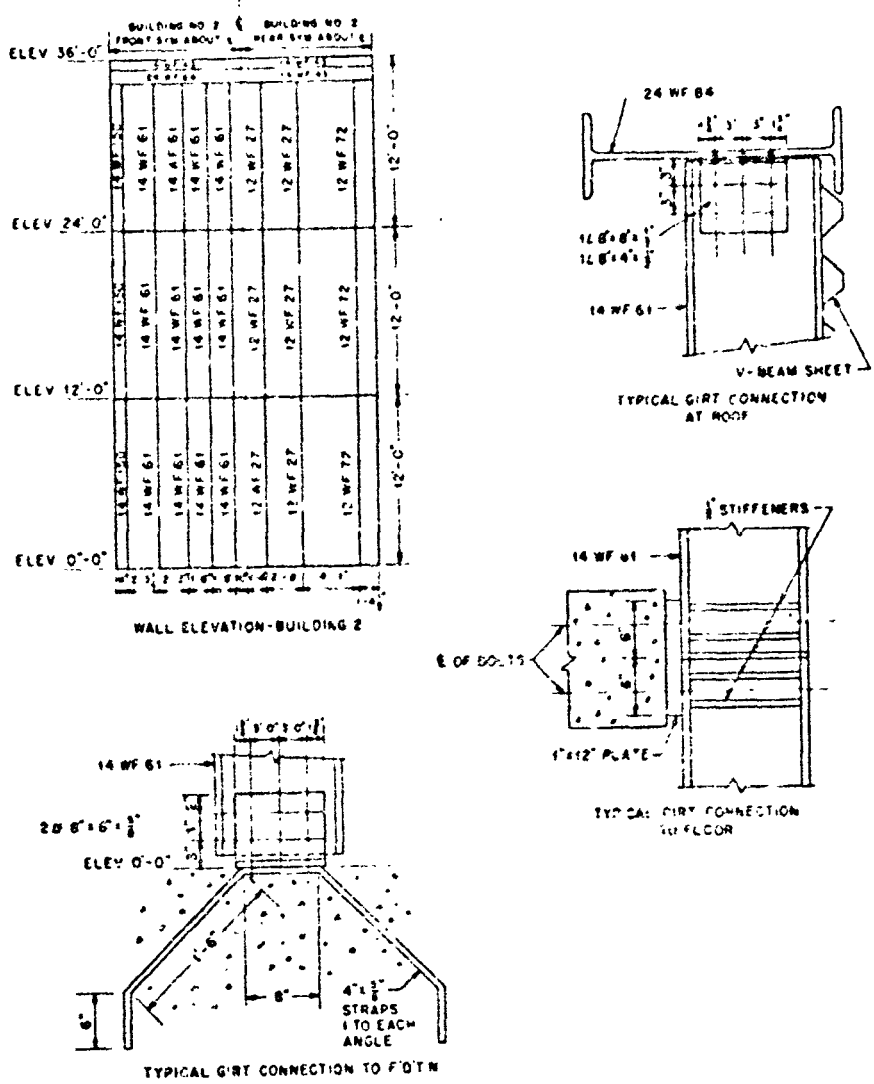

Fig. 3.39 — Front elevation and wall details, Building 2.

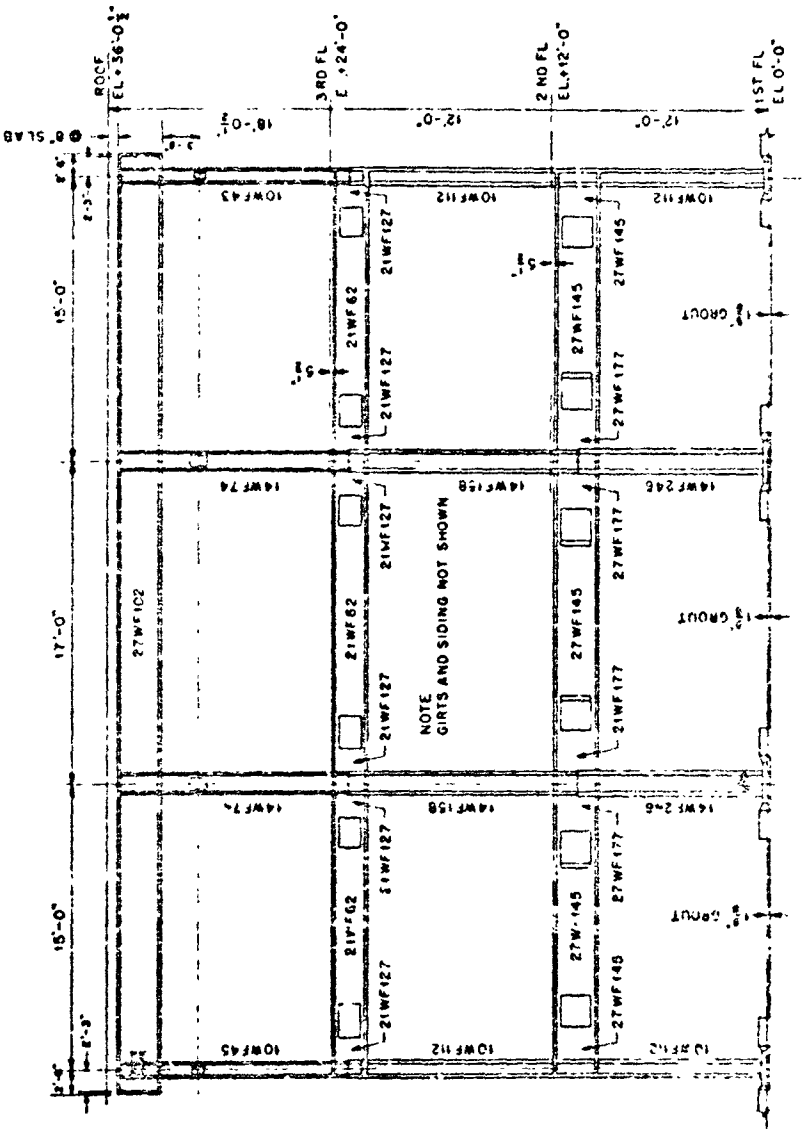

Fig. 2.40 — Transverse section through frame of Building 2.

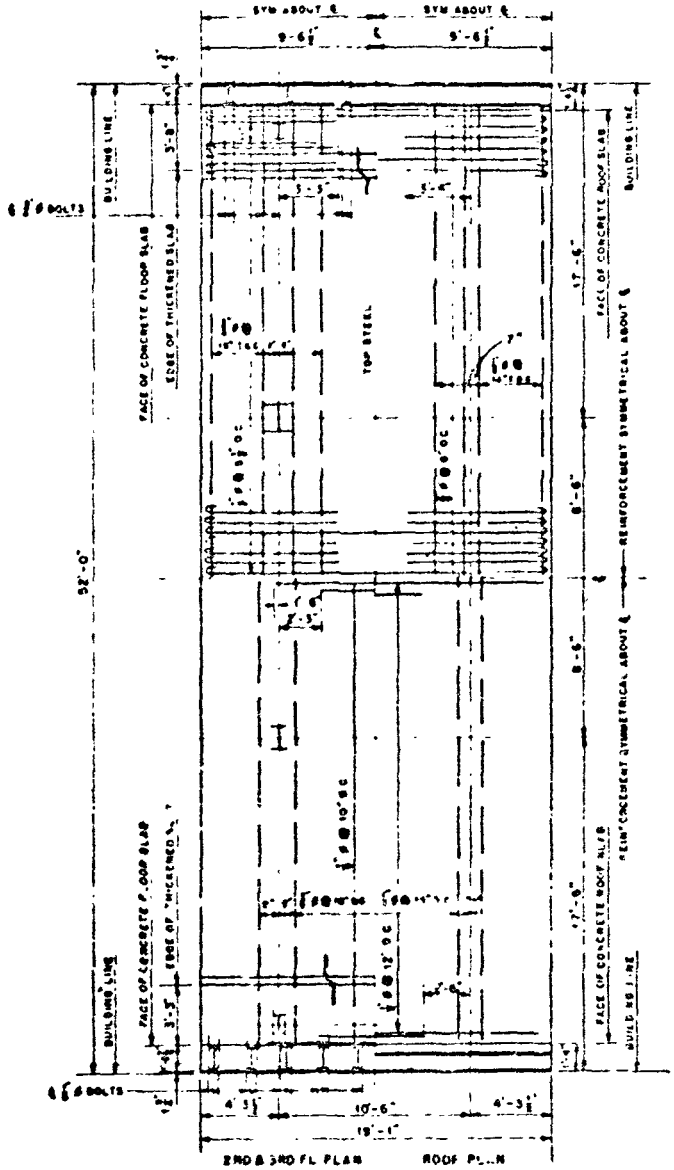

Fig. 2.41—Second-floor, third-floor, and roof plans of Building 2.

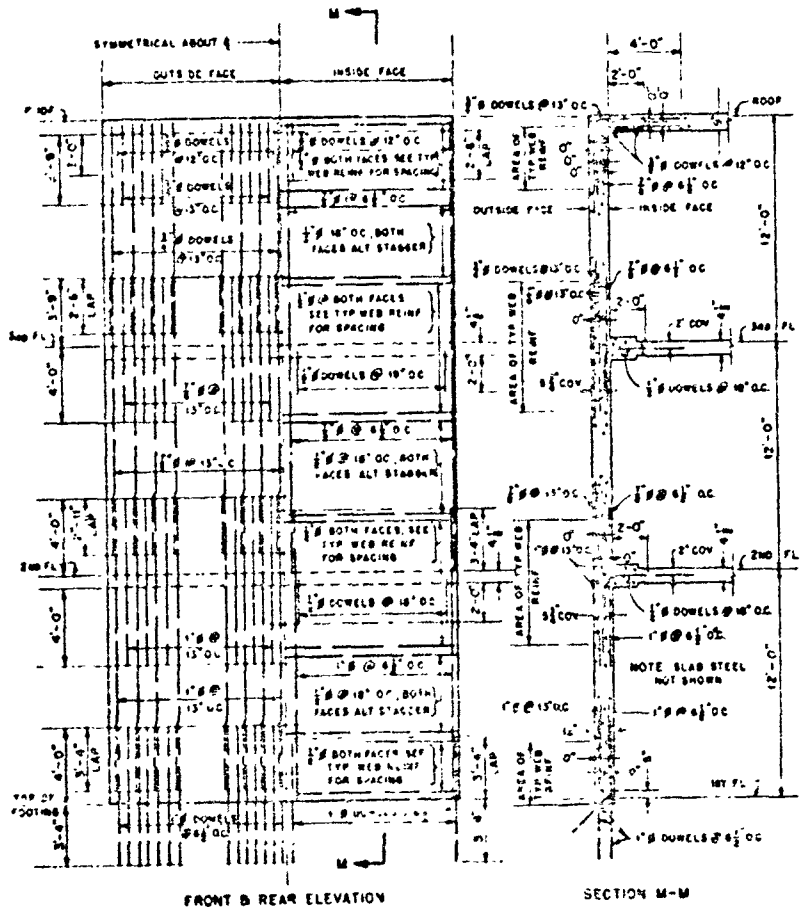

Fig. 2.42—Front and rear elevations and wall details, Building 3.

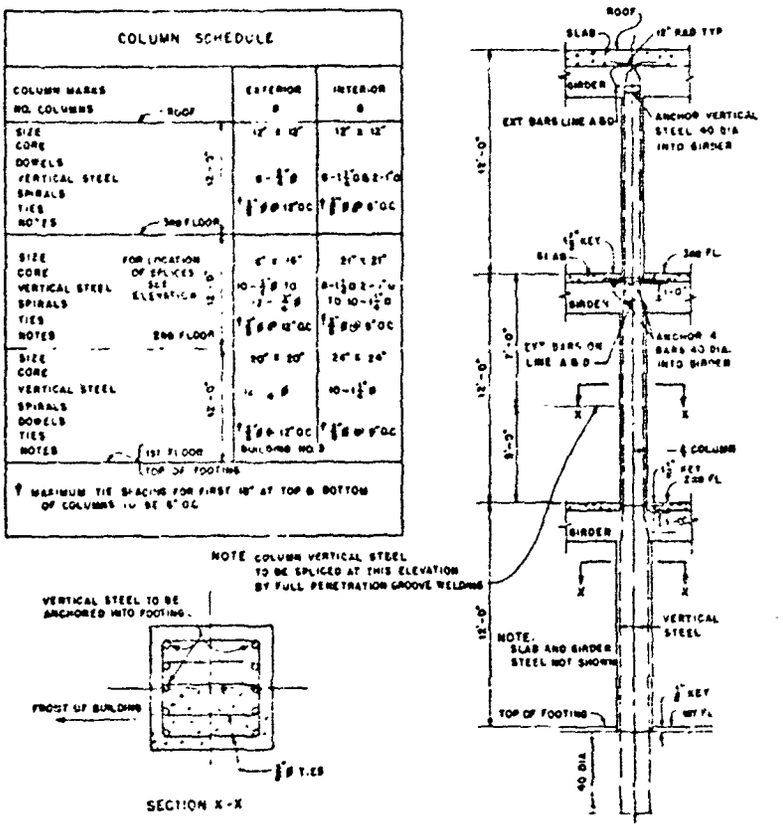

Fig. 2.13—Transverse section through frame of Building 3.

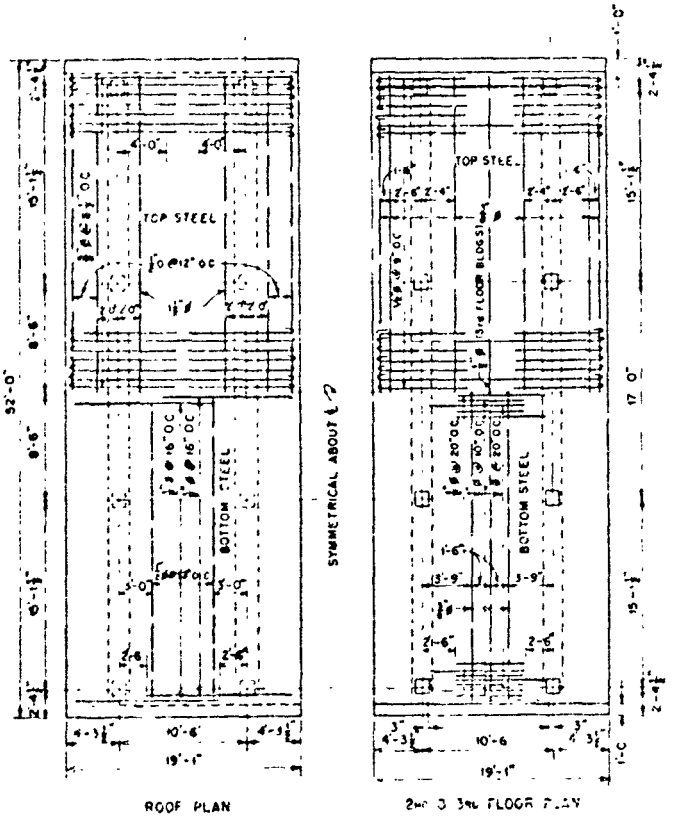

Fig. 2.44 — Second-floor, third-floor, and roof plans of Building 3.

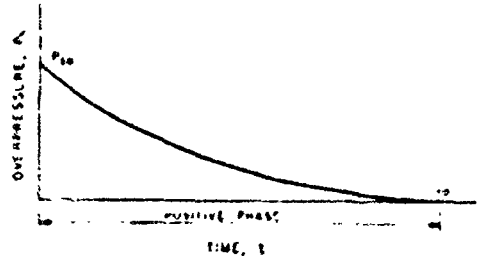

Fig. 2.45 — Free-stream overpressure vs time curve.

$$P_s = P_{so}\left(1 - \frac{t}{t_o}\right)e^{-t/t_o}$$

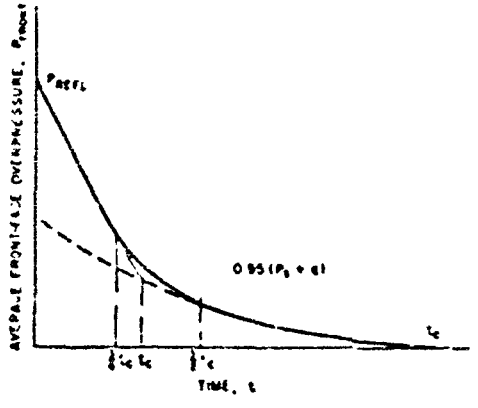

Fig. 2.46 — Average front-face overpressure vs time curve. Note that the average front-face overpressure curve fared between $\frac{1}{4}t_c$ and $\frac{3}{4}t_c$.

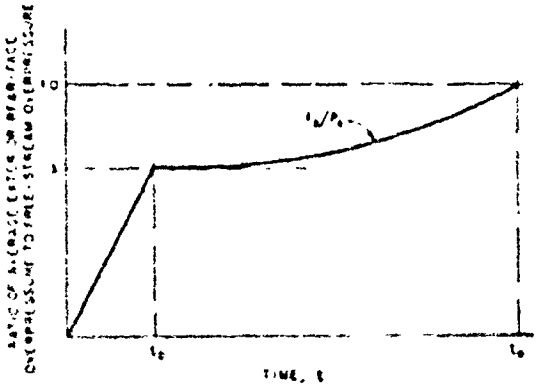

Fig. 2.47 Ratio of average exterior rear-face overpressure to free-stream overpressure vs time.

$$(P_s - P_1) = A + (1 - A)[1 - t_a/(t_a - t_b)]^2$$

$$A = \tfrac{1}{2}[1 + (1 - e^{-\delta})]$$

$$\delta = 0.5\,\frac{P_{so}}{14.7}$$

$$t_b = \frac{4h'}{c_o}$$

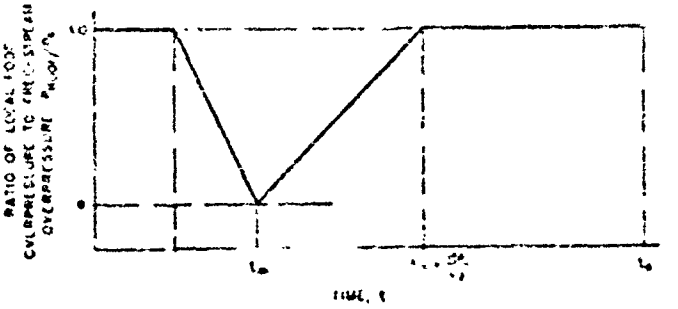

Fig. 2.48 — Ratio of local roof overpressure to free-stream overpressure vs time.

$$t_m = \frac{L'}{v}$$

$$v = \left(0.042 + 0.105\,\frac{L}{l}\right)c_o$$

$$a = 4\left(\frac{P_{so}}{14.7}\right)\left(\frac{L'}{c_o t_a}\right)\left(1 - \frac{x}{L}\right)$$

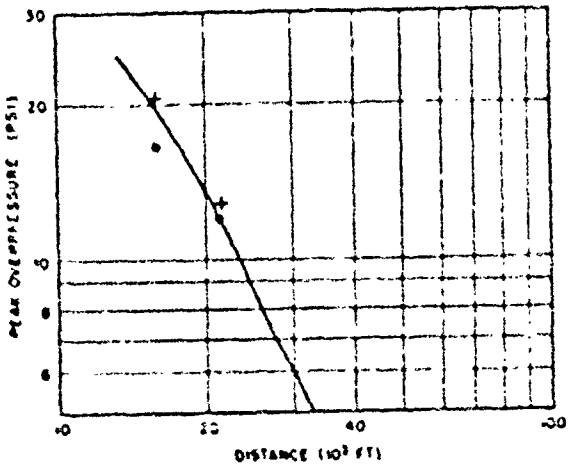

Fig. 2.49—Peak overpressure vs distance from Ground Zero, Mike shot. ●, side-on baffle +, Pitot static tube.

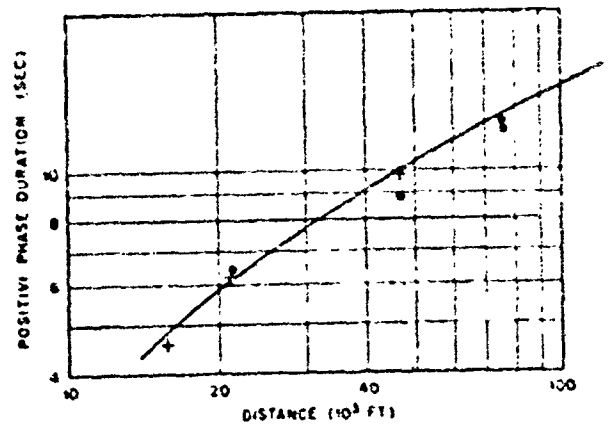

Fig. 2.50—Positive-phase duration vs distance from Ground Zero, Mike shot. ●, side-on baffle. +, Pitot-static tube.

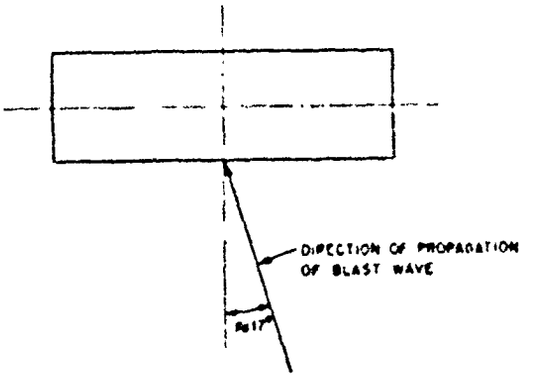

Fig. 2.51—Angle of incidence on Structure 3.1.1, Mike shot.

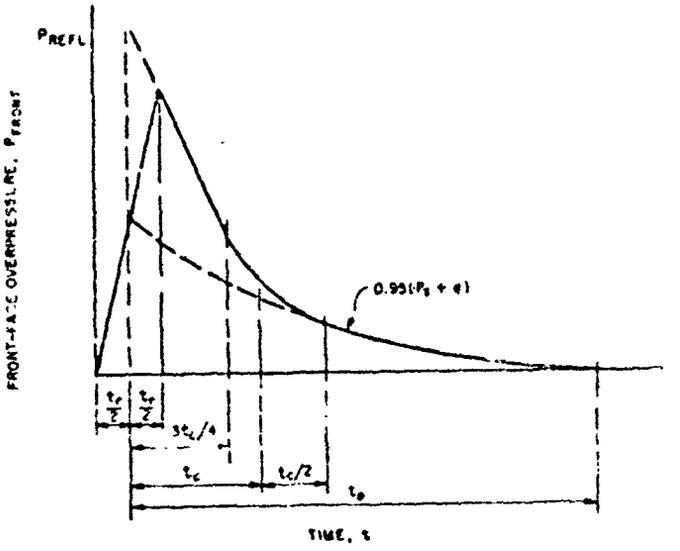

Fig. 2.52—Front-face overpressure vs time, incorporating time of r[illegible], t_r.

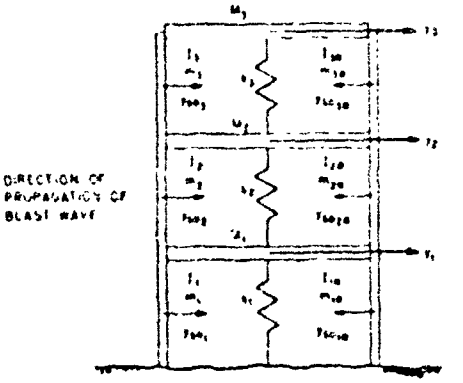

Fig. 2.53 — Idealized dynamic system for three-story frame building.

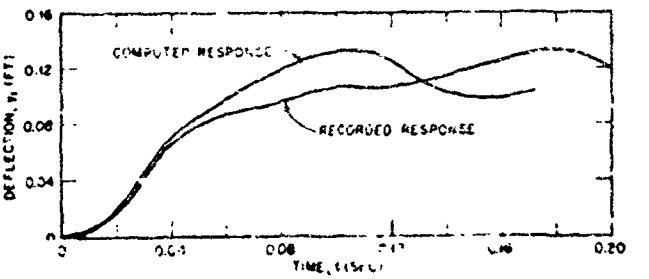

Fig. 2.54 — Comparison of computed and recorded response of first story of Building 2, Operation Greenhouse, h_g = 9.29 ft.

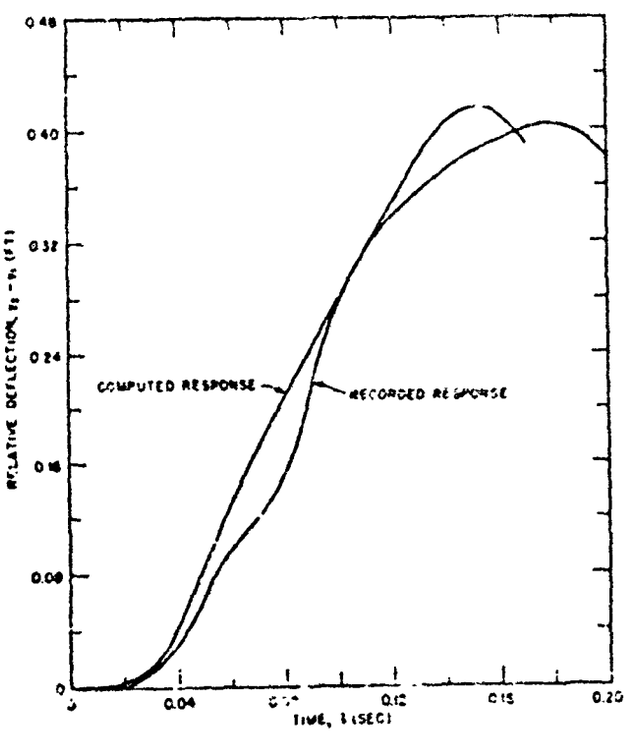

Fig. 2.55 – Comparison of computed and recorded response of second story of Building 2, Operation Greenhouse. h_2 = 10.25 ft.

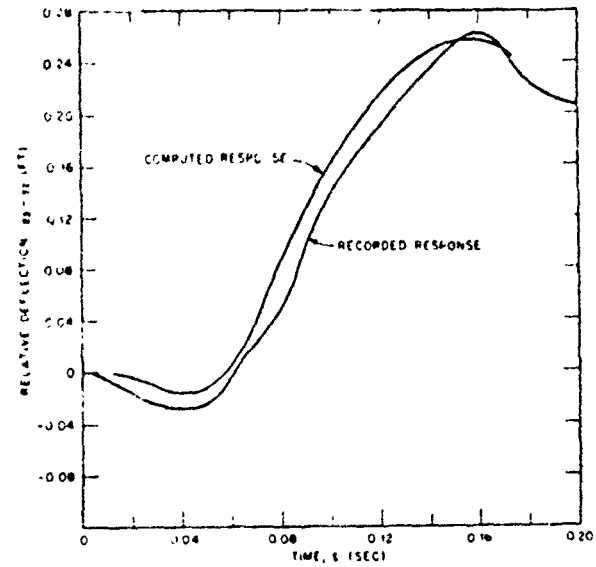

Fig. 2.56 — Comparison of computed and recorded response of third story of Building 4, Operation Greenhouse. h_0 = 9.12 ft.

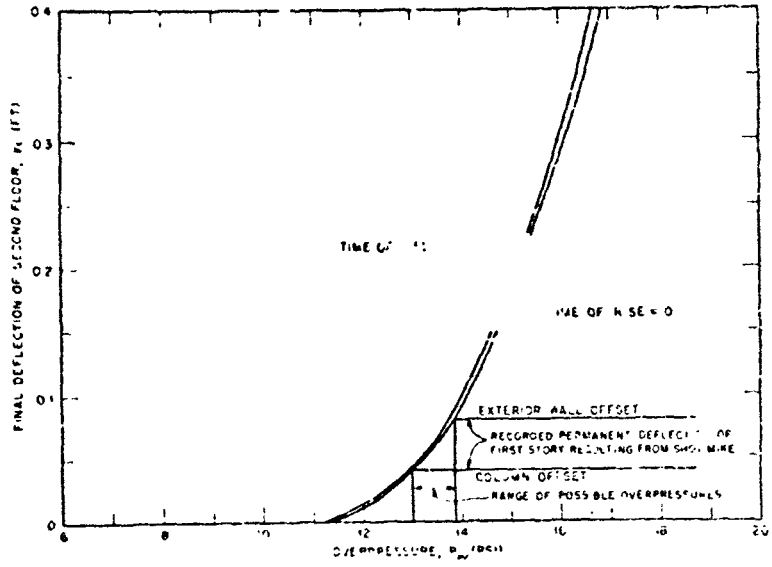

Fig. 2.57 — Final deflection vs overpressure for first story of Building 2, Mike shot, Operation Ivy

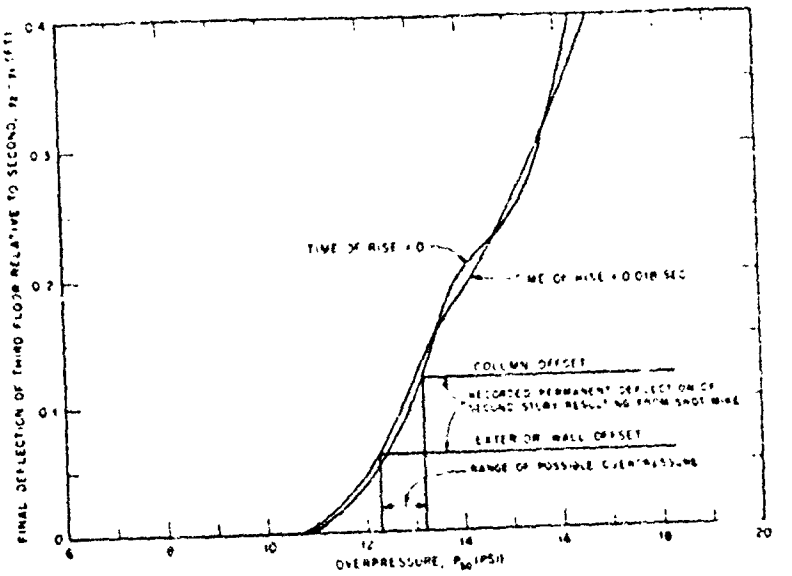

Fig. 2.58 — Final deflection vs overpressure for second story of Building 2, Mike shot, Operation Ivy.

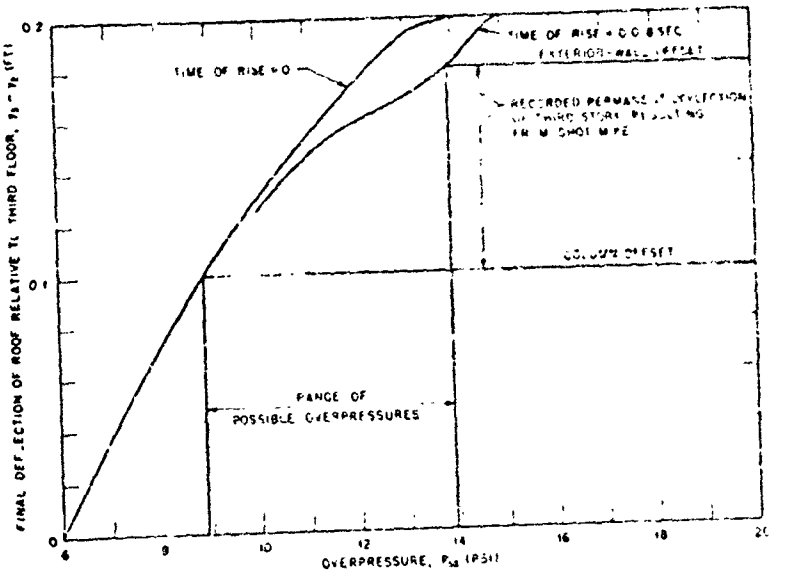

Fig. 2.59 — Final deflection vs overpressure for third story of Building 2, Mike shot, Operation Ivy.

CHAPTER 3

DAMAGE SURVEY OF MISCELLANEOUS STRUCTURES

3.1 GENERAL

The damage caused by shots Mike and King of Operation Ivy to the various structures, other than 3.1.1, located on the islands of the Enlwetok Atoll (Fig. 3.1) was observed and recorded. The structures consisted of heavily reinforced concrete shelters, both buried and above ground, air-blast and thermal measuring and recording stations, lightly constructed wood and metal timing shacks, and other miscellaneous items.

The damage observations were of a visual nature. Detailed measurements were made for only two structures, where it appeared that it might be possible to analyze their dynamic behavior. One of these was an overturned blast wall used in previous tests to house blast-measuring instruments. A simple overturning analysis of this structure is contained in Appendix F. Photographs were obtained of all significant damage.

Because there were two atomic bursts at different points in Operation Ivy, there was an overlap of the air-blast effects at some locations. In some cases the blast-wave overpressures from one shot were insignificant compared to the overpressures from the other shot. In these cases it was apparent that the larger overpressure caused the observed damage. At other locations the overpressures from both shots were of the same order of magnitude; in these cases the observed damage would probably not have been caused by the observed overpressure from only one of the shots. The tabulation of the observed structural damage, Table 3.1, lists the distances of each structure from the Ground Zeros for both the Mike and King shots with the corresponding air-blast overpressures for each. A brief description of the structure and the damage caused to it is also given, along with references to the photographs and plans.

The localities of the structures with respect to the Ground Zeros for the two atomic bursts were obtained from maps in reference 17. In many cases the location of the structure on the map was not given and had to be estimated. The overpressures corresponding to the distances thus determined were obtained from overpressure curves in reference 2.

A summary of general damage observations made as a result of the damage survey is contained in Sec. 3.2.

3.2 SUMMARY OF GROSS-DAMAGE OBSERVATIONS

The gross damage observed at various points caused by shots Mike and King of Operation Ivy may be summarized as follows:

1. All reinforced-concrete semiburied instrumentation shelters appeared to have performed their function satisfactorily without exhibiting any primary structural failures.

2. Of the many one-story reinforced-concrete surface and semiburied structures observed, none were badly damaged. The only serious structural failures observed were confined to wing

walls designed to retain portions of the fill on the semiburied structures. These structures were exposed to overpressures of 11 psi and greater.

3. Small buildings covered with thin sheet metal over diagonal wood sheathing generally withstood overpressures up to 5 and 6 psi. However, one structure of this type was observed badly damaged by an overpressure of 4 ½ psi.

4. Lightly constructed wood-frame shacks apparently sheathed only with corrugated metal and located in regions with overpressures greater than 4 psi were completely destroyed. No structures of this type were observed in regions subjected to less than 4 psi overpressure.

5. Palm trees were destroyed by air-blast overpressures of 4 to 5 psi and greater, but none were destroyed by overpressures less than 4 psi.

Table 3.1 — GROSS-DAMAGE OBSERVATIONS

Site	Description	Figure	Damage	Air-blast intensity			
				Mike		King	
				Distance from G. Z., ft	Over-pressure, psi	Distance from G. Z., ft	Over-pressure, psi
Alice	Station 300: massive reinforced-concrete above-ground structure; walls and roof 5 ft thick with 1¼% reinforcement in two directions; clear span of roof 12 ft; 12-in.-thick retaining wall reinforced with ¾-in.-diameter bars at 12 in. center to center in each face in two directions	3.2 to 3.12	Wing wall adjacent to rear of structure moved 2 to 3 in.; reinforcement exposed and concrete spalled at top of wall, no major structural damage	17,500	17	77,300	0.25
Belle	No structure	3.13, 3.14	All trees blown away	13,400	25	75,200	0.25
Clara	— Station 220: massive reinforced-concrete semi-buried structure; walls and roof 4 ft thick with 1¼% reinforcement in each face in two directions, clear span of roof 6 ft; earth-fill cover 4 ft deep	3.15 to 3.24	Top of retaining wall at rear of structure collapsed, no major damage	7,100	74*	71,900	0.3
Irene	— Station 200: massive reinforced-concrete semi-buried structure; walls 4 ft thick; roof 3 ft thick, wall reinforcement ½% vertical and 1¼% horizontal in each face, roof slab reinforced with steel I-beams over 14, 12, and 9 ft clear spans, earth fill cover 2 ft deep	3.25 to 3.35	Heavy concrete wall with pipe inserts at front of structure was badly dented, in rear of structure a heavy steel beam on roof was bent through 180°, a retaining wall was separated from structure but not severely damaged; no major structural damage	8,600	52*	63,600	0.35
Janet	— Structure 3.1.2: Army semi-buried shelter	3.36 to 3.39	Structurally undamaged, surface on vent pipe charred on side facing G. Z.; doors removed prior to test; wood-frame air lock destroyed	17,060	16	54,600	0.42
	Structure 3.1.1: Army Test Structure	See Chap. 2	See Chap. 2	18,500	15	53,300	0.45
	Air-blast wall	3.40 to 3.42	Overturned on side exposing footing	18,450	15.5	52,400	0.48
Kate	Wood-frame shack sheathed with corrugated metal	3.43 to 3.48	Completely demolished down to foundation; generator blown 70 ft and overturned	21,300	12	48,200	0.5
Lucy	Time shack: 8½ ft by 12½ ft by 8½ ft high, 2 by 4 wood framing covered with corrugated aluminum roofing and siding	3.49	Completely demolished	24,000	9.4	46,300	0.55
Sand bar between Lucy and Mary	Aluminum sheathed thermal station on cylindrical pentcone	3.50, 3.51	Front pentcone flattened by blast, front aluminum covering scorched by thermal radiation; exposed wood scorched	27,400	7.1	42,400	0.6
Mary	Station 600: reinforced-concrete structure, walls and roof 1 ft thick with ¾% main reinforcement for 8 ft clear span	3.53 to 3.54	No damage				
	Several small wood buildings covered with thin sheet metal over diagonal wood sheathing	3.54 to 3.56	One building destroyed; others damaged	31,000	5.8	39,300	0.7
	Photographic tower	3.54	Destroyed				
	Trees	3.54 to 3.56	Destroyed				
Nancy	Trees	3.57	7 trees remaining; numerous trunks and stumps	34,300	4.8	38,300	0.8

Table 3.1—(Continued)

Site	Description	Figure	Damage	Air-blast intensity: Mike Distance from G. Z., ft	Mike Overpressure, psi	King Distance from G. Z., ft	King Overpressure, psi
Vera	Trees	3.58	Numerous trees undamaged	55,200	2.0	17,900	8.6
Wilma	Trees	3.59 to 3.62	No trees remaining				
	Sheet metal and diagonal wood sheathed building at north end of island	3.60	No damage				
	Corrugated-metal shack at east center of island	3.58, 3.60	Collapsed onto foundation	57,300	1.9	13,400	4.5
	Sheet metal and diagonal wood sheathed building at west end of island	3.60, 3.61	Roof and one side destroyed				
	Sheet metal and diagonal wood sheathed building at south end of island	3.58 to 3.62	Moderate damage	57,300	1.9	13,400	4.5
Yvonne	Station 208: reinforced concrete semiburied structure; walls and roof 1 ft 2 in. thick with 1% main reinforcement for 13 ft clear span; no earth cover over roof	3.64 to 3.66	Wood parapet and sandbags blown over entrances, no damage to concrete structure				
	Heavy concrete structure at center of island	3.63	Pipe and brackets bent; no damage to concrete structure	73,500	1.35	8,500	18
	Station 605: reinforced-concrete structure; walls and roof 1 ft 3 in. thick with 1% main reinforcement for 11 ft clear span	3.67 to 3.69	No damage				
	Wood-pile pier	3.70 to 3.72	Deck of pier destroyed				
	Telephone station 200 ft north of airstrip, heavy concrete structure	3.73	No damage				
	Station 307: reinforced concrete semiburied structure; walls and roof 1 ft 2 in. thick with 1% main reinforcement for 9 ft clear span; earth cover 2 ft thick over roof	3.74 to 3.76	12-in. pipe outlet bent; no damage to concrete structure				
Bruce	Station 604: wooden structure (tower at north end of island; wooden tub on 23 ft by 13 ft by 9 ft high supported with top 35 ft above grade on four 10 by 10 wooden bents, chain sheathed with two layers of 1-in. diagonal wood sheathing	3.77 to 3.81	No damage	103,000	0.76	37,300	0.73
	Palm groves.		No damage				
David	Miscellaneous wood structures	3.82 to 3.84	No damage	112,100	0.64	50,500	0.47
	Palm groves		No damage				
Elmer	Miscellaneous corrugated-metal structures	3.85, 3.86	Minor damage	117,000	0.58	58,300	0.39
Mack	Station 803: exposed concrete pier with wood deck, wood tubing shack with 2 in. by 6 in. framing members sheathed with ¼-in. plywood	3.87 to 3.89	No damage	48,100	2.5	35,400	0.78

* Estimated.

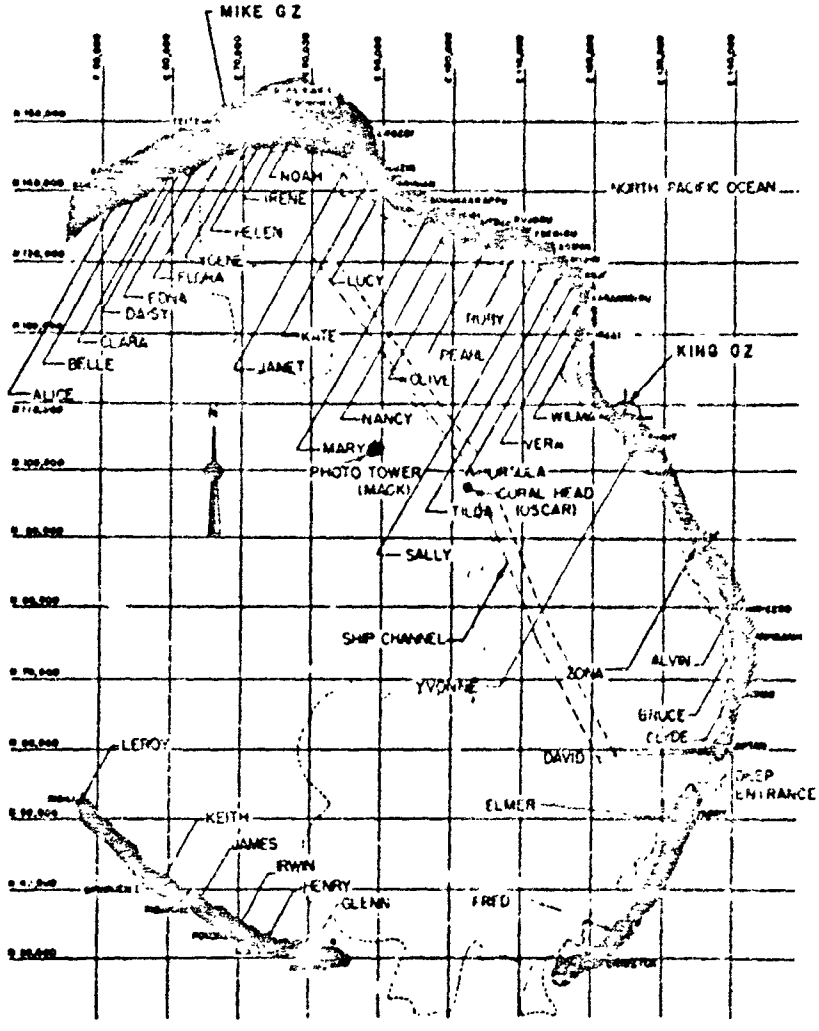

Fig. 3.1—Enlwetok Atoll.

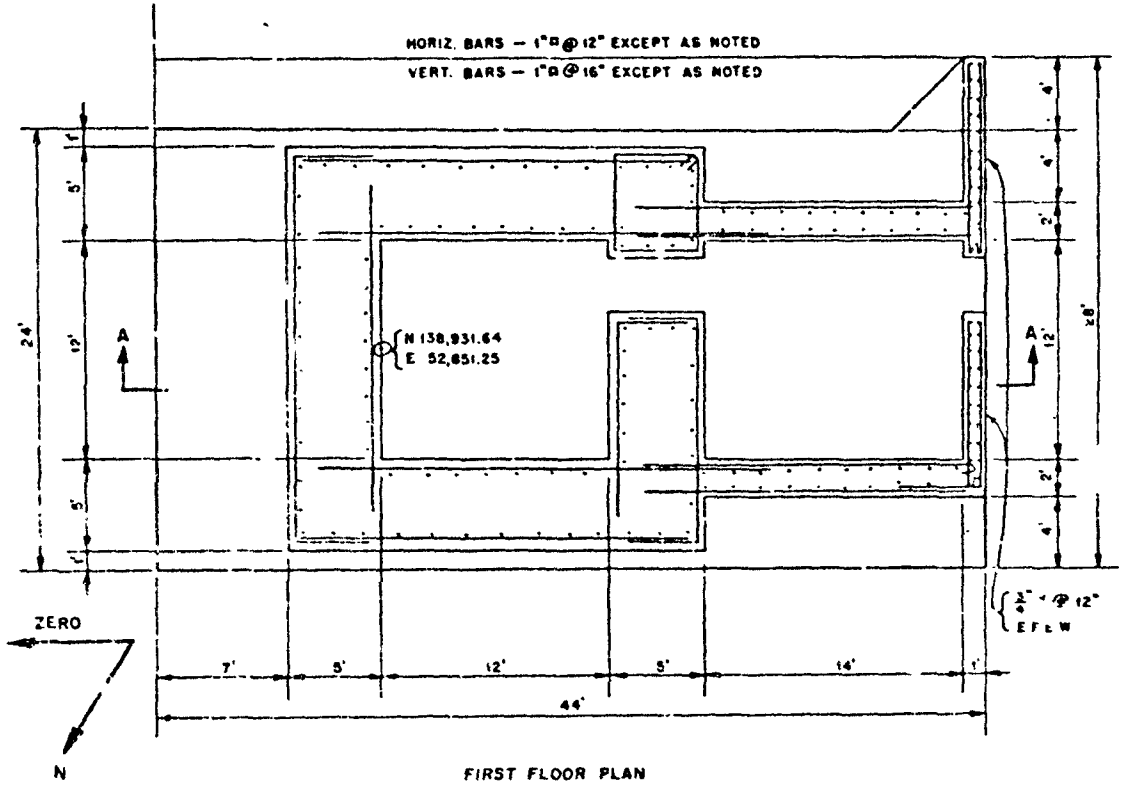

FIRST FLOOR PLAN

Fig. 3.2—General details, Station 300 on Alice. Pressure levels: Mike, 17 psi; King, 0.25 psi.

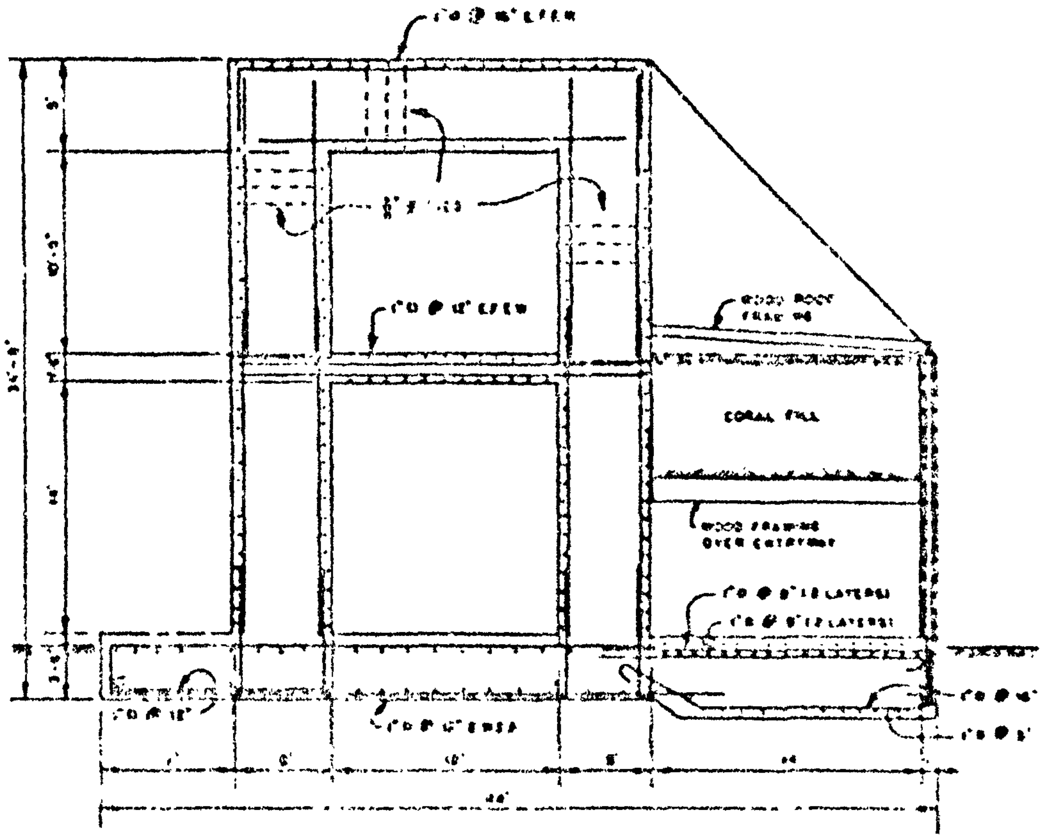

Fig. 3.3—General details, Station [illegible] on Alice. Pressure levels: Mike, 17 psi, King, [illegible] psi

Fig. 3.4 — Pretest, Station 9.0 on Alice. Mike Ground Zero is to right of camera. Note wing wall on near side at rear of structure (left side of passageway). Pressure levels: Mike, 17 psi; King, 0.25 psi.

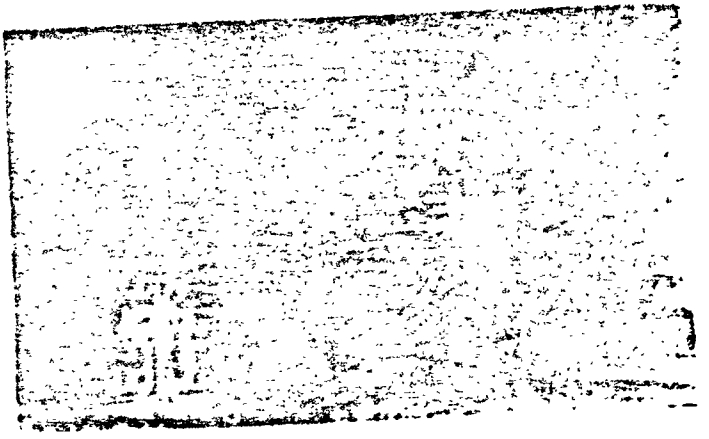

Fig. 3.5 — Pretest, Station 3.0 on Alice. Note main beams on roof of structure. Pressure levels: Mike, 17 psi; King, 0.25 psi.

Fig. 3.6—Precast, roof of Station 300 on Alice. Note steel beams and instrumentation attached to roof. Camera is pointed in general direction of Mike Ground Zero. Pressure levels: Mike, 17 psi; King, 0.25 psi.

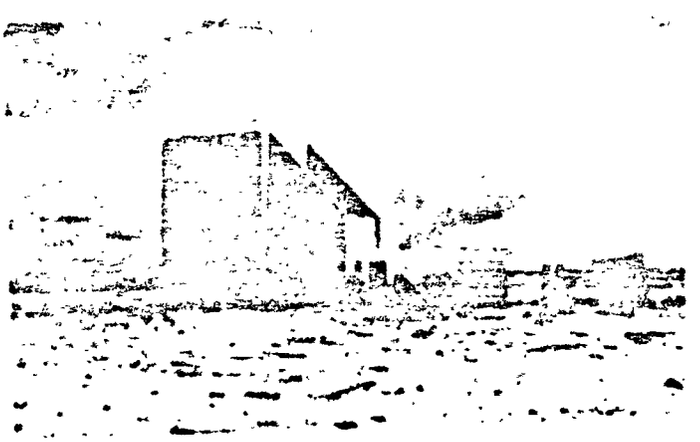

Fig. 3.7—Fourteen, Station 300 on Alice. Mike Ground Zero is located to left of camera. Note large open vertical crack at top of wing wall where it joins main body of structure. Pressure levels: Mike, 17 psi; King, 0.25 psi.

Fig. 3.8—Postcast, Station 300 on Alice. Aerial view showing roof with steel beams and exposed instrumentation destroyed. Pressure levels: Mike, 17 psi; King, 0.25 psi.

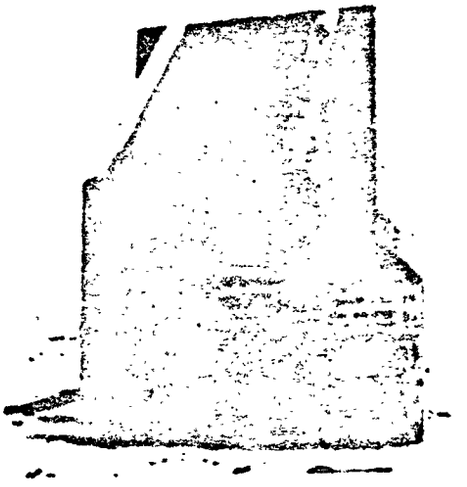

Fig. 3.9—Postcast, Station 300 on Alice. Camera facing Mike Ground Zero. Note attempts to repair top of damaged wing wall with grout. Pressure levels: Mike, 17 psi; King, 0.25 psi.

Fig. 3.10—Postest, Station 300 on Alice. Camera facing Mike Ground Zero. Note attempt to repair top of damaged wing wall with grout. Pressure levels: Mike, 17 psi; King, 0.75 psi.

Fig. 3.11—Postest, Station 300 on Alice. Camera facing away from Mike Ground Zero. Note damaged wing wall in background. Pressure levels: Mike, 17 psi; King, 0.25 psi.

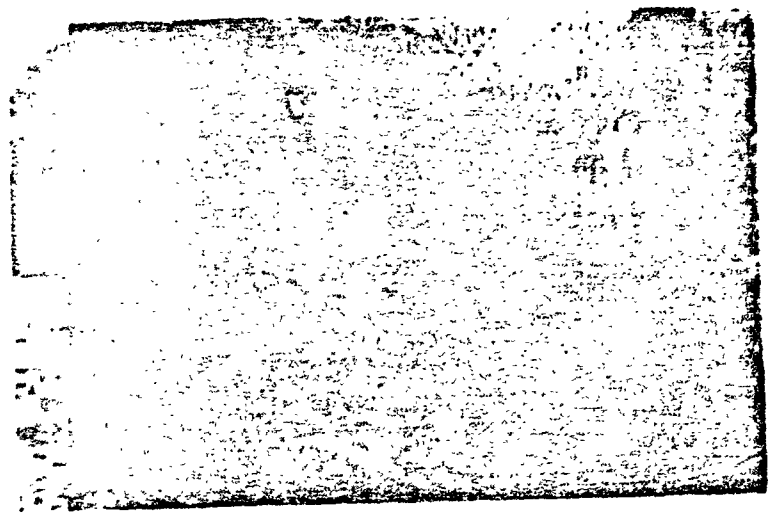

Fig. 3.12 — Postshot, damaged wing wall of Station 900 on Aleng. Camera facing away from Mike Ground Zero. Note diagonal cracks and grouting of cracks along base of wing wall. Pressure levels: Mike, 17 psi; King, 0.25 psi.

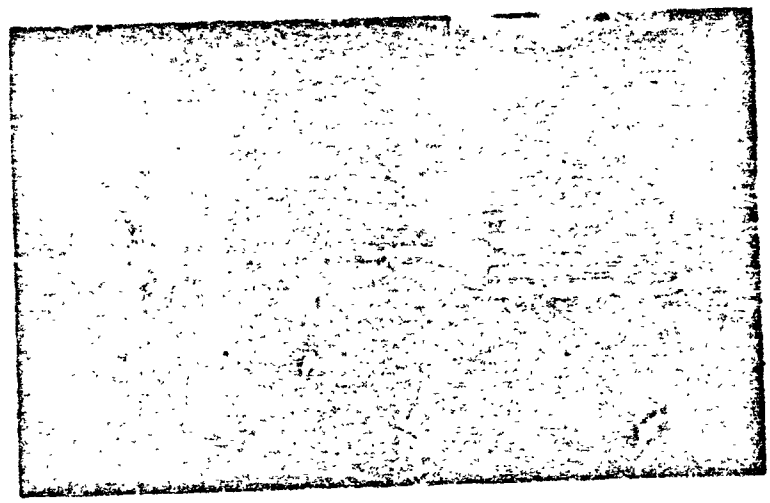

Fig. 3.13 — Postshot, Belle. Mike Ground Zero to right of camera. Note that all trees and vegetation have been burned or blown off island. Pressure levels: Mike, 25 psi; King, 0.25 psi.

Fig. 3.14—Fortress, Belle. Camera facing away from Mike Ground Zero. Note coarse vegetation and absence of trees. Pressure levels: Mike, 25 psi; King, 0.25 psi.

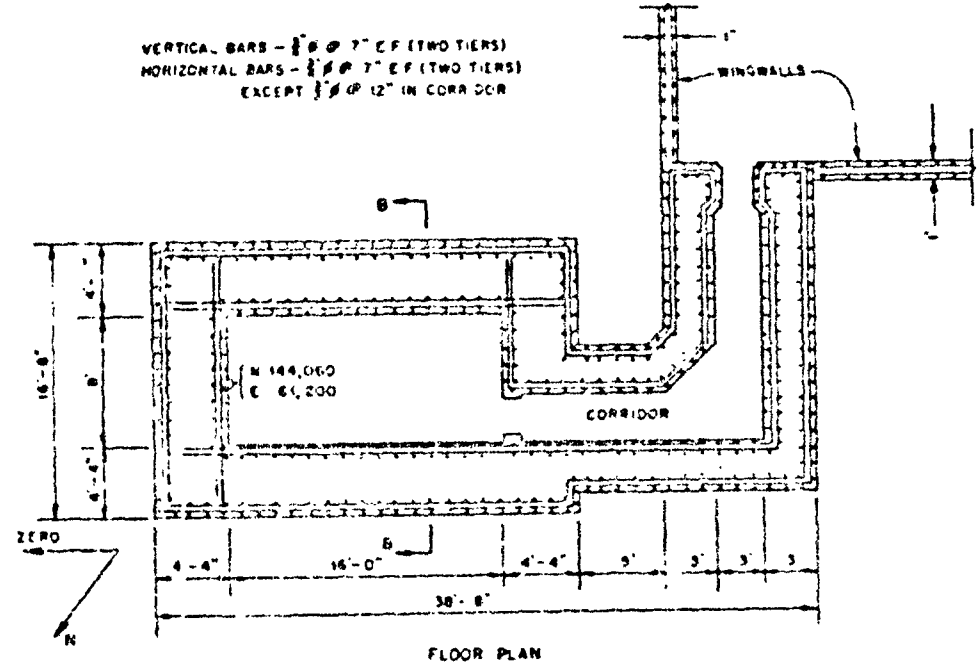

Fig. 3.18—General details, Station 320 on Clara. Pressure levels: Mike, 74 psi; King 3.3 psi.

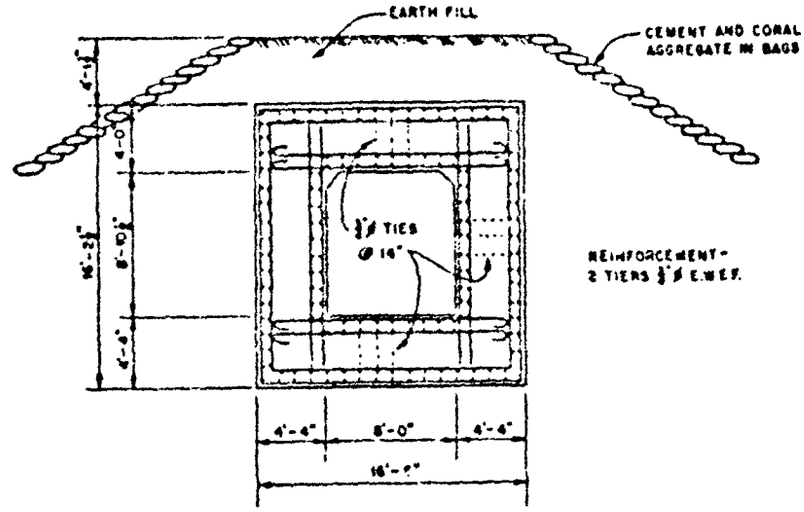

SECTION B-B

Fig. 9.18—General details, Station 520 on Clara. Pressure levels: Mike, 74 psi; King, 0.5 psi.

Fig. 3.17— Pretest, Station 820 on Clara. Mike Ground Zero to right of camera. Pressure levels: Mike, 74 psi; King, 0.3 psi.

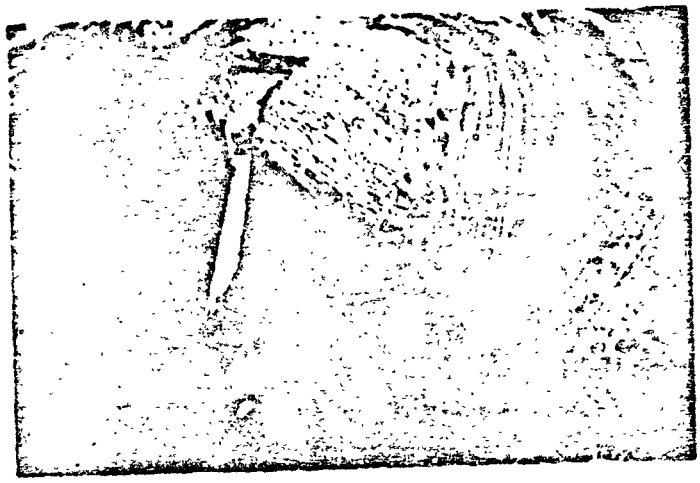

Fig. 3.18— Pretest, Station 820 on Clara. Camera facing in general direction of Mike Ground Zero. Note instrumentation cabinet on concrete platform above doorway. Pressure levels: Mike, 74 psi; King, 0.3 psi.

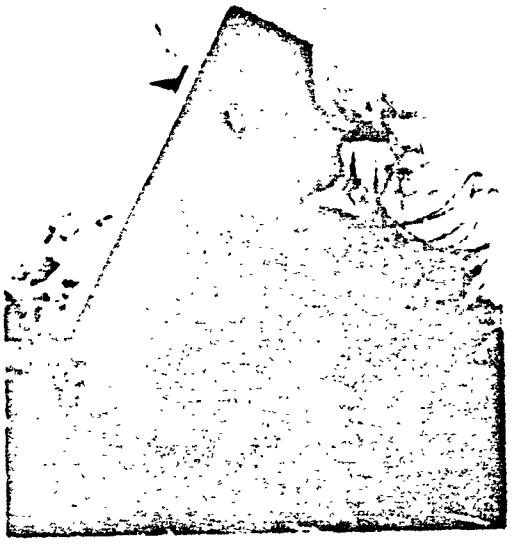

Fig. 3.19—Posttest, Station 520 on C'lara. Note failures of wing wall and of concrete platform behind undamaged wall. Pressure levels: Mike, 74 psi; King, 0.3 psi.

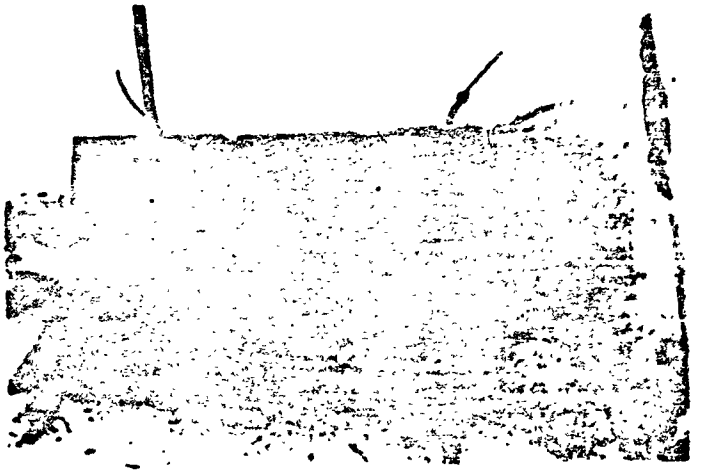

Fig. 3.20—Posttest, Station 520 on Clara. Note failure of concrete platform behind undamaged wing wall. Pressure levels: Mike, 74 psi; King, 0.3 psi.

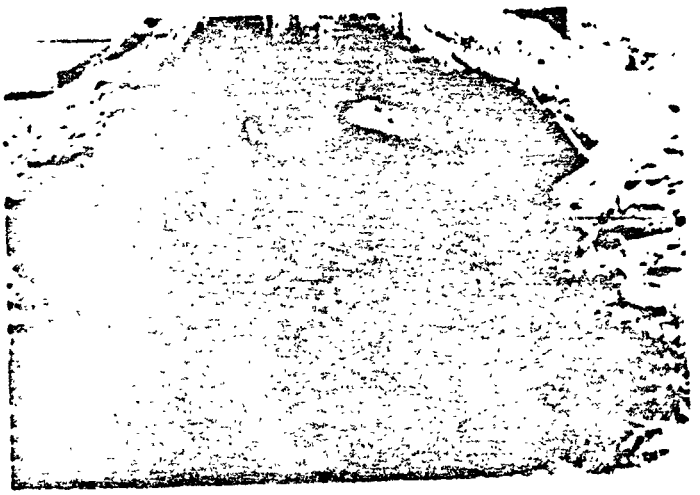

Fig. 3.21—Posttest, Station 520 on Clara. Note damaged retaining wall. Pressure levels: Mike, 74 psi; King, 0.3 psi.

Fig. 3.22—Posttest, Station 520 on Clara. Close-up of damaged retaining wall. Pressure levels: Mike, 74 psi; King, 0.3 psi.

Fig. 3.23—Posttest. Station 520 on Clara. Close-up of damaged instrumentation. Camera facing away from Mike Ground Zero. Pressure levels: Mike, 74 psi; King, 0.3 psi.

Fig. 3.24—Posttest. Station 520 on Clara. Mike Ground Zero to right of camera. Note flowed and eroded appearance of the earth cover on the structure. Pressure levels: Mike, 74 psi; King, 0.3 psi.

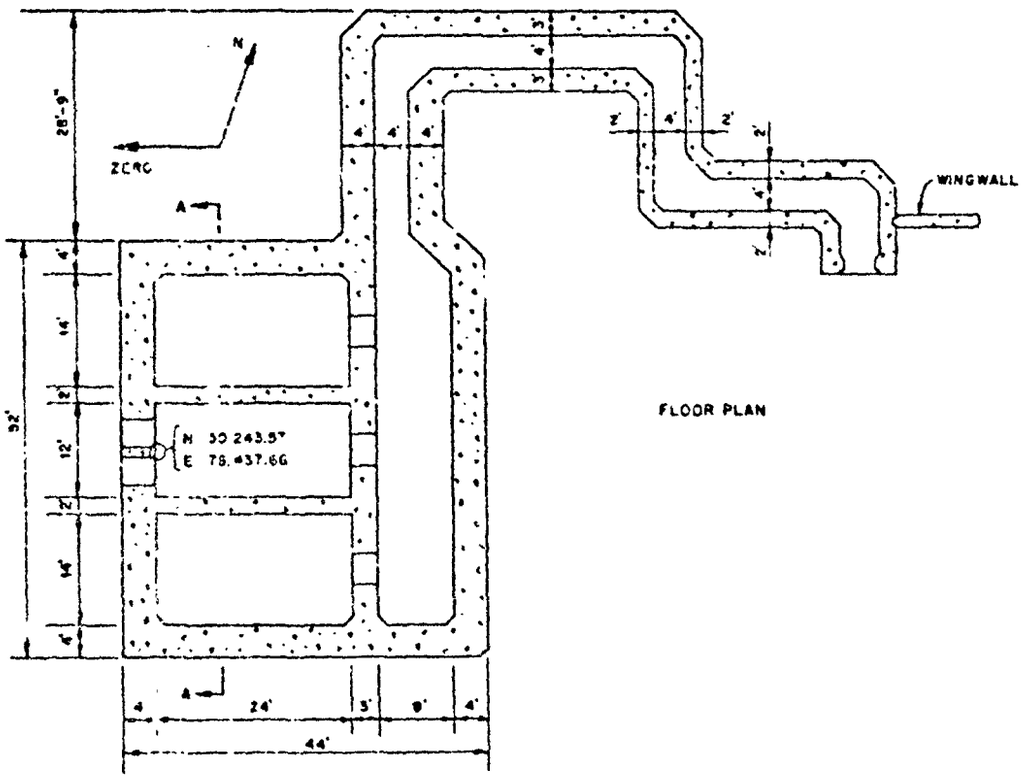

Fig. 3.28—General details, Station 200 on Irene. Pressure levels: Mike, 52 psi; King, 0.35 psi.

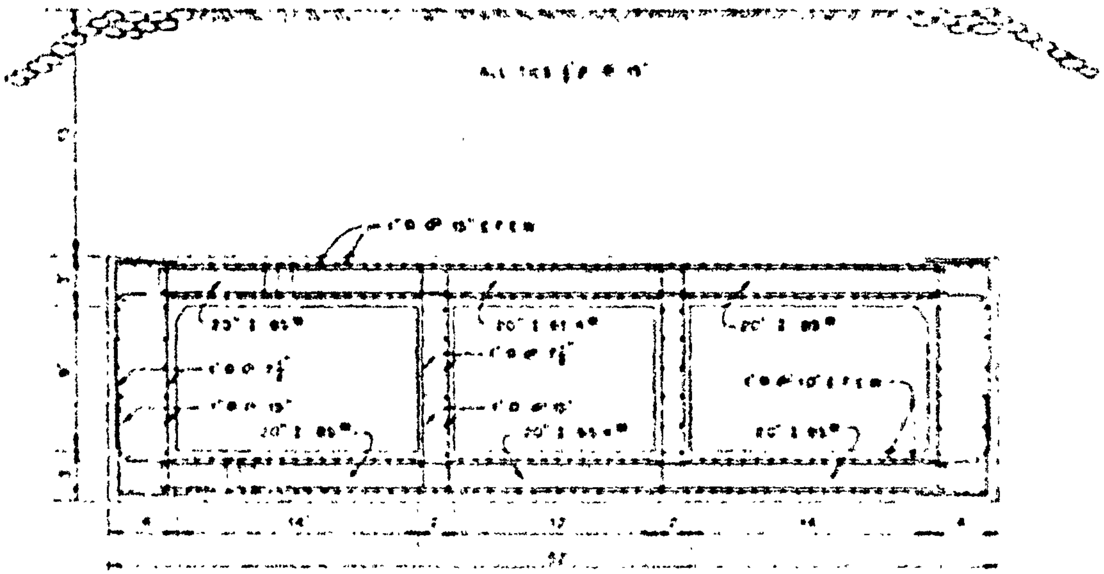

SECTION A-A

Fig. 3.[illegible]—General details, Station [illegible] on [illegible]. Pressure levels: [illegible]

Fig. 3.27—Project. Station 300 on Irene. Camera facing Mike (ground zero distance to structure on near side). Pressure levels: Mike, 32 psi; King, 9.35 psi.

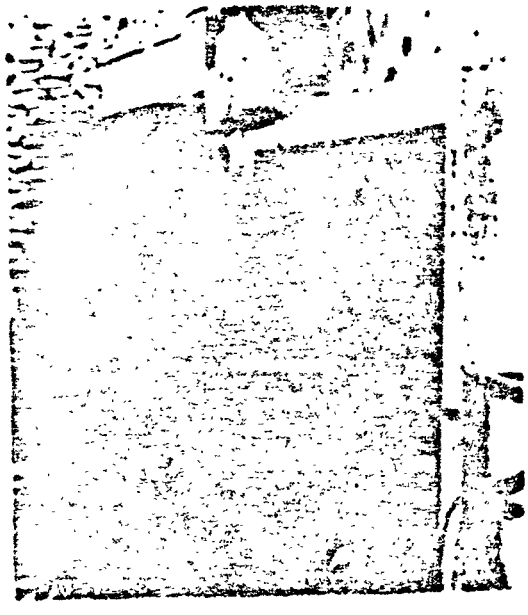

Fig. 3.28—Project. Station 200 on Irene. Close-up of doorway in rear of structure. Pressure levels: Mike, 32 psi; King, 9.35 psi.

Fig. 3.29— Position. Station 250 on brace. Mike Ground Zero to left of camera. Nose front of structure at left and entranceway at rear. Pressure levels: Mike, 52 psi; King, 0.50 psi.

Fig. 3.30— Position. Station 250 on brace. Entranceway to rear of structure. Pressure levels: Mike, 52 psi; King, 0.55 psi.

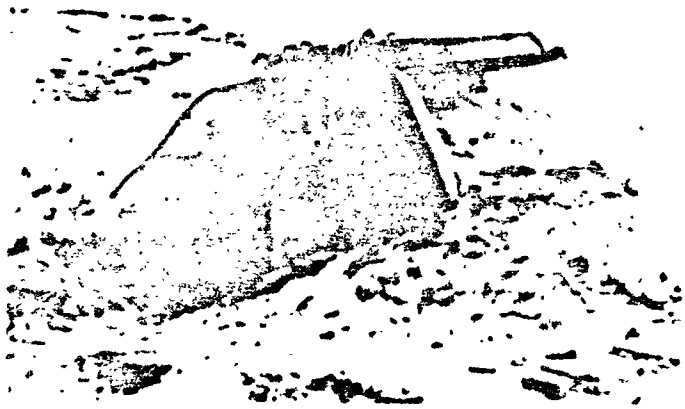

Fig. 3.31 — Portent, Station 300 m Irene. Close-up of entranceway, [illegible] steel beam, damaged wing wall, and hole cut in door to gain access to structure. Pressure levels: Mike, 52 psi, King, 0.35 psi.

Fig. 3.32 — Portent, Station 300 m Irene. Close-up of entranceway. Pressure levels: Mike, 52 psi; King, 0.35 psi.

Fig. 3.33—Postcut, Station 200 on Irene. Camera facing away from Mike Ground Zero. Pressure levels: Mike, 52 psi; King, 0.35 psi.

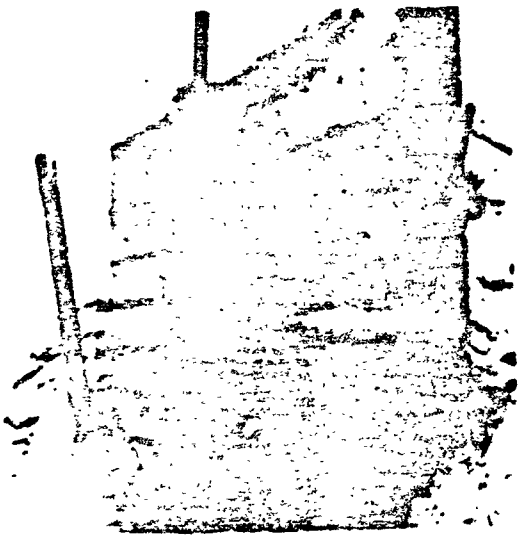

Fig. 3.34—Postcut, Station 200 on Irene. Close-up of post facing Mike Ground Zero. Pressure levels: Mike, 52 psi; King, 0.35 psi.

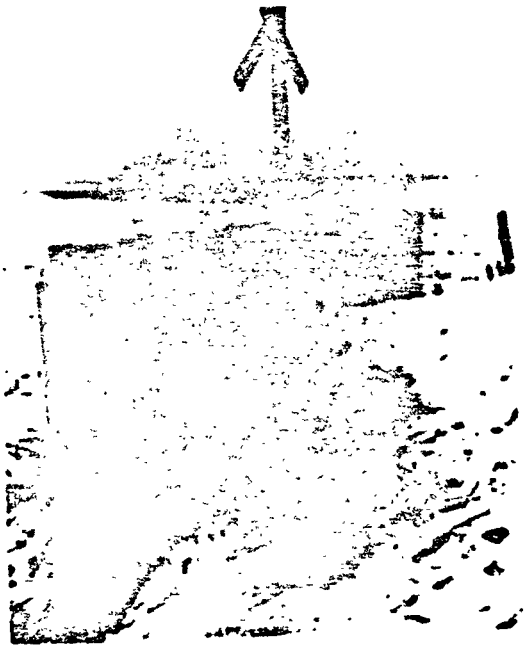

Fig. 3.35 — Portent, Station 200 on frame. Close-up of b[illegible] on wall supporting parts in front of structure. Pressure levels: Mike, 82 psi; King, [illegible]

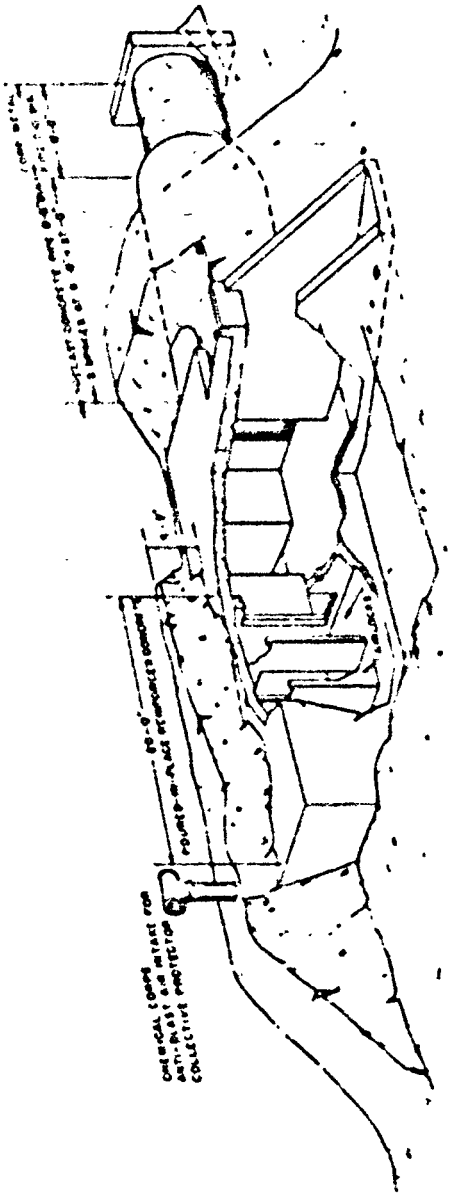

Fig. 3.36—Structure 3.1.3 on Johnston Atoll, Army composite-type reinforced shelter.

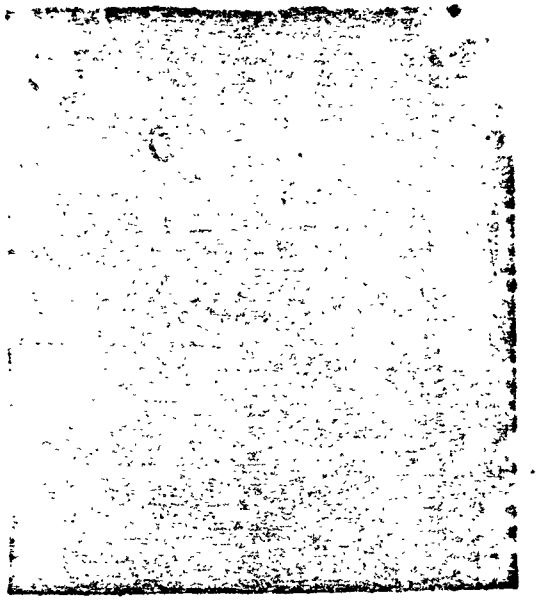

Fig. 3.37— Pootest. Structure 3.1.3 on Janet. Looking into rectangular portion of shelter. Note remnants of destroyed wooden air lock. Steel blast door removed prior to test. Pressure levels: Mike, 18 psi; King, 0.42 psi.

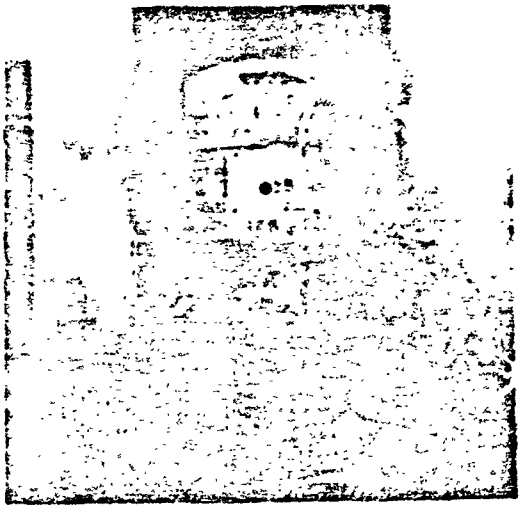

Fig. 3.38— Pootest. Structure 3.1.3 on Janet. Entrance to circular shelter units. Note steel blast door removed prior to test. Pressure levels: Mike, 18 psi; King, 0.42 psi.

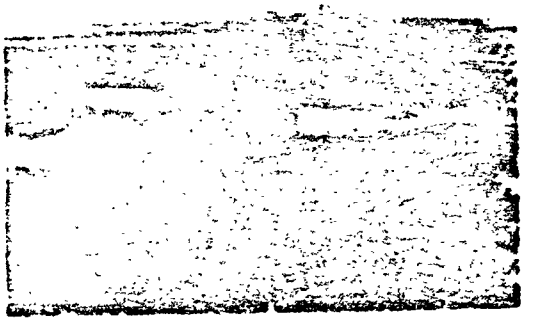

Fig. 3.39—Pretest, Structure 9.1.9 on Janet. Close-up of exhaust vent protruding from above fill over structure. Mike Ground Zero to left of camera. Note inclination of vent pipe away from Ground Zero and burned surface on side facing Ground Zero. Pressure levels: Mike, 18 psi; King, 0.42 psi.

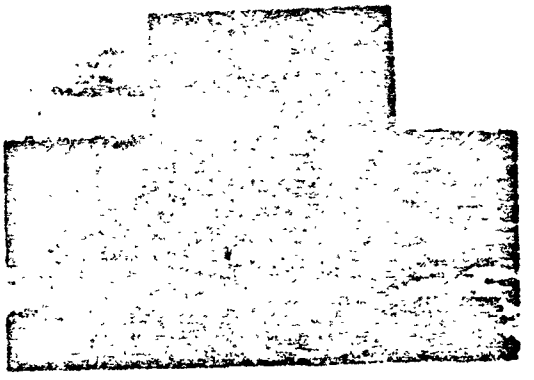

Fig. 3.40—Pretest, blast wall for mounting air-pressure instrumentation. Mike Ground Zero to left of camera. Pressure levels: Mike, 15.5 psi; King, 0.45 psi.

Fig. 3.41 — Postest, blast wall on Jemet. Camera facing in general direction of Mike Ground Zero. Pressure levels: Mike, 15.5 psi; King, 0.45 psi.

Fig. 3.42 — Postest, blast wall on Jemet. Mike Ground Zero to left of camera. Note completely exposed foundation. Pressure levels: Mike 15.5 psi; King, 0.45 psi.

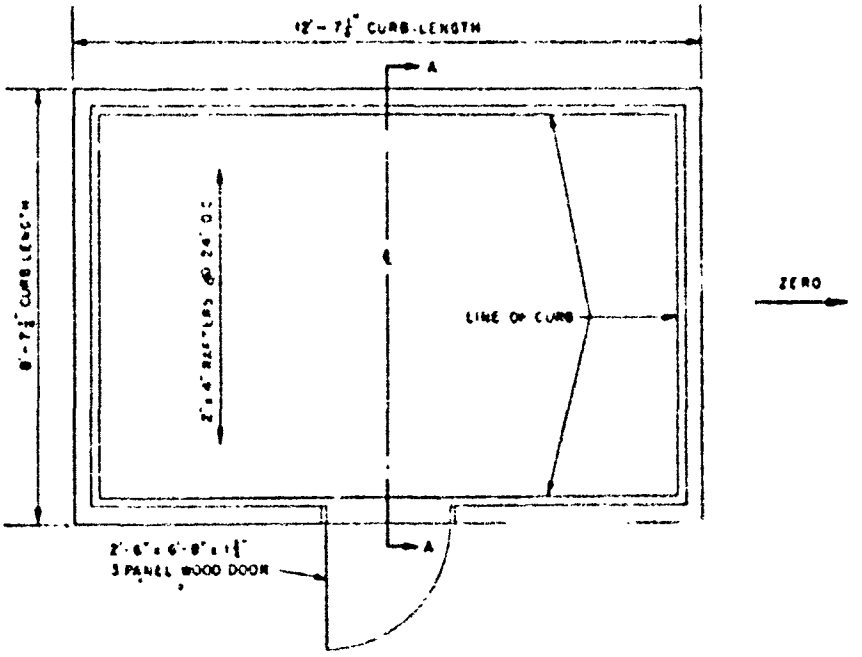

Fig 3.43 — General details of typical building No. 8.

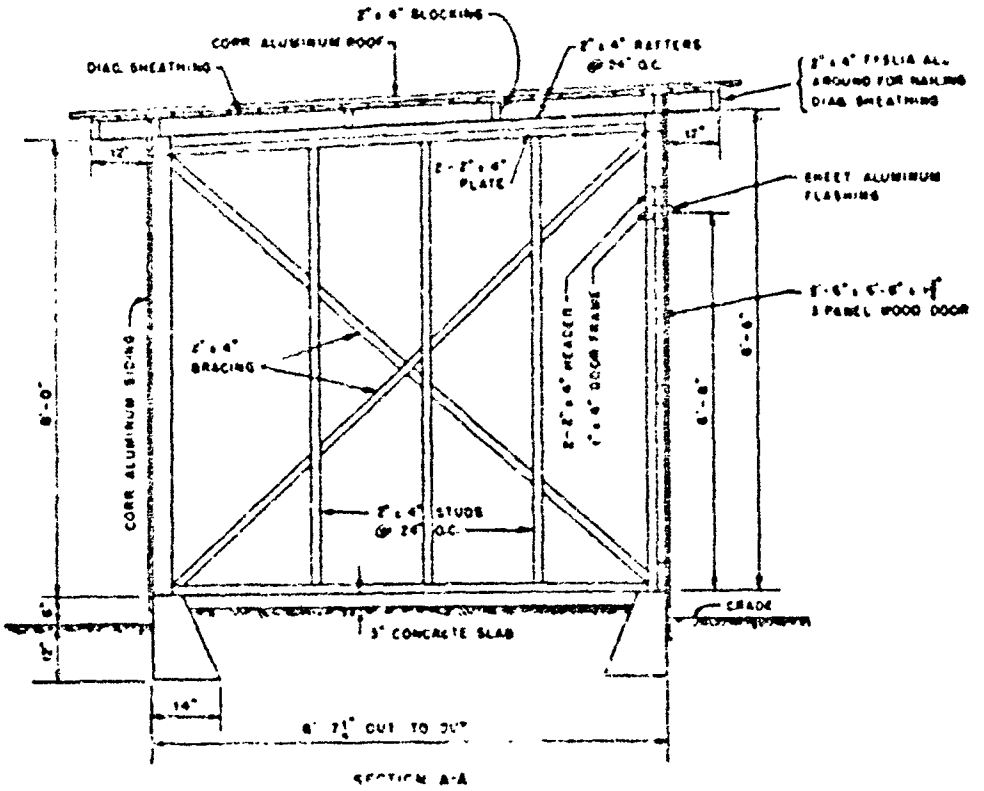

Fig. 3.44—General details of typical timing shack.

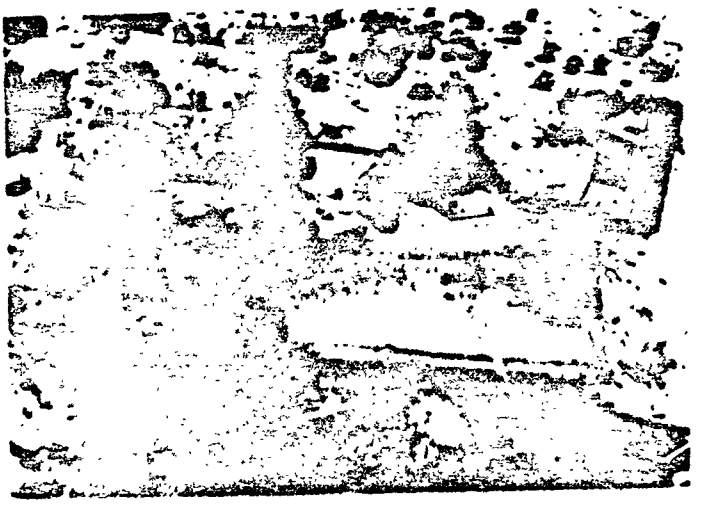

Fig. 3.45—Posttest, site of lightly constructed timing shack on Kate. Pressure levels: Mike, 12 psi; King, 0.5 psi.

Fig. 3.46—Posttest, generator of Kate blown 70 ft from site of timing shack. Camera facing Mike Ground Zero. Pressure levels: Mike, 12 psi; King, 0.5 psi.

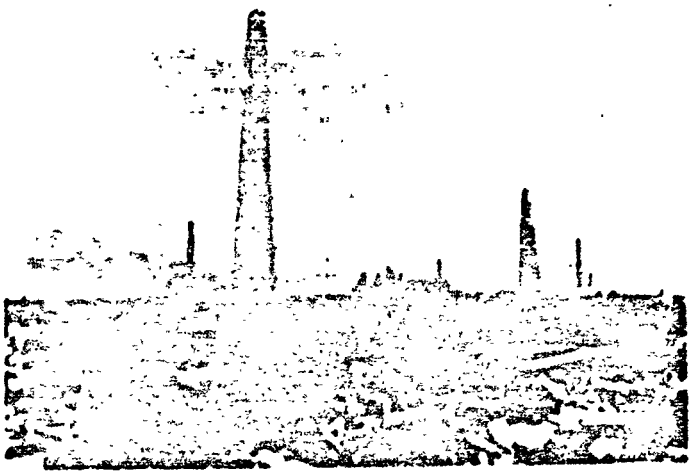

Fig. 3.47—Postest, instrumentation pylons on Kate. Three pylons still remain standing. Pressure levels: Main, 12 psi; King, 0.8 psi.

Fig. 3.48—Postest, instrumentation pylons on Kate. Pressure levels: Main, 12 psi; King, 0.8 psi.

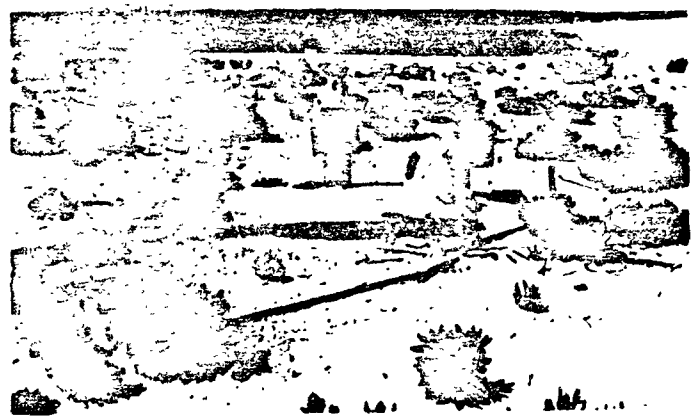

Fig. 3.49—Posttest, site of lightly constructed timing shack on Lucy. Shack was completely demolished by air blast. Pressure levels: Mike, 9.4 psi; King, 0.55 psi.

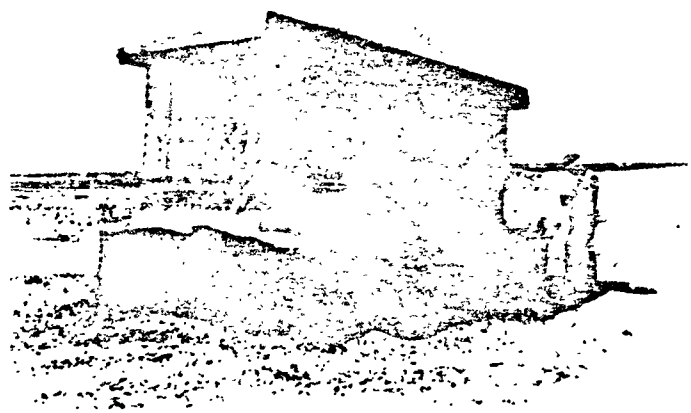

Fig. 3.50—Posttest, thermal station on sand bar between Lucy and Mary. Mike Ground Zero to right of camera. Note flattening of iron of round portions and the scorched surface of aluminum. Pressure levels: Mike, 7.1 psi; King, 0.6 psi.

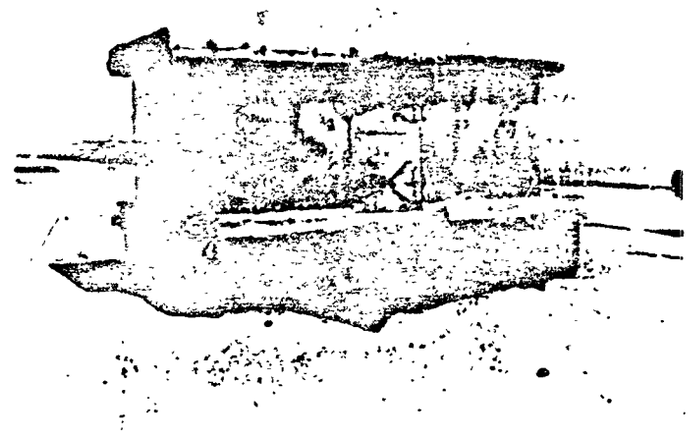

Fig. 3.61 — Posttest, thermal station on sand bar between Lucy and Mary. Mike Ground Zero to left of camera. Note damaged rear portions of structure. Pressure levels: Mike, 7.1 psi; King, 0.6 psi.

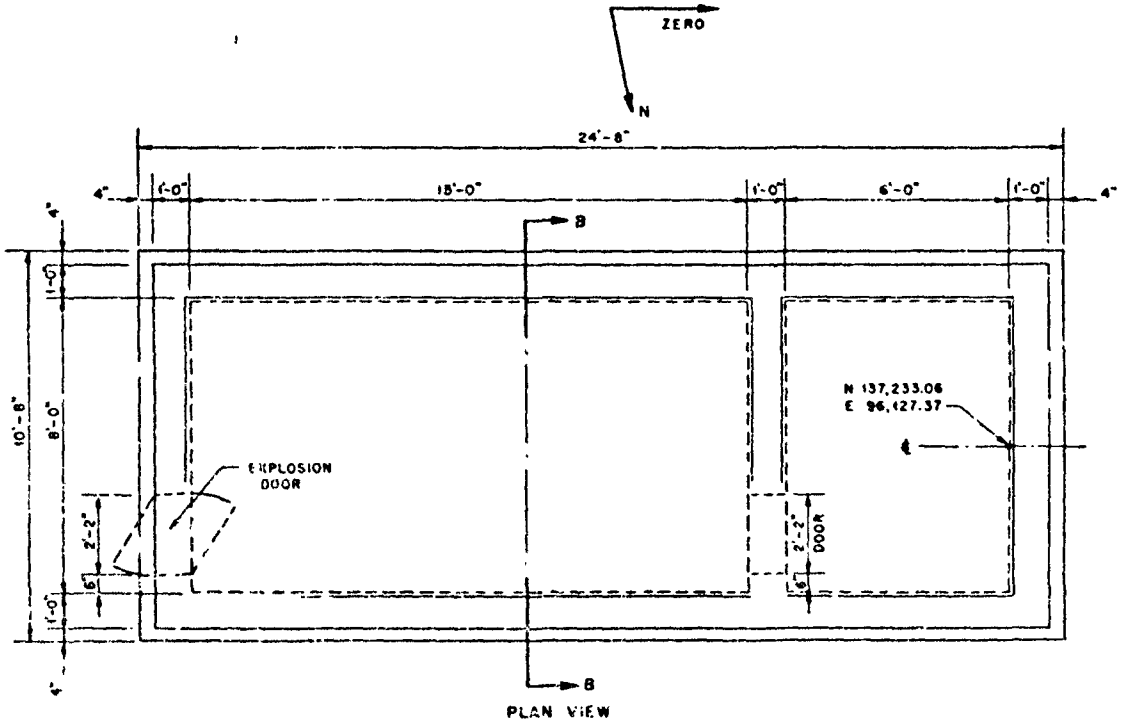

Fig 3.52—General details, Station 603 on Mary. Pressure levels: Mike, 5.6 psi; King, 0.7 psi.

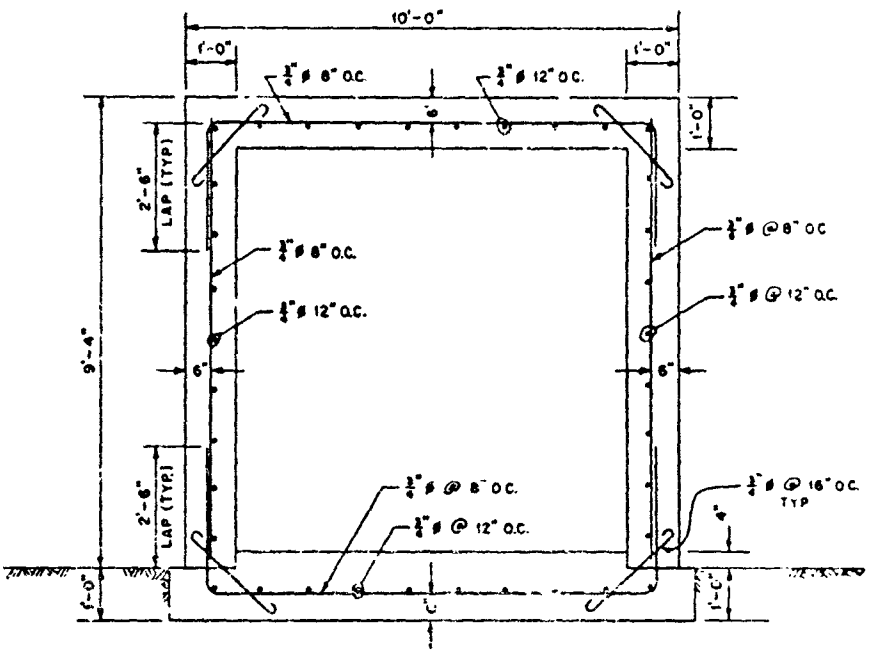

SECTION B-B

Fig. 3.53—General details Station 600 on Mary. Pressure levels: Mike, 5.6 psi; King, 0.7 ps.

Fig. 3.54—Posttest, Mary Mike Ground Zero to right of camera. Note destroyed photographic tower and numerous small wooden structures. Pressure levels: Mike, 5.6 psi; King, 0.7 psi.

Fig. 3.55—Posttest, Mary. Mike Ground Zero to left of camera. Site of destroyed timing shack near base of photographic tower. Pressure levels: Mike, 5.6 psi; King, 0.7 psi.

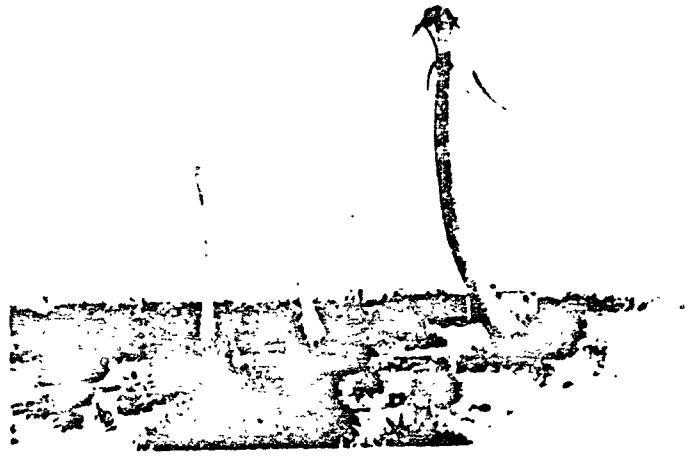

Fig. 3.56—Posttest, Mary. Facing toward Mike Ground Zero. Note remains of only trees left on island. Pressure levels: Mike, 5.6 psi; King, 0.7 psi.

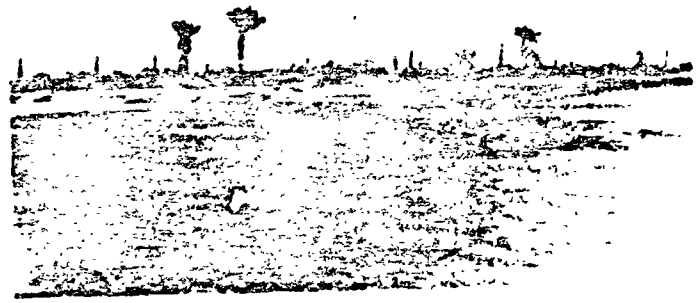

Fig. 3.57—Posttest, Nancy. Mike Ground Zero to left of camera. Note trees and vegetation on island. Pressure levels: Mike, 4.6 psi; King, 0.8 psi.

Fig. 3.58—Postest, Vera. Note trees and vegetation on island. Pressure levels: Mike, 2.0 psi; King, 2.6 psi.

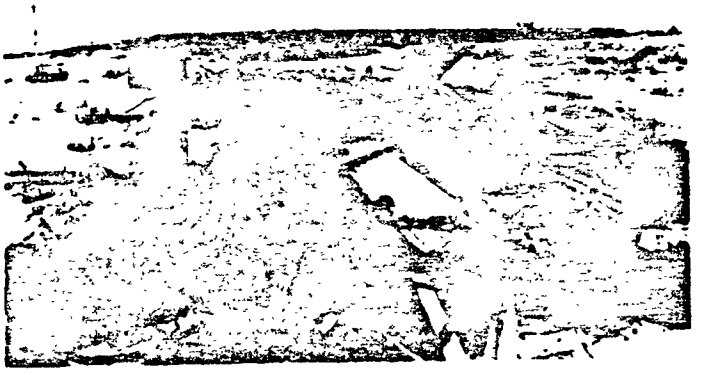

Fig. 3.59—Postest, Wilma. Timing shack on east center of island collapsed on foundation. Looking in southwestern direction. King Ground Zero to left. Pressure levels: Mike, 1.9 psi; King, 4.5 psi.

Fig. 3.60—Posttest, Wilma. Same location as Fig. 3.59 but looking northwest. King Ground Zero to left. Pressure levels: Mike, 1.9 psi; King, 4.5 psi.

Fig. 3.61—Posttest, Wilma. Recording station on west center of island. Note heavy construct[illegible] King Ground Zero to left. Pressure levels: Mike, 1.9 psi; King, 4.5 psi.

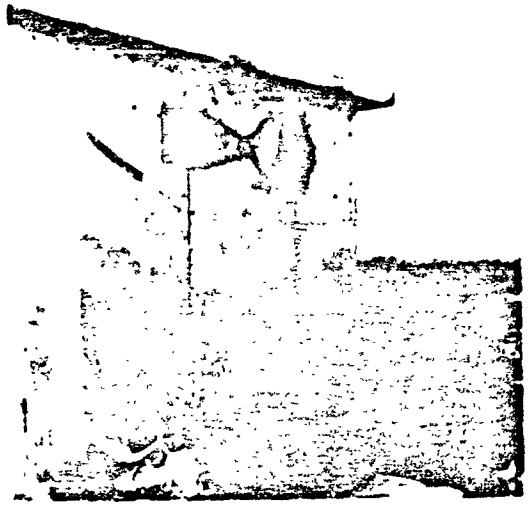

Fig. 3.62—Posttest, Wilma. Timing shack at south end of island. King Ground Zero to left of camera. Door damaged and jammed in 5 in. at base. Pressure levels: Mike, 1.9 psi; King, 4.5 psi.

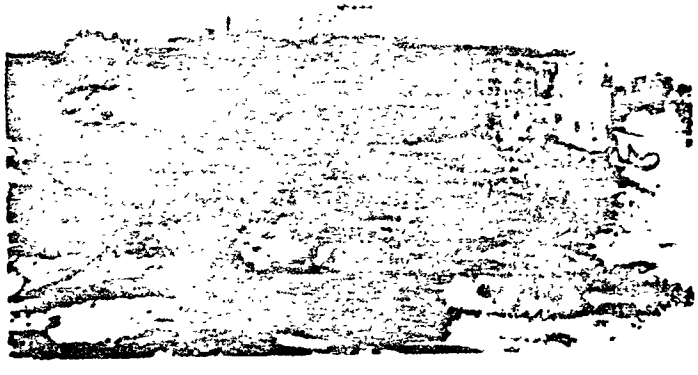

Fig. 3.63—Posttest, heavy concrete structure located about middle of Yvonne. Exterior pipe and brackets bent but no damage to concrete. King Ground Zero in left rear. Pressure levels: Mike, 1.35 psi; King, 18 psi.

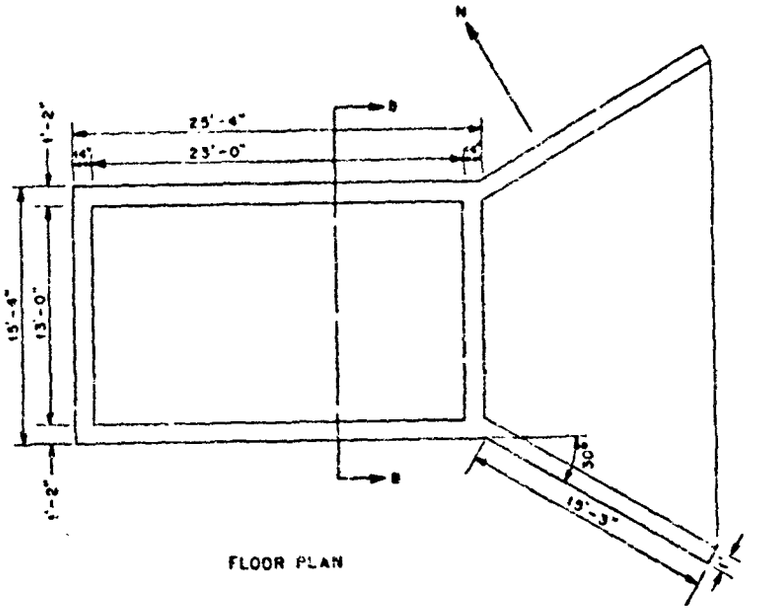

Fig. 3.64—General details, Station 252 on Yvonne. Pressure levels: Mike, 1.36 psi; King, 18 psi.

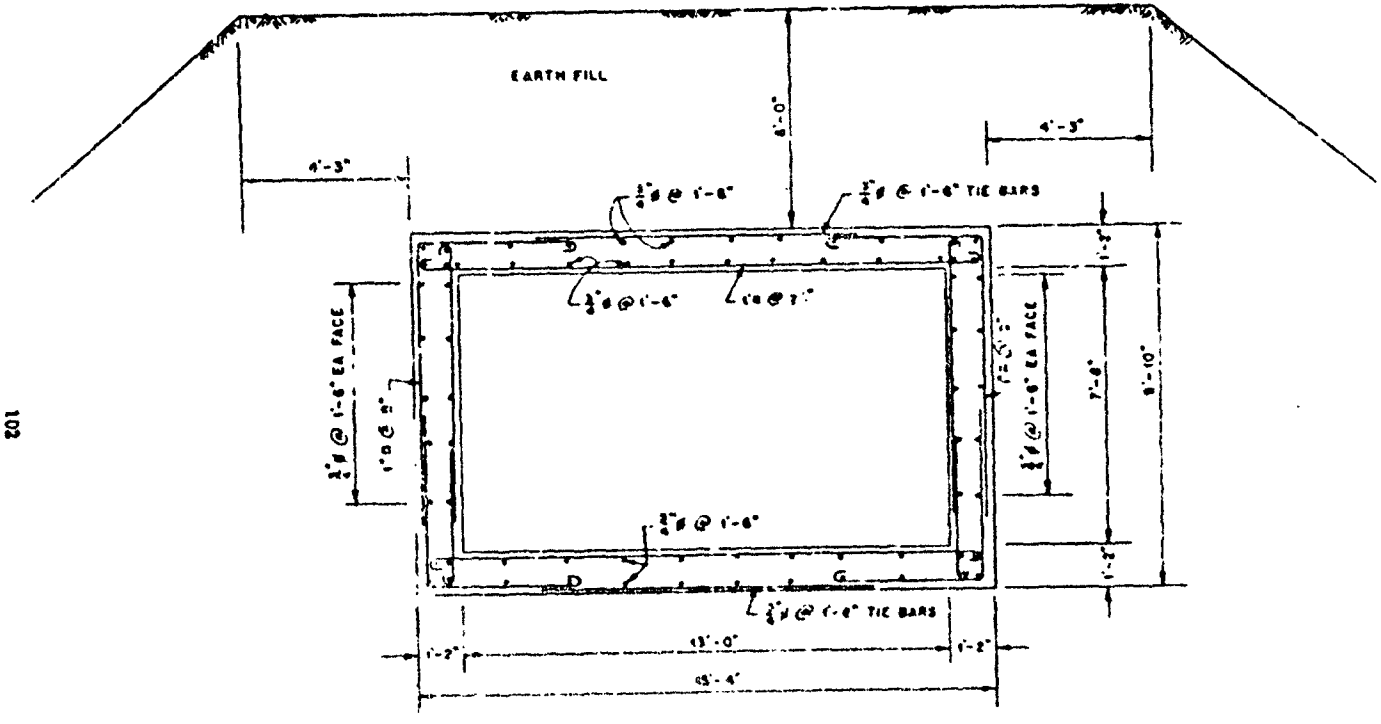

SECTION B-B

Fig. 3.66—General details, Station 252 on Yvonne. Pressure levels: Mike, 1.35 psi; King, 18 psi.

Fig. 3.68 — Poston, Station 282 on Yvonne. Wood parapet and sandbags blown over entrances. No damage to concrete. Camera facing toward King Ground Zero. Pressure levels: Mike, 1.35 psi; King, 15 psi.

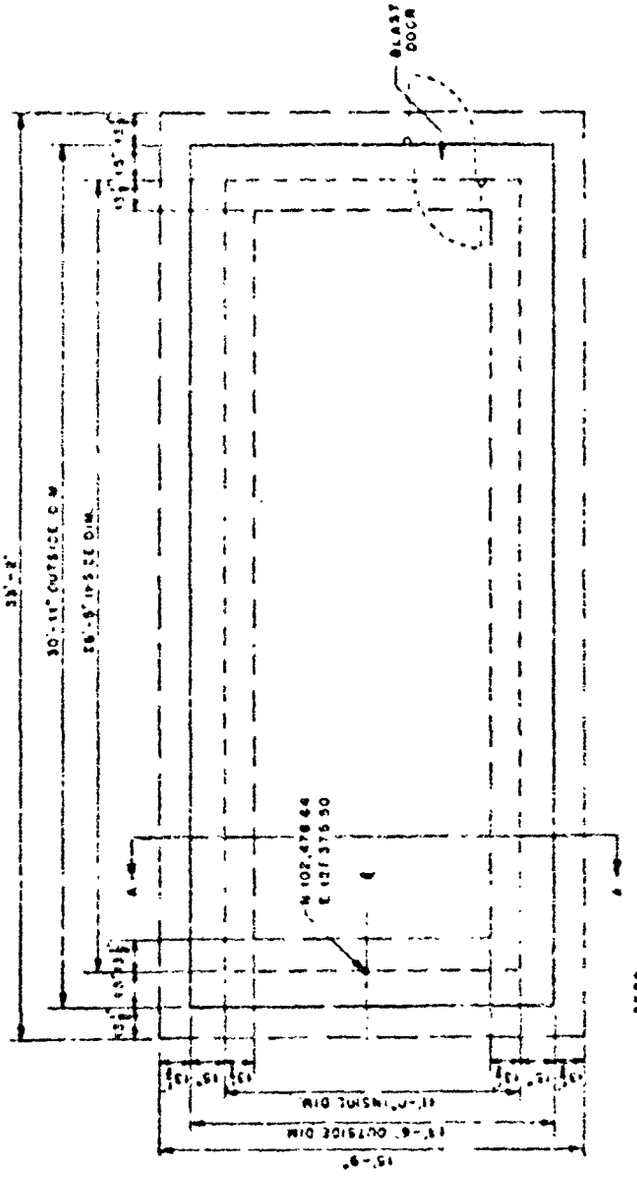

Fig. 3.37—General Details, Station 600 on Tracks. Pressure levels: Mike, 1.35 psi; King, 10 psi.

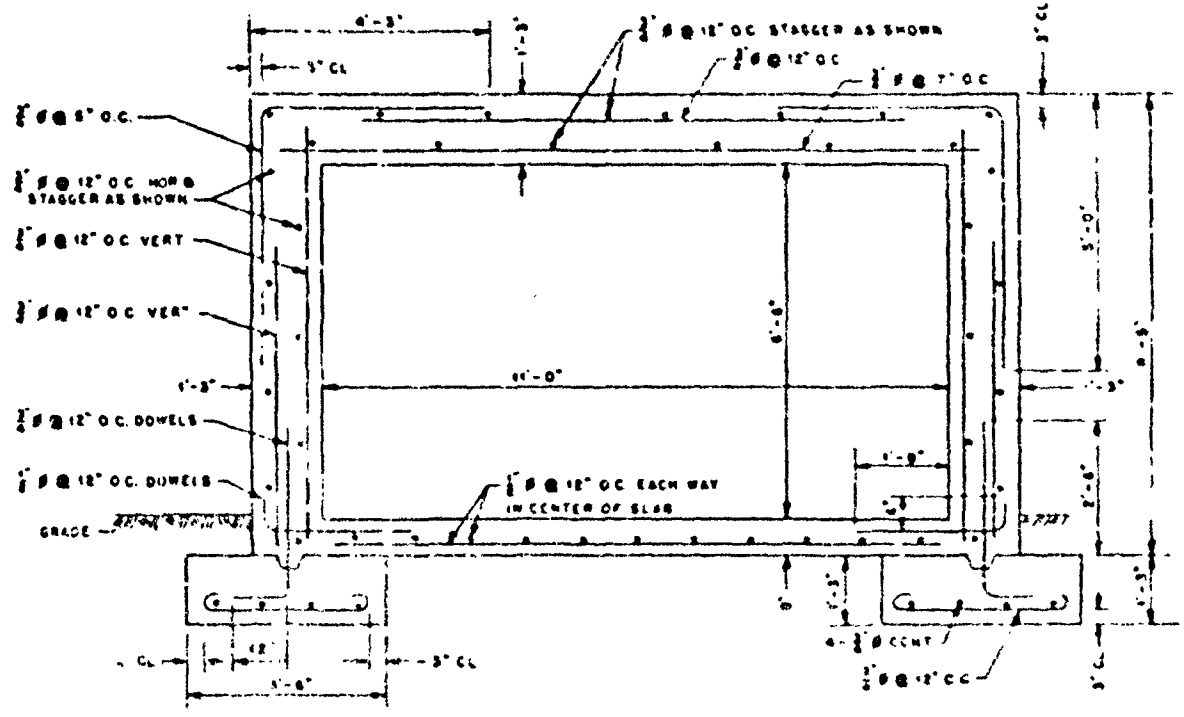

Fig. 3-76—General details. Station 605 on Yvonne. Pressure levels: Mike, 1 35 psi, King, 18 psi.

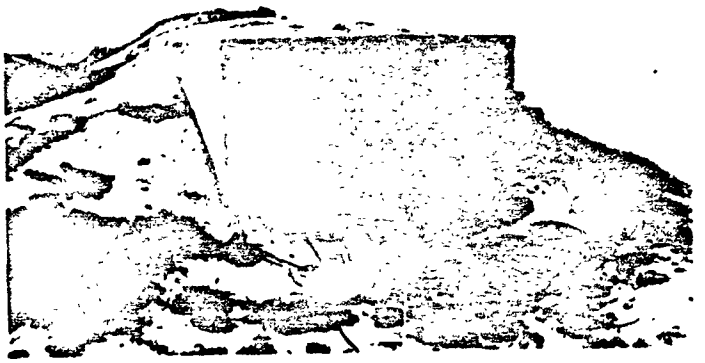

Fig. 3.69—Postshot, Station 605 on east side of Yvonne, opposite dock. No structural damage. King Ground Zero in left rear. Pressure levels: Mike, 1.35 psi; King, 18 psi.

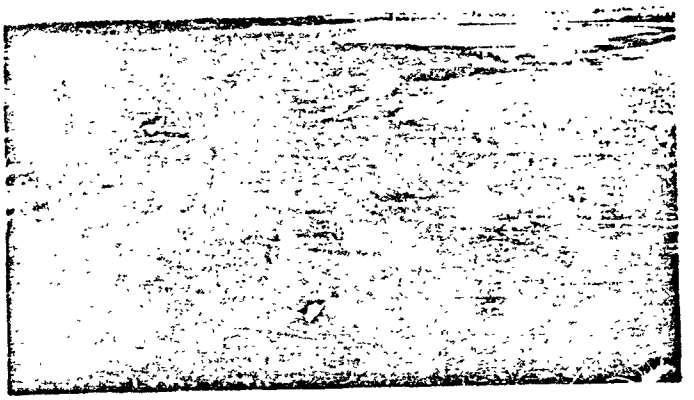

Fig. 3.70—Pretest, pier on Yvonne. King Ground Zero to left of camera. Pressure levels: Mike, 1.35 psi; King, 11 psi.

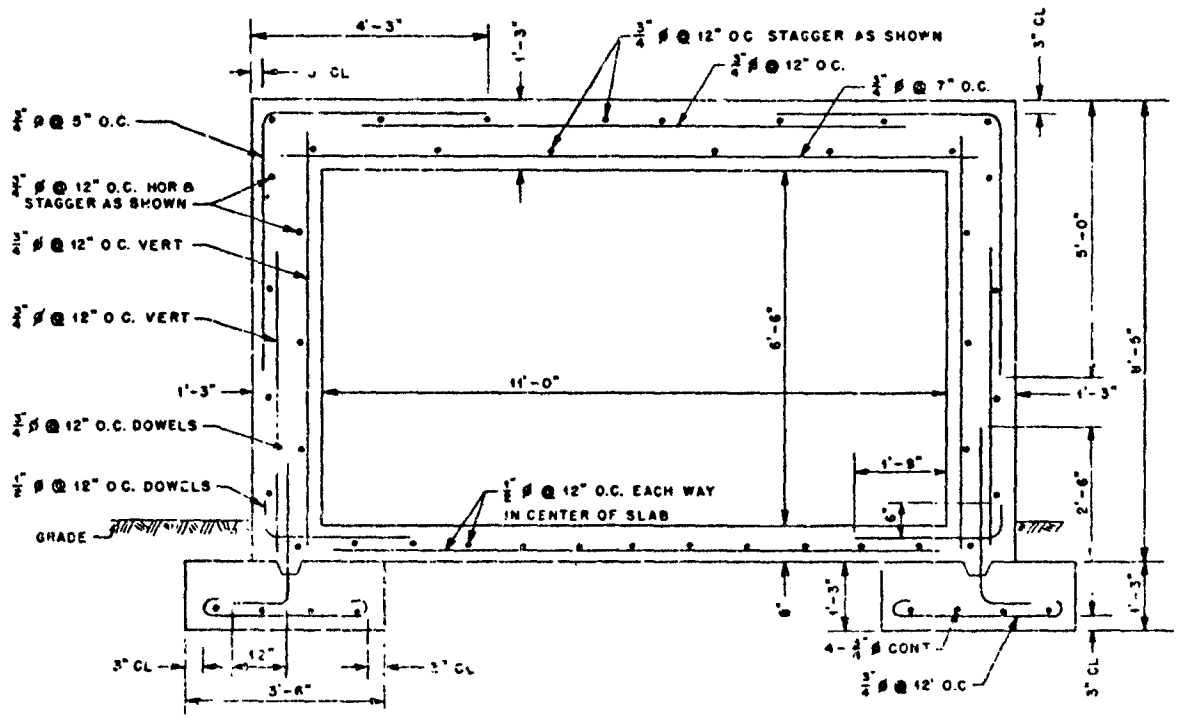

SECTION AA

Fig. 3.66—General details, station 605 on Yvonne. Pressure levels: Mike, 1.35 psi; King, 18 psi.

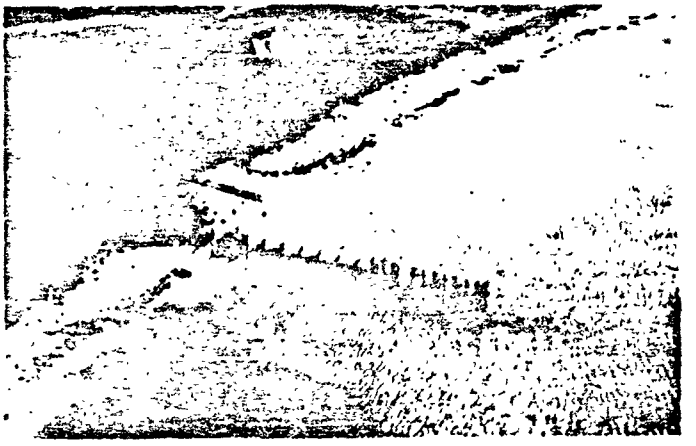

Fig. 3.71—Posttest, pier on Yvonne. King Ground Zero to left rear of camera. Pressure levels: Mike, 1.35 psi; King, 11 psi.

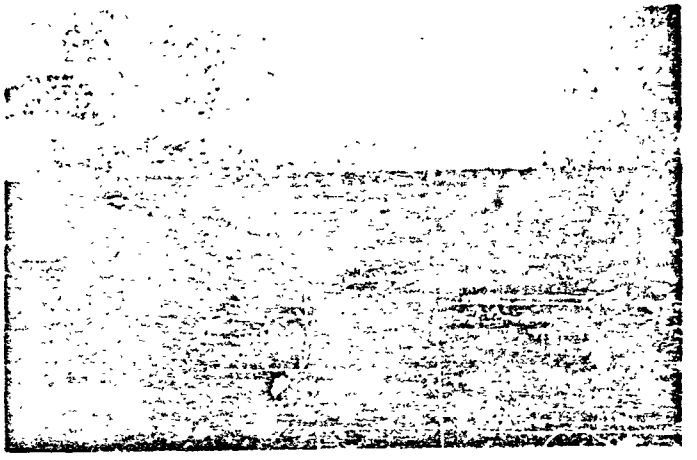

Fig. 3.72—Posttest, pier on Yvonne. Close-up of damage. Pressure levels: Mike, 1.35 psi; King, 11 psi.

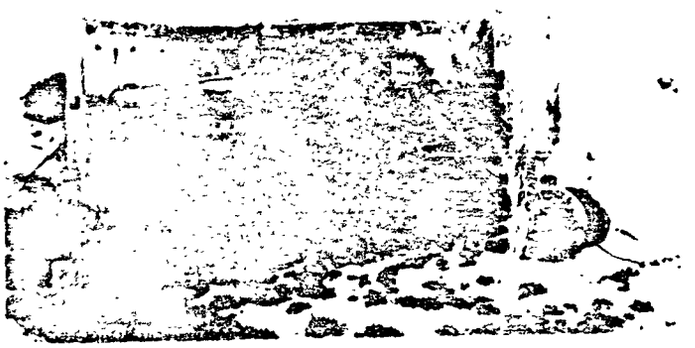

Fig. 3.73—Posttest, telephone station on Yvonne. Located 200 ft north of airstrip and east of Station 207. Only superficial damage to structural appurtenances. Camera facing to left of King Ground Zero. Pressure levels: Mike, 1.35 psi; King, 11 psi.

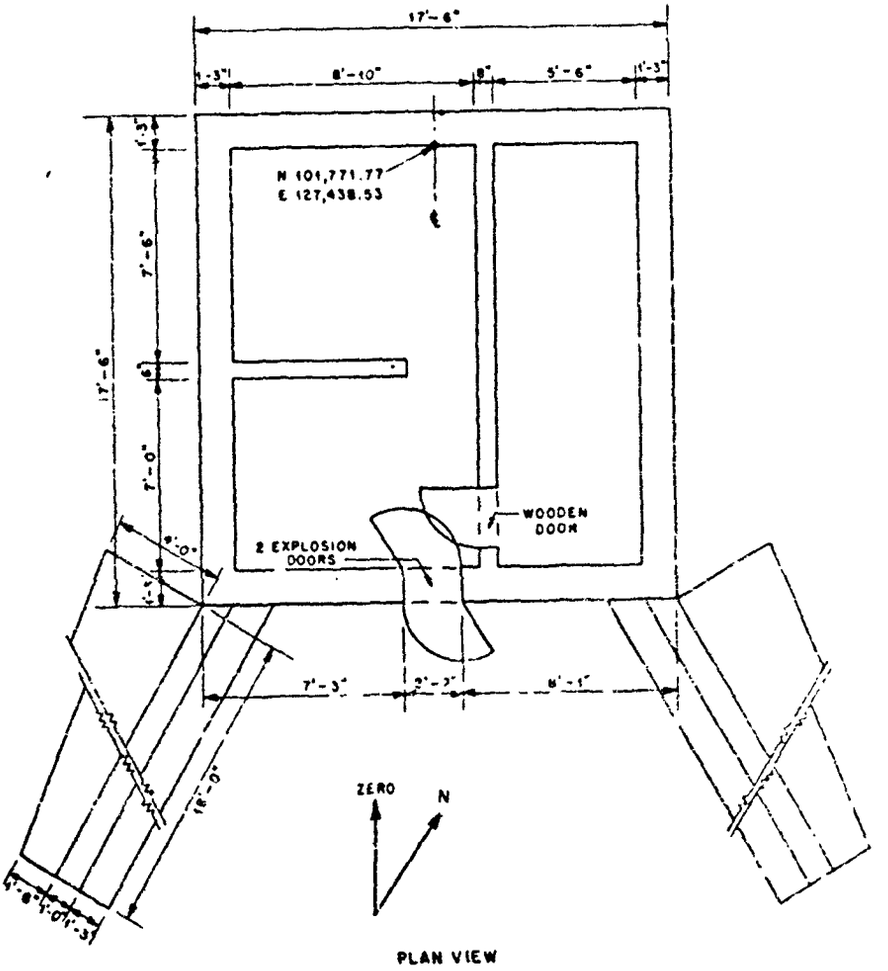

PLAN VIEW

Fig. 3.74—General details, Station 307 on Yvonne. Pressure levels: Mike, 1.[illegible] psi; King, 11 psi

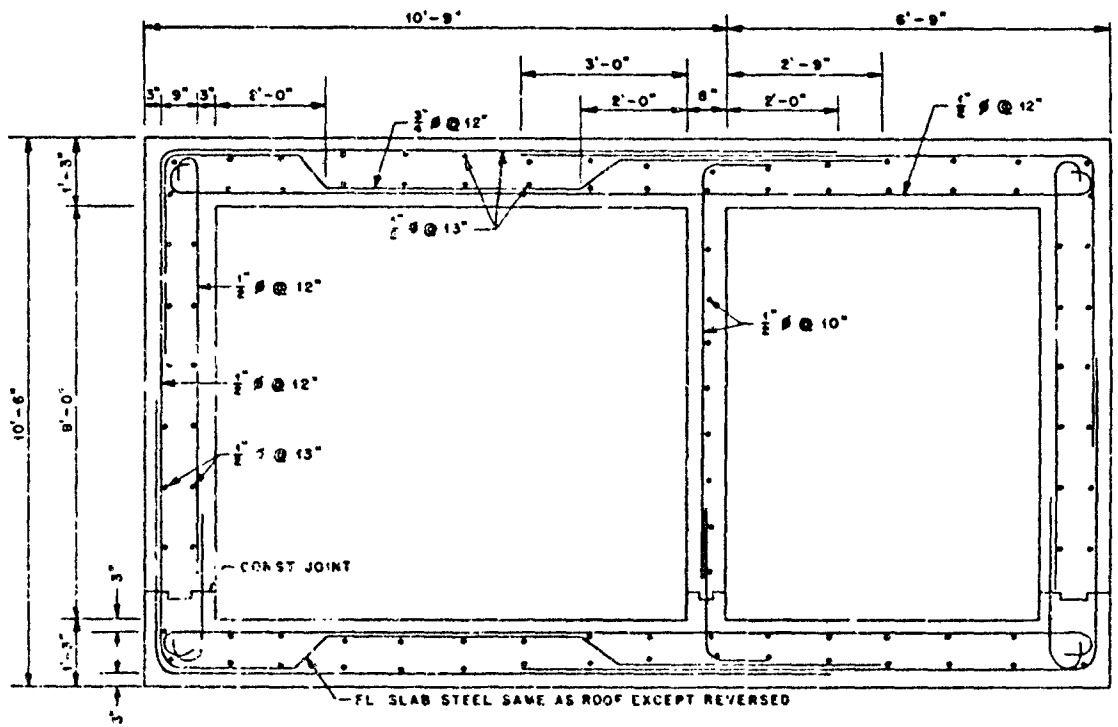

SECTION B-B

Fig. 3 5—General details, Station 307 on Yvonne. Pressure levels: Mike, 1.35 psi; King, 11 psi.

Fig. 3.76—Forrest, Station 307 on Yvonne. Located on south end of island, 100 ft north of airstrip. Note damage to exposed 12-in. pipe. Camera facing to left of King Ground Zero. Pressure levels: Mike, 1.75 psi; King 11 psi

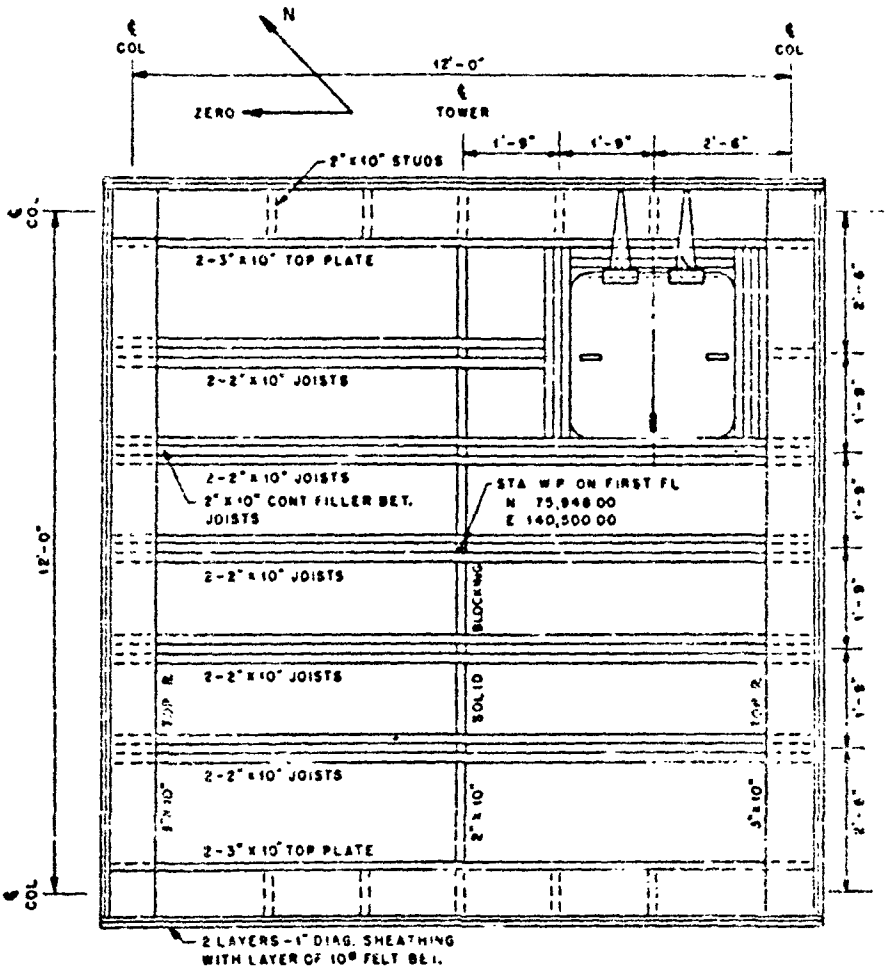

SECOND FLOOR FRAMING PLAN

Fig. 3.77—General details, Station 804 on Bruce. Pressure levels: Mike, 0.15 psi; X-ray, 0.15 psi.

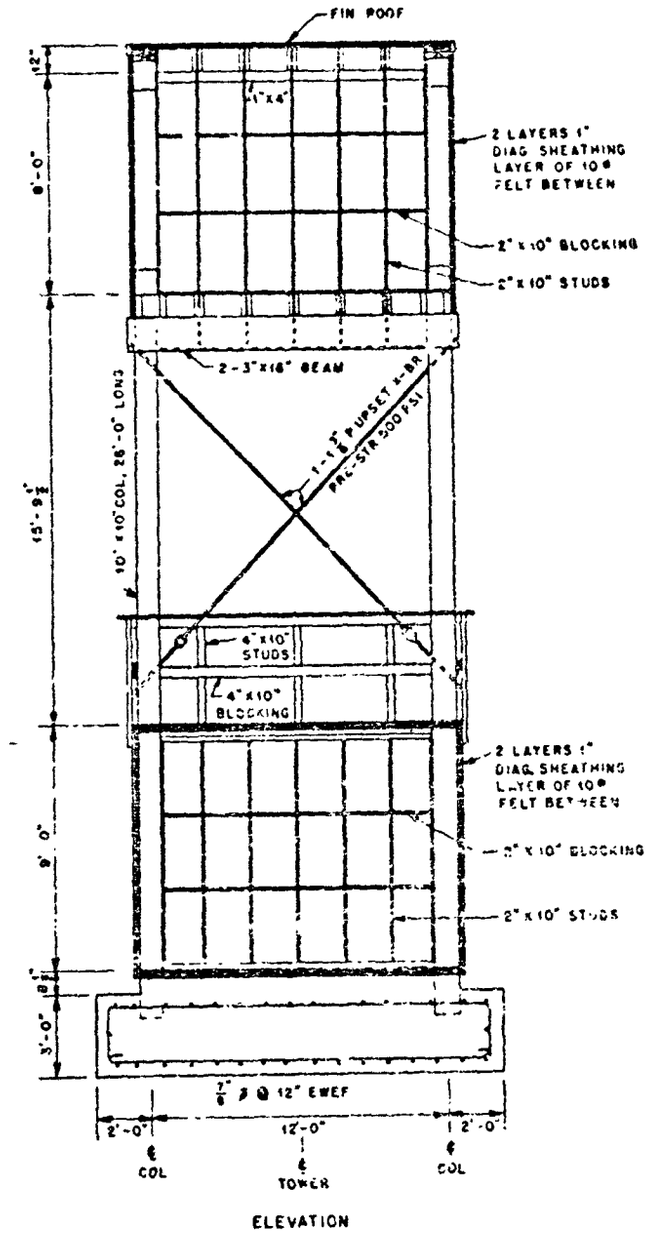

ELEVATION

Fig. 3.78—Station 804 on Bruce. Pressure levels: Mike, 0.76 psi; King, 0.73 psi.

Fig. 3.79—Pretest, camera tower on north end of Bruce. General view. Note outline of concrete foundation. Pressure levels: Mike, 0.76 psi; King, 0.73 psi.

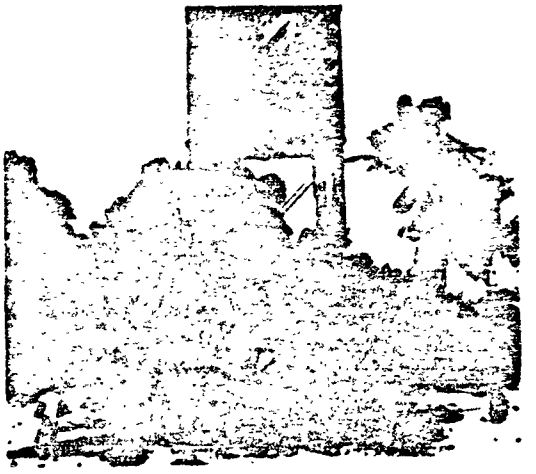

Fig. 3.80—Posttest, camera tower on north end of Bruce. View facing away from Ground Zero. Note undamaged trees in background. Pressure levels: Mike, 0.76 psi; King, 0.73 psi.

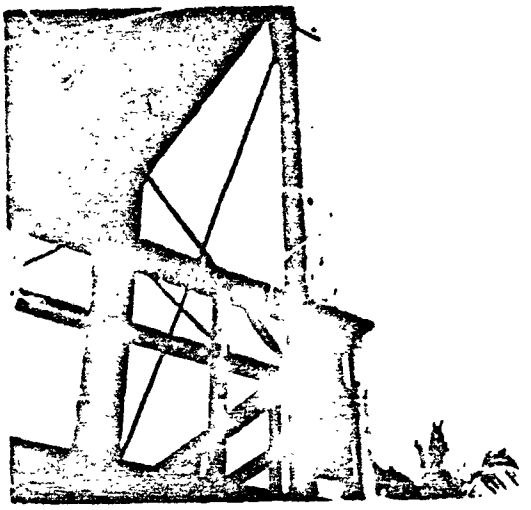

Fig. 3.81 — Posttest, camera tower on north end of Bruce. Close-up showing construction details. Note 10 by 10 in. timber columns and $1\frac{1}{4}$-in. steel tie rods for cross-bracing. Pressure levels: Mike, 0.76 psi; King, 0.73 psi.

Fig. 3.82 — Posttest, David. Miscellaneous structures. No apparent blast damage. Pressure levels: Mike, 0.64 psi; King, 0.47 psi.

Fig. 3.83—Poettest, David. General view of trees near pier. Pressure levels: Mike, 0.64 psi; King, 0.47 psi.

Fig. 3.84—Poettest, David. General view from pier. Note [illegible] trees. Pressure levels: Mike, 0.64 psi; King, 0.47 psi.

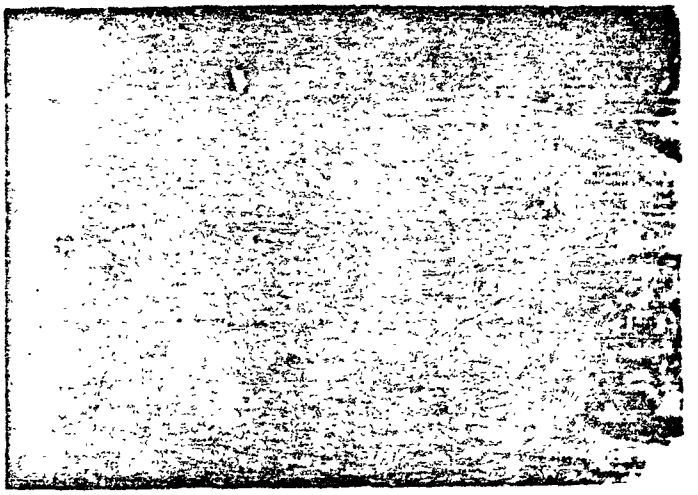

Fig. 3.85—Postest, Elmer. Damage to warehouse 3 from Mike shot. Pressure levels: Mike, 0.58 psi; King, 0.39 psi.

Fig. 3.86—Postest, Elmer. Damage to H&N warehouse from Mike shot. Pressure levels: Mike, 0.58 psi; King, 0.39 psi.

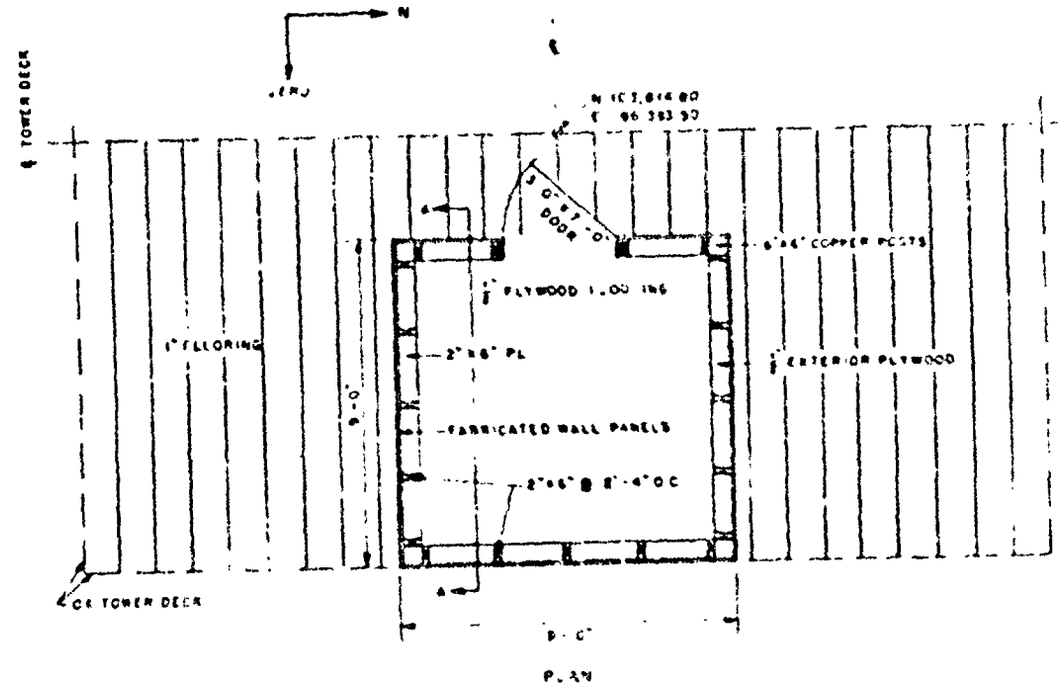

Fig. 3.87—Station 806 on Mack. Pressure levels: Luke, 2.5 psi; King, 0.79 psi.

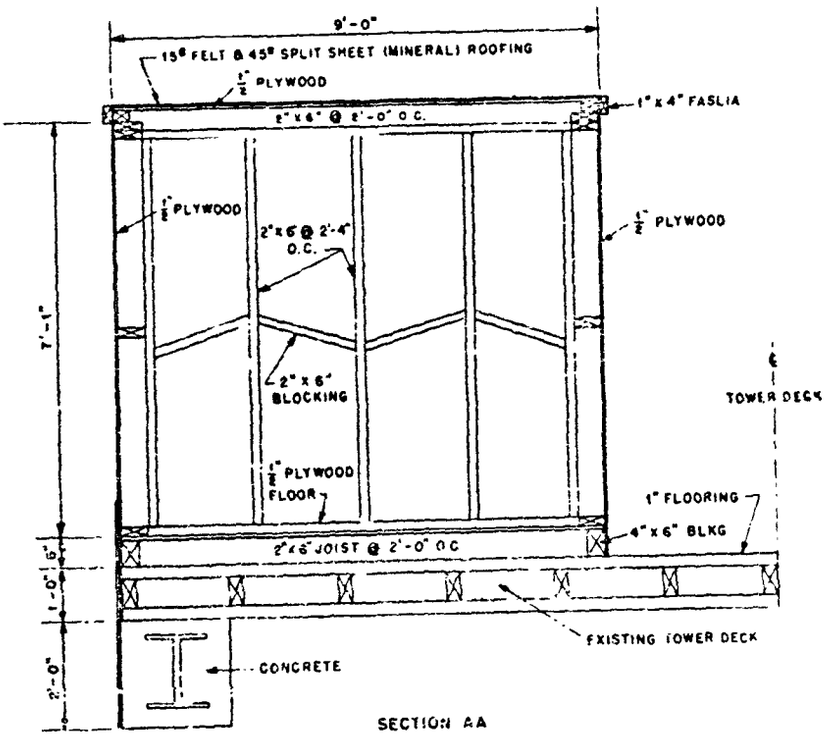

Fig. 3.88—Station 803 on Mack. Pressure levels: Mike, 2.5 psi; King, 0.79 psi.

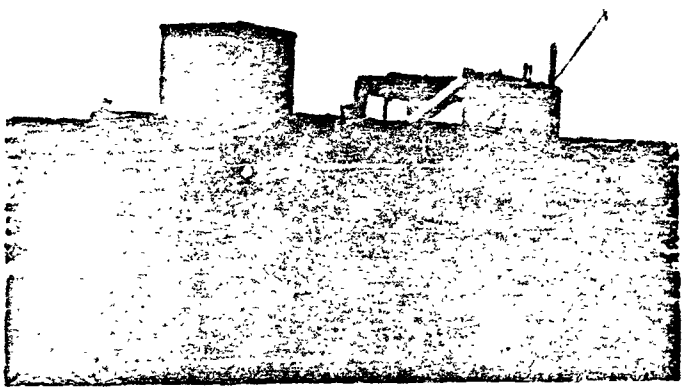

Fig. 3.89—Posttest, Station 806 on Mack. Timing shack on wooden deck of concrete pier. No blast damage to structure. Pressure levels: Mike, 2.5 psi; King, 0.79 psi.

CHAPTER 4

CONCLUSIONS

The following conclusions can be drawn from the damage survey performed for Operation Ivy.

1. The damage sustained by the various buildings of Structure 3.1.1 due to shot Mike was as follows: The test panels of Buildings 1 and 7 sustained only slight additional damage due to air blast. The steel frames of Building 2 suffered moderate plastic deformation, and the steel sheeting of the rear face was distorted inward between girts. The steel frame and siding of Building 6 received no apparent additional damage. The concrete frames of Buildings 3 and 5 suffered moderate plastic deformation. The rear wall of Building 5 was blown off by the air blast. The shear walls of Building 4 were undamaged. However, large cracks were opened in the roof slabs adjacent to the shear walls and roof girders. The overpressure was approximately 14 psi.

2. Structure 3.1.3 suffered no major structural damage. The blast doors were removed prior to the test. The wood frame air lock, which was left in place, was destroyed by the air blast. The painted surface of the vent pipe was charred on the side facing Ground Zero. The gage overpressure was approximately 18 psi.

3. All reinforced-concrete semiburied instrumentation shelters appeared to have performed their function satisfactorily without exhibiting any primary structural failures.

4. Of the many one-story reinforced-concrete surface and semiburied structures observed, none were badly damaged. The only serious structural failures observed were confined to wing walls designed to retain portions of the fill on the semiburied structures. Exposed steel beams and pipes attached to these structures were damaged and destroyed by overpressures of 11 psi and greater.

5. Small buildings covered with thin sheet metal over diagonal wood sheathing generally withstood overpressures up to 5 and 6 psi. However, one structure of this type was observed badly damaged by an overpressure of 4.5 psi.

6. Lightly constructed wood frame shacks apparently sheathed with corrugated metal and located in regions with overpressures greater than 4 psi were completely destroyed. No structures of this type were observed in regions subjected to less than 4 psi overpressure.

7. Palm trees were destroyed by air-blast overpressures of 4 to 5 psi and greater, but none were destroyed by overpressures less than 4 psi.

From the results of the dynamic analysis of Structure 3.1.1 presented in Sec. 2.6, the following conclusions can be drawn:

1. The free-air overpressure existing in the vicinity of Structure 3.1.1 for shot Mike of Operation Ivy was between 12 and 14 psi.

2. Pressures measured by the side-on baffle gage at Station 611-01 on Engebi were more reliable than those measured by the Pitot-static tube gage at the same station.

3. The effect on structural response of rise times of the order of magnitude investigated is small.

APPENDIX A

REPORT OF FIELD TRIP

A.1 GENERAL

T. O. Stark of the Office of the Chief of Engineers and John C. Archer of Massachusetts Institute of Technology arrived at Eniwetok Atoll on Aug. 16, 1953, and left Aug. 26, 1953. Section A.2 consists of excerpts from a letter report on the field trip written by Stark to the Chief, Engineering Division, Office of the Chief of Engineers.

A.2 EXCERPTS FROM REPORT OF FIELD TRIP

A. Purpose of Trip

To accomplish a physical damage survey of the multi-story Army test structure, to examine other structures and items for damage which would provide data of military or technical interest, and to evaluate or suggest structural modifications necessary to conduct a future program of blast and displacement measurements.

. . . . . .

B. Observation and Activities

. . . . . .

On Tuesday, 18 August, we proceeded to Engebi (JANET) a run of about 2 hours. The survey was begun immediately and consisted of establishing a base line and measuring offsets from existing "ramset" pins on vertical panels and/or walls to the vertical plane established. This provides a relative measurement of deflection from base to top of wall. The level was set up on the roof and shots were taken on 41 rows of 7 "ramset" pins each.

. . . . . .

The survey of the building was completed, except for photography, on Friday, 21 August. Saturday was spent in completing notes, examining the photographs which had already been taken, and arranging for an M-boat and "Duck" for Monday and Tuesday with which to make examination and photos of miscellaneous structures on all the islands. This survey was completed on Tuesday and the undersigned departed on Wednesday, 26 August.

1. General Description of Multi-story Building

The building did not show extensive damage from the front but it was determined that Buildings 2 and 3 had deflected about 7 inches. This contrasts with approximately 3½ inches of permanent deflection from GREENHOUSE test. The rear panel of Building 5 was completely out and lying on the ground. Large blocks of concrete were suspended from unsevered reinforcing bars in the roof. The roof slab of Building 4 showed marked depression in two places. One of these depressions was initiated from the

second GREENHOUSE shot. The underside of the roof slab showed considerable spalling and approximate failure from shear cracks at the end of bottom reinforcing bars about 33 inches from each end wall and the same distance from girders. These cracks were thoroughly photographed.

Reinforced concrete columns exhibited additional spalling on the compression side and cracking on the opposite side. Offsets of permanent deflection were measured on all reinforced concrete and steel columns.

Wall panels and roofs were examined for additional cracking. Very few additional cracks were noted and these were fine hair cracks.

2. General Description of Buried Shelter

The buried shelter, Structure 3.1.3 was examined for damage. The blast-proof doors had been removed and laid inside the shelters prior to the test. No damage occurred to the ramp-type concrete entrance. The air locks, of timber, in the rectangular shelter, were shattered and debris was lying inside. No damage was noted in the circular-type shelter. The air intake pipe protruding through the backfill over the rectangular shelter approximately 3½ feet was bent away from the blast source. Photographs were made of the pipe as well as the doorways and interiors of the shelters.

3. General Description of Miscellaneous Structures

Inspection of miscellaneous structures, primary instrumentation shelters and timing shacks was begun at ALICE, the most remote island on the northwest extremity of the Atoll. Enroute a shelter on a coral reef, MACK, was inspected and photographed. Examination of very heavy concrete shelters was made on ALICE, CLARA, IRENE, JANET, etc. Little damage occurred on basic structures; however, wing walls which were keyed rather than doweled to the basic structures were damaged. Steel doors of the Navy type held up well. One door had an opening out with acetylene torch; a heavy steel I-beam above the door used for hoisting, was folded 180 degrees in a horizontal plane. A wall for measuring blast pressures on JANET was overturned. It appeared to be oriented about 45 degrees from normal in direction of blast. A shack on [illegible]TE, about 4½ miles, was completely demolished. The timing portable generator was overturned approximately 100 feet away and severely damaged. Three concrete pylons, out of 6, used for instrumenting of AF hangar in GREENHOUSE tests remained standing. Timing shacks further down the Atoll sustained lesser degrees of damage. Photographs were made of all damage details and tree-stands were photographed for comparison with pre-shot conditions—all trees were of the coconut-palm variety. The dock on JANET was examined but it appeared to have been damaged severely from wave action and general weathering. Other causeways and trestles in the vicinity of the URSULA group were being used for current construction. It appears impossible to specifically attribute damage to any of these docks and causeways to blast effects.

4. Estimate of Modification of Multi-story Building for Future Instrumentation Program

At the request of Capt. Kingsley, AFSWP, the undersigned examined the Army test structure with a view to making recommendations on structural modifications necessary for a future blast measurement program. The instruments are to be mounted on Buildings 1, 2 and 3. Mr. Dave Self, J-5, at the request of Commander McClellan, AEC Liaison Officer at Sandia Corporation, discussed the requirements with the undersigned. The following suggestions were made:

a. The panels (2) blown out on 2nd floor rear of Building 1 would be replaced by timber bulkheads of a strength comparable to 12" brick walls which have withstood all previous blast loads. They would be braced by wales and shoring.

b. The separation cracks between Buildings 1 through 4 would be closed by 2-inch timber where alignment of surface is consistent (roof and undeflected walls). This timber could be anchored by metal straps spanning between existing bolts with wedges driven between the timber and the strap. Where the building lines are offset, continuous wedges would be driven against timbers.

c. The access hatches in Building 4 (at Building 5) would be closed with bulkhead timbers in existing stop-log channels.

d. Existing instrument mounts on Buildings 1, 2 and 3 are in usable condition. All will require retapping and redieing to clean up rust on threads.

e. Displacement gage pipes, approximately 3", 2" and 1¼" were examined. The large pipe are in fair condition and usable; the 2" pipe are about 75% usable, some having been bent; and the 1¼ pipe are mostly bent and probably cannot be re-used.

f. A later examination of the roof of Building 4 indicated that the two outside spans of the 3-span continuous roof should be shored along the crack line for future tests.

E. Conclusions

1. The survey developed all necessary information on which to accomplish a dynamic analysis of the multi-story structure.

2. The observation of other structures should provide general information on damage to structures and particularly to design of elements of heavy concrete instrumentation shelters. Very few of the test-type structures remained on islands in the vicinity of tests.

. . . . . .

APPENDIX B

DAMAGE-SURVEY DATA FOR STRUCTURE 3.1.1

B.1 EXTERIOR-WALL-DISPLACEMENT MEASUREMENTS

The locations of the survey points are shown in Fig. 2.3. Offsets were measured from a vertical plane to these survey points after Operation Ivy. Similar pretest measurements are available as posttest measurements of Operation Greenhouse.[9,10] For each vertical row of survey points, the distance to the base point was subtracted from all measurements, the remainder being the horizontal distance between the base point and the survey point, shown in Table B.1 as "offset from vertical at base point." The difference between the pre-Ivy and post-Ivy measurements is then shown as "net lateral displacement." The displacement for front and back is positive if away from Ground Zero, and for the ends it is positive if it is toward the inside of the building.

B.2 COLUMN-OFFSET MEASUREMENTS

The locations of the columns in Buildings 2, 3, 5, and 6 are shown in Fig. B.1. Horizontal-offset measurements were made from a vertical line to the front or rear face at the top and bottom of each column of each story of these buildings. The difference of the offset measurements indicates the total permanent displacement of the top of the column relative to the bottom of the column. The relative displacements thus determined are tabulated in Table B.2, a positive sign indicating motion of the column top away from Ground Zero.

B.3 ROOF-ELEVATION MEASUREMENTS

The locations of the roof survey points are shown in Fig. 2.3. In the level survey the elevations of the points were determined relative to an arbitrary datum plane since no bench marks were available with which to determine the absolute elevations. In reducing the field data, the posttest elevations were tied to the pretest elevations by assuming that the average elevation of the four corner points of Building 4 remained unchanged. The post-Ivy elevations thus obtained and the pre-Ivy elevations obtained from references 9 and 10 are tabulated in Table B.3. The difference between these elevations for each point gives the vertical displacement of the roof, upward displacements being indicated by a positive sign.

Table B.1 — EXTERIOR-WALL-DISPLACEMENT MEASUREMENTS

Survey point	Offset from vertical at base point, ft		Net lateral displacement, ft	Survey point	Offset from vertical at base point, ft		Net lateral displacement, ft
	Pre-Ivy	Post-Ivy			Pre-Ivy	Post-Ivy	
			Front of Building 1				
A-1	0.000	0.000	0.00	D-4	−0.060	−0.054	+0.01
A-2	0.000	0.000	0.00	D-5	−0.095	−0.089	+0.01
A-3	0.000	0.000	0.00	D-6	−0.050	−0.061	−0.01
A-4	0.000	0.000	0.00	D-7	−0.015	−0.026	−0.01
A-5	0.000	0.000	0.00	E-1	+0.035	+0.033	−0.00
A-6	0.000	0.000	0.00	E-2	+0.005	+0.009	+0.00
A-7	0.000	0.000	0.00	E-3	+0.020	−0.037	−0.06
B-1	0.000	−0.005	−0.00	E-4(lower)	−0.020	−0.012	+0.01
B-2	+0.035	+0.009	−0.03	E-4(upper)	−0.025	−0.021	+0.00
B-3	+0.010	+0.008	−0.00	E-5	−0.030	−0.016	+0.00
B-4	+0.005	+0.000	−0.00	E-6	−0.040	−0.048	−0.01
B-5	+0.030	+0.011	−0.02	E-7	+0.015	−0.012	−0.00
B-6	+0.030	+0.019	−0.01	F-1	+0.004	−0.030	+0.01
B-7	+0.020	+0.000	−0.02	F-2	−0.030	−0.056	0.00
C-1	−0.020	−0.026	−0.01	F-3	−0.055	−0.057	−0.00
C-2	−0.020	0.023	−0.00	F-4	−0.015	−0.023	−0.01
C-3	−0.040	−0.038	+0.00	F-5	−0.025	−0.033	−0.01
C-4(lower)	0.000	−0.001	−0.00	F-6	−0.045	−0.054	−0.01
C-4(upper)	−0.075	−0.072	+0.00	F-7	−0.015	−0.029	−0.01
C-5	−0.030	−0.031	−0.00	G-1	+0.040	+0.029	−0.01
C-6	−0.005	−0.009	−0.00	G-2	0.000	+0.005	+0.00
C-7	+0.020	+0.020	0.00	G-3	−0.020	−0.016	+0.00
D-1	+0.020	+0.023	+0.00	G-4	+0.015	−0.010	−0.02
D-2	−0.015	−0.012	+0.00	G-5	+0.010	+0.009	−0.00
D-3	−0.060	−0.053	+0.01	G-6	−0.030	−0.053	−0.02
				G-7	−0.015	−0.028	−0.01
			Front of Building 2				
A-8*	0.000	0.000	0.00	E-8	0.220	0.356	+0.14
B-8	0.032	0.055	+0.02	F-8	0.277	0.476	+0.20
C-8	0.044	0.122	+0.08	G-8	0.352	0.648	+0.32
D-8	0.139	0.253	+0.10				
			Front of Building 4				
A-13	0.000	0.000	0.00	C-13	0.070	0.136	+0.06
A-14	0.000	0.000	0.00	C-14	0.055	0.126	+0.08
A-15	0.000	0.000	0.00	C-15	0.070	0.144	+0.07
A-16	0.000	0.000	0.00	C-16	0.045	0.125	+0.05
A-17	0.000	0.000	0.00	C-17	0.035	0.116	+0.08
B-13	0.020	0.060	+0.04	D-13	0.130	0.269	+0.14
B-14	0.035	0.084	+0.05	D-14	0.155	0.294	+0.14
B-15	0.025	0.081	+0.06	D-15	0.155	0.270	+0.11
B-16	0.025	0.058	+0.03	D-16	0.130	0.262	+0.13
B-17	0.010	0.045	+0.04	D-17	0.085	0.219	+0.13

Table B.1 — (Continued)

Survey point	Offset from vertical at base point, ft		Net lateral displacement, ft	Survey point	Offset from vertical at base point, ft		Net lateral displacement, ft
	Pre-Ivy	Post-Ivy			Pre-Ivy	Post-Ivy	
			Front of Building 3 (Continued)				
E-13	0.180	0.371	+0.19	F-16	0.225	0.496	+0.27
E-14	0.185	0.388	+0.20	F-17	0.185	0.454	+0.27
E-15	0.190	0.392	+0.20	G-13	0.295	0.615	+0.32
E-16	0.145	0.353	+0.21	G-14	0.305	0.650	+0.35
E-17	0.135	0.337	+0.20	G-15	0.285	0.634	+0.35
F-13	0.230	0.507	+0.28	G-16	0.275	0.602	+0.33
F-14	0.255	0.539	+0.28	G-17	0.290	0.625	+0.34
F-15	0.230	0.501	+0.27				
			Front of Building 4				
A-18	0.000	0.000	0.00	D-22	−0.055	−0.065	−0.01
A-19	0.000	0.000	0.00	D-23	−0.010	−0.002	+0.01
A-20	0.000	0.000	0.00	D-24	−0.070	−0.068	+0.00
A-21	0.000	0.000	0.00	E-18	−0.025	−0.032	−0.01
A-22	0.000	0.000	0.00	E-19	+0.015	+0.009	+0.01
A-23	0.000	0.000	0.00	E-20	0.000	−0.004	−0.00
A-24	0.000	0.000	0.00	E-21	+0.005	+0.004	−0.00
B-18	−0.015	+0.020	−0.00	E-22	−0.005	−0.011	−0.01
B-19	0.000	+0.001	+0.00	E-23	−0.020	−0.025	−0.00
B-20	+0.015	+0.011	−0.00	E-24	−0.040	−0.043	−0.00
B-21	−0.010	−0.006	+0.00	F-18	+0.005	−0.010	−0.02
B-22	−0.015	−0.015	0.00	F-19	+0.040	+0.027	−0.01
B-23	+0.010	0.000	−0.01	F-20	+0.005	+0.002	−0.00
B-24	0.000	−0.007	−0.01	F-21	+0.025	+0.024	−0.00
C-18	−0.045	−0.040	+0.00	F-22	+0.035	+0.025	−0.01
C-19	−0.025	−0.030	−0.00	F-23	+0.010	+0.008	−0.00
C-20	−0.020	−0.025	−0.00	F-24	0.000	−0.014	−0.01
C-21	−0.022	−0.016	+0.01	G-18	+0.005	−0.001	−0.01
C-22	−0.015	−0.020	−0.00	G-19	+0.020	+0.013	−0.01
C-23	−0.020	−0.010	+0.01	G-20	+0.030	+0.025	−0.00
C-24	−0.050	−0.065	−0.02	G-21	+0.050	+0.038	−0.01
D-18	−0.035	−0.030	+0.00	G-22	+0.030	+0.020	−0.01
D-19	−0.010	0.012	−0.00	G-23	0.000	+0.020	−0.01
D-20	−0.020	−0.017	+0.00	G-24	0.000	−0.022	−0.02
D-21	+0.005	+0.012	+0.01				
			Front of Building 5				
A-25	0.000	0.000	0.00	C-25	+0.110	+0.249	+0.14
A-26	0.000	0.000	0.00	C-26	+0.075	+0.216	+0.14
A-28	0.000	0.000	0.00	C-27	+0.080	+0.228	+0.15
A-29	0.000	0.000	0.00	C-28	+0.070	+0.208	+0.14
A'-27†	+0.010	+0.026	+0.02	C-29	+0.100	+0.231	+0.13
B-25	+0.035	+0.179	+0.14	C'-27†	+0.135	+0.303	+0.17
B-26	+0.065	+0.156	+0.09	D-25	+0.130	+0.320	+0.19
B-28	+0.035	+0.141	+0.10	D-26	+0.160	+0.346	+0.19
B-29	+0.060	+0.157	+0.10	D-28	+0.125	+0.314	+0.19
B'-27†	+0.065	+0.204	+0.14	D-29	+0.165	+0.343	+0.18

Table B.1 — (Continued)

Survey point	Offset from vertical at base point, ft		Net lateral displacement, ft	Survey point	Offset from vertical at base point, ft		Net lateral displacement, ft
	Pre-Ivy	Post-Ivy			Pre-Ivy	Post-Ivy	
			Front of Building 5 (Continued)				
D'-27†	+0.200	+0.397	+0.20	F-26	+0.175	+0.458	+0.28
E-25	+0.180	+0.386	+0.21	F-28	+0.210	+0.487	+0.28
E-26	+0.155	+0.371	+0.21	F-29	+0.220	+0.476	+0.26
E-27	+0.180	+0.385	+0.20	G-25	+0.245	+0.643	+0.40
E-28	+0.170	+0.373	+0.20	G-26	+0.225	+0.615	+0.39
E-29	+0.195	+0.394	+0.20	G-27	+0.260	+0.637	+0.38
E'-27†	+0.183	+0.394	+0.21	G-28	+0.250	+0.621	+0.37
F-25	+0.190	+0.456	+0.27	G-29	+0.275	+0.656	+0.38
			Front of Building 7				
A-39	0.000	0.000	0.00	D-41	−0.060	+0.023	+0.08
A-40	0.000	0.000	0.00	E-39	+0.280	+0.053	−0.33
A-41	0.000	0.000	0.00	E-40	−0.100	−0.046	+0.05
B-39	−0.010	−0.035	−0.02	E-41	−0.085	+0.051	+0.14
B-40	−0.040	−0.018	+0.02	F-39	+0.250	−0.060	−0.31
B-41	−0.020	+0.016	+0.04	F-40	−0.090	−0.055	+0.04
C-39	−0.040	−0.028	+0.01	F-41	−0.040	+0.023	+0.06
C-40	−0.080	−0.061	+0.02	G-39	+0.265	−0.043	−0.31
C-41	−0.060	+0.004	+0.06	G-40	−0.110	−0.032	+0.04
D-39	+0.270	−0.042	−0.31	G-41	−0.040	+0.003	+0.04
D-40	−0.100	−0.034	+0.07				
			Back of Building 7				
A-39	0.000	0.000	0.00	D-41	−0.060	−0.063	−0.00
A-40	0.000	0.000	0.00	E-39	+0.280	−0.087	−0.37
A-41	0.000	0.000	0.00	E-40	−0.100	−0.095	+0.00
B-39	−0.010	−0.019	−0.01	E-41	−0.085	−0.087	−0.00
B-40	−0.040	−0.033	+0.01	F-39	+0.250	−0.098	−0.35
B-41	−0.020	−0.023	−0.00	F-40	−0.090	−0.098	−0.01
C-39	−0.040	−0.060	−0.02	F-41	−0.040	−0.042	−0.00
C-40	−0.080	−0.078	+0.00	G-39	+0.265	−0.083	−0.35
C-41	−0.060	−0.064	−0.00	G-40	−0.110	−0.053	+0.06
D-39	+0.270	−0.082	−0.35	G-41	−0.040	−0.019	+0.00
D-40	−0.100	−0.108	−0.01				
			End of Building 1				
A-H	0.000	0.000	0.00	B-I	−0.035	+0.046	+0.01
A-J‡				B-M	+0.010	−0.003	−0.01
A-K	0.000	0.000	0.00	B-N	+0.035	+0.055	+0.02
A-L	0.000	0.000	0.00	B-P	−0.050	0.018	+0.03
A-M‡	0.000	0.000	0.00	C-H	+0.030	+0.008	−0.02
A-N‡				C-J	0.040	+0.051	+0.01
A-P	0.000	0.000	0.00	C-K	+0.020	+0.009	−0.01
B-H	+0.020	+0.007	−0.01	C-L	+0.035	+0.033	−0.00
B-J	+0.060	+0.064	+0.00	C-M	−0.015	+0.010	+0.00
B-K	−0.010	+0.004	+0.01	C-N	+0.015	+0.016	+0.00

Table B.1 — (Continued)

Survey point	Offset from vertical at base point, ft		Net lateral displacement, ft	Survey point	Offset from vertical at base point, ft		Net lateral displacement, ft
	Pre-Ivy	Post-Ivy			Pre-Ivy	Post-Ivy	
			End of Building 1 (Continued)				
C-P‡				F-H	0.000	−0.021	−0.02
D-H	+0.050	+0.033	−0.02	F-J	+0.030	+0.018	−0.01
D-J	−0.005	−0.027	−0.02	F-K	−0.010	−0.030	−0.02
D-K	−0.045	−0.051	−0.01	F-L	−0.005	+0.006	+0.01
D-L	−0.025	−0.026	−0.00	F-M	+0.015	+0.015	0.00
D-M	−0.015	−0.026	−0.01	F-N	+0.005	+0.013	+0.01
D-N‡				F-P	+0.020	+0.048	+0.03
D-P‡				G-H	+0.015	+0.005	−0.01
E-H	+0.035	+0.011	−0.02	G-J	+0.005	+0.001	−0.00
E-J	+0.010	+0.001	−0.01	G-K	+0.020	+0.019	−0.00
E-K		−0.014		G-L	+0.005	+0.018	+0.01
E-L	0.035	−0.034	+0.00	G-M	+0.010	+0.013	+0.00
E-M	−0.020	−0.024	−0.00	G-N	+0.025	+0.035	+0.01
E-N	+0.010	+0.016	+0.01	G-P	+0.010	+0.036	+0.03
E-P‡							
			Back of Building 1				
A-1	0.000	0.000	0.00	D-5	−0.080	−0.074	+0.01
A-2	0.000	0.000	0.00	D-6	−0.050	−0.056	−0.01
A-3	0.000	0.000	0.00	D-7	+0.040	+0.051	+0.01
A-4	0.000	0.000	0.00	E-1			
A-5	0.000	0.000	0.00	E-2	−0.050	−0.057	−0.01
A-6	0.000	0.000	0.00	E-3	+0.030	+0.032	+0.00
A-7	0.000	0.000	0.00	E-4(lower)	−0.045	−0.044	+0.00
B-1	−0.005	+0.079	+0.08	E-4(upper)	−0.065	−0.069	+0.00
B-2	−0.015	−0.026	+0.01	E-5	−0.060	−0.056	+0.00
B-3	−0.010	−0.010	0.00	E-6(lower)	−0.045	−0.054	−0.01
B-4	−0.005	−0.006	+0.00	E-6(upper)	−0.035	−0.044	−0.01
B-5	−0.030	−0.032	−0.00	E-7	−0.020	−0.018	+0.00
B-6	−0.019	−0.016	−0.01	F-1	−0.060	−0.051	+0.01
B-7	+0.030	+0.033	+0.00	F-2	−0.070	−0.072	−0.00
C-1	−0.025			F-3	−0.055	−0.050	+0.00
C-2	−0.010	−0.022	−0.01	F-4	−0.100	−0.096	+0.00
C-3	+0.025	+0.028	+0.00	F-5	−0.145	−0.141	+0.00
C-4	−0.015	−0.014	+0.00	F-6	−0.100	−0.079	+0.00
C-5	−0.035	−0.033	+0.00	F-7	0.000	+0.016	+0.02
C-6(lower)	−0.035	−0.033	+0.00	G-1	−0.040	+0.051	+0.09
C-6(upper)	−0.065	−0.076	−0.01	G-2	−0.050	−0.049	+0.00
C-7	+0.035	+0.048	+0.01	G-3	−0.030	−0.024	+0.01
D-1	−0.055			G-4	−0.070	−0.068	+0.00
D-2	−0.095			G-5	−0.090	−0.091	−0.00
D-3	+0.015	+0.018	+0.00	G-6	−0.030	−0.025	+0.00
D-4	−0.035	−0.048	−0.01	G-7	+0.015	+0.035	+0.02

* None of the survey points could be found in the corrugated metal siding. Therefore the posttest offsets were measured to flat flange of edge angle at locations adjacent to line 7 on Building 1.

† Base point assumed as average of points A-26 and A-28.

‡ No survey points at this location.

Table B.2 — COLUMN-OFFSET MEASUREMENTS

Column	Story level	Relative displacement*	Av. displacement per story	Column	Story level	Relative displacement*	Av. displacement per story
		Building 2				Building 5	
5A	First	+0.129	+0.10	13A	First	+0.248	+0.22
5B		+0.092		13B		+0.232	
5C		+0.091		13C		+0.200	
5D		+0.091		13D		+0.240	
6A		+0.091		14A		+0.208	
6B		+0.107		14B		+0.209	
6C		+0.080		14C		+0.217	
6D		+0.101		14D		+0.232	
5A	Second	+0.240	+0.24	13A	Second	+0.084	+0.11
5B		+0.232		13B		+0.089	
5C		+0.247		13C		+0.111	
5D		+0.244		13D		+0.116	
6A		+0.241		14A		+0.103	
6B		+0.258		14B		+0.098	
6C		+0.241		14C		+0.110	
6D		+0.226		14D		+0.141	
5A	Third	+0.236	+0.24	13A	Third	+0.192	+0.21
5B		+0.237		13B		+0.198	
5C		+0.2[illegible]		13C		+0.220	
5D		+0.230		13D		+0.193	
6A		+0.23[illegible]		14A		+0.221	
6B		+0.252		14B		+0.202	
6C		+0.250		14C		+0.220	
6D		+0.246		14D		+0.242	
		Building 3				Building 6	
7A	First	+0.118	+0.13	15A	First	+0.022	+0.03
7B		+0.132		15B		+0.023	
7C		+0.111		15C		+0.037	
7D		+0.148		15D		+0.029	
8A		+0.143		16A		+0.048	
8B		+0.129		16B		+0.031	
8C		+0.110		16C		+0.03[illegible]	
8D		+0.148		16D		+0.032	
7A	Second	+0.151	+0.18	15A	Second	+0.0[illegible]	[illegible]
7B		+0.190		15B		+0.072	
7C		+0.210		15C		+0.0[illegible]	
7D		+0.210		15D		+0.073	
8A		+0.195		16A		+0.063	
8B		+0.180		16B		+0.089	
8C		+0.174		16C		+0.071	
8D		+0.197		16D		+0.068	
7A	Third	+0.206	+0.21	15A	Third	+0.0[illegible]	+0.05
7B		+0.218		15B		+0.[illegible]59	
7C		+0.224		15C		+0.066	
7D		+0.215		15D		+0.041	
8A		+0.215		16A		+0.054	
8B		+0.205		16B		+0.060	
8C		+0.218		16C		+0.067	
8D		+0.215		16D		+0.054	

*Relative displacement is total permanent displacement of top of column relative to bottom of column. Positive sign indicates movement of top of column away from Ground Zero.

Table B.3—ROOF-ELEVATION MEASUREMENTS

Survey point	Pre-Ivy elev., ft	Post-Ivy elev., ft	Net vert. displ., ft	Survey point	Pre-Ivy elev., ft	Post-Ivy elev., ft	Net vert. displ., ft
			Roof o	Building 1			
H-1	48.174	48.184	+0.01	L-5	48.099	48.108	+0.01
H-2	48.124	48.127	+0.00	L-6	48.099	48.107	+0.01
H-3	48.119	48.125	+0.01	L-7	48.074	48.077	+0.00
H-4	48.094	48.096	+0.00	M-1	48.114	48.127	+0.01
H-5	48.084	48.096	+0.01	M-2	48.104	48.119	+0.02
H-6	48.104	48.109	+0.00	M-3	48.095	48.107	+0.01
H-7	48.125	48.125	+0.00	M-4			
J-1	48.144	48.151	+0.01	M-5	48.084	48.095	+0.01
J-2	48.119	48.129	+0.00	M-6	48.099	48.104	+0.00
J-3	48.124	48.129	+0.00	M-7	48.079	48.085	+0.01
J-4	48.104	48.109	+0.00	N-1	48.164	48.172	+0.01
J-5	48.104	48.108	+0.00	N-2	48.094	48.102	+0.01
J-6	48.079	48.076	-0.00	N-3	48.084	48.099	+0.02
J-7	48.074	48.074	0.00	N-4	48.099	48.094	+0.01
K-1	48.114	48.120	+0.01	N-5	48.079	48.089	+0.01
K-2	48.089	48.095	+0.01	N-6	48.074	48.077	+0.00
K-3	48.099	48.104	+0.00	N-7	48.074	48.077	+0.00
K-4				P-1	48.184	48.193	+0.01
K-5	48.104	48.109	+0.00	P-2	48.104	48.107	+0.00
K-6	48.104	48.114	+0.01	P-3	48.099	48.109	+0.01
K-7	48.084	48.089	+0.00	P-4	48.064	48.075	+0.01
L-1	48.109	48.119	+0.01	P-5	48.079	48.087	+0.01
L-2	48.064	48.075	+0.01	P-6	48.034	48.031	-0.00
L-3	48.084	48.097	+0.01	P-7	48.104	48.112	+0.01
L-4	48.069	48.076	+0.01				
			Roof of	Building 2			
H-8	48.099	48.095	-0.00	L-11	48.099	48.[illegible]	-0.01
H-9	48.134	48.149	+0.02	L-12	48.044	48.[illegible]	-0.02
H-10	48.124	48.134	+0.01	M-8	48.[illegible]	[illegible]	-0.02
H-11	48.139	48.148	+0.01	M-9	[illegible]	[illegible]	-0.01
H-12	48.094	48.091	-0.00	M-10	48.014	48.007	-0.01
J-8	48.054	48.055	+0.00	M-11	48.[illegible]	48.049	-0.00
J-9	48.114	48.119	+0.00	M-12	[illegible]	[illegible]	-0.02
J-10	48.089	48.097	+0.01	N-9	48.039	[illegible]	-0.01
J-11	48.114	48.120	+0.01	N-9	48.094	48.083	-0.01
J-12	48.074	48.070	-0.00	N-10	48.044	48.015	-0.00
K-8	48.054	48.047	-0.01	N-11	48.089	48.[illegible]	+0.00
K-9	48.104	48.114	+0.01	N-12	48.054	48.029	-0.02
K-10	48.069	48.078	+0.01	P-8	48.079	48.078	-0.00
K-11	48.099	48.099	0.00	P-9	48.119	48.[illegible]	[illegible]
K-12	48.079	48.075	-0.00	P-10	48.054	48.050	-0.00
L-8	48.044	48.026	-0.02	P-11	48.114	48.112	-0.00
L-9	48.074	48.071	-0.00	P-12	48.[illegible]	48.029	-0.03
L-10	48.034	48.034	0.00				

Table B.3—(Continued)

Survey point	Pre-Ivy elev., ft	Post-Ivy elev., ft	Net vert. displ., ft	Survey point	Pre-Ivy elev., ft	Post-Ivy elev., ft	Net vert. displ., ft
			Roof of Building 3				
H-13	48.104	48.133	+0.02	L-16	48.104	48.143	+0.04
H-14	48.114	48.135	+0.02	L-17	48.064	48.098	+0.03
H-15	48.094	48.117	+0.02	M-13	48.114	48.[illegible]	+0.02
H-16	48.094	48.[illegible]13	+0.02	M-14	48.114	48.[illegible]	+0.04
H-17	48.068	48.080	+0.01	M-15	48.114	48.[illegible]34	+0.[illegible]
J-13	48.104	48.130	+0.03	M-16	48.104	48.138	+0.03
J-14	48.099	48.133	+0.03	M-17	48.064	48.096	+0.03
J-15	48.104	48.137	+0.03	N-13	48.094	48.120	+0.03
J-16	48.054	48.087	+0.03	N-14	48.094	48.121	+0.01
J-17	48.054	48.080	+0.03	N-15	48.119	48.148	+0.01
K-13	48.104	48.140	+0.04	N-16	48.084	48.115	+0.03
K-14	48.084	48.134	+0.05	N-17	48.074	48.099	+0.02
K-15	48.084	48.124	+0.04	P-13	48.078	48.[illegible]	+0.01
K-16	48.074	48.109	+0.04	P-14	48.104	48.119	+0.02
K-17	48.054	48.083	+0.03	P-15	48.079	48.091	+0.01
L-13	48.129	48.117	-0.01	P-16	48.084	48.100	+0.02
L-14	48.134	48.174	+0.05	P-17	48.041	48.068	+0.01
L-15	48.134	48.180	+0.08				
			Roof of Building 4				
H-18	48.084	48.083	-0.00	L-22	48.024	48.026	+0.[illegible]
H-19	48.029	48.030	+0.00	L-23	48.[illegible]	47.[illegible]	-0.03
H-20	48.019	48.019	0.00	L-24	48.074	48.[illegible]71	-0.[illegible]
H-21	48.039	48.039	0.00	M-18	48.074	48.[illegible]75	+0.[illegible]
H-22	48.049	48.048	0.00	M-19	47.954	47.[illegible]57	-0.[illegible]
H-23	48.079	48.080	0.00	M-20	48.034	48.031	-0.[illegible]
H-24	48.094	48.101	+0.01	M-21	47.999	47.[illegible]93	-0.[illegible]
J-18	48.084	48.047	-0.01	M-22	48.014	48.008	-0.01
J-19	47.974	47.962	-0.01	M-23	47.[illegible]	47.[illegible]	-0.[illegible]
J-20	47.994	47.990	-0.00	M-24	48.074	48.[illegible]77	+0.[illegible]
J-21	48.034	48.[illegible]18	-0.00	N-18	48.084	[illegible]61	-0.[illegible]
J-22	48.041	48.042	-0.00	N-19	48.[illegible]	47.[illegible]	-0.[illegible]
J-23	48.054	48.052	-0.00	N-20	48.[illegible]	48.[illegible]	0.00
J-24	48.084	48.[illegible]	+0.00	N-21	47.994	47.[illegible]	0.[illegible]
K-18	48.039	48.039	0.00	N-22	48.014	48.010	-0.[illegible]
K-19	47.[illegible]	47.885	-0.06	N-23	47.999	47.983	-0.[illegible]
K-20	47.958	47.957	+0.00	N-24	48.054	48.050	-0.00
K-21	48.009	48.008	-0.00	P-18	48.074	48.079	0.00
K-22	48.044	48.043	-0.00	P-19	48.034	48.035	+0.[illegible]
K-23	48.019	48.007	-0.01	P-20	48.044	48.[illegible]	0.00
K-24	48.064	48.065	+0.[illegible]	P-21	48.049	[illegible]48	-0.00
L-18	48.034	48.029	-0.00	P-22	48.044	48.04[illegible]	-0.[illegible]
L-19	47.904	47.788	-0.12	P-23	48.054	48.[illegible]54	0.[illegible]
L-20	47.969	47.970	+0.[illegible]	P-24	48.069	48.067	-0.[illegible]
L-21	48.099	47.999	-0.10				

Table B 5—(Continued.

Survey point	Pre-Ivy elev., ft	Post-Ivy elev., ft	Net vert. displ., ft	Survey point	Pre-Ivy elev., ft	Post-Ivy elev., ft	Net vert. displ., ft
			Roof of Building 5				
H-25	48.124	48.147	+0.02	L-28	48.074	48.110	+0.04
H-26	48.124	48.150	+0.03	L-29	48.069	48.097	+0.03
H-27	48.099	48.141	+0.04	M-25	48.074	48.093	+0.02
H-28	48.114	48.149	+0.04	M-26	48.084	48.114	+0.03
H-29	48.089	48.121	+0.03	M-27	48.039	48.071	+0.03
J-25	48.099	48.133	+0.03	M-28	48.074	48.101	+0.03
J-26	48.084	48.123	+0.04	M-29	48.084	48.107	+0.02
J-27	48.094	48.138	+0.04	N-25	48.069	48.086	+0.02
J-28	48.084	48.125	+0.04	N-26	48.044	48.066	+0.02
J-29	48.094	48.127	+0.03	N-27		48.065	
K-25	48.074	48.104	+0.03	N-28	48.074	48.103	+0.03
K-26	48.049	48.113	+0.06	N-29	48.074	48.095	+0.02
K-27	48.079	48.121	+0.04	P-25	48.069	47.878	−0.19
K-28	48.084	48.124	+0.04	P-26	48.079	48.099	+0.02
K-29	48.084	48.115	+0.03	P-27	48.084	48.112	+0.03
L-25	48.044	48.073	+0.03	P-28	48.114	48.137	+0.02
L-26	48.044	48.079	+0.04	P-29			
L-27							
			Roof of Building 6				
H-30	48.129	48.128	−0.00	L-33	48.114	48.115	+0.00
H-31	48.164	48.165	+0.00	L-34	48.084	48.077	−0.01
H-32	48.159	48.161	+0.00	M-30	48.079	48.074	−0.00
H-33	48.184	48.182	−0.00	M-31	48.114	48.109	−0.00
H-34	48.169	48.166	−0.00	M-32	48.134	48.136	+0.00
J-30	48.114	48.105	−0.01	M-33	48.134	48.137	+0.00
J-31	48.124	48.124	0.00	M-34	48.114	48.097	−0.02
J-32	48.124	48.130	+0.01	N-30	48.134	48.128	−0.01
J-33	48.124	48.127	+0.00	N-31	48.129	48.126	−0.00
J-34	48.124	48.117	−0.01	N-32	48.144	48.144	0.00
K-30	48.089	48.082	−0.01	N-33	48.144	48.131	−0.01
K-31	48.124	48.105	−0.02	N-34	48.139	48.119	−0.02
K-32	48.119	48.122	+0.00	P-30	48.134	48.119	−0.02
K-33	48.124	48.126	+0.00	P-31	48.154	48.143	−0.01
K-34	48.119	48.109	−0.01	P-32	48.121	48.116	−0.01
L-30	48.084	48.075	−0.01	P-33	48.154	48.134	−0.02
L-31	48.114	48.111	−0.00	P-34	48.144	48.113	−0.03
L-32	48.124	48.130	+0.01				
			Roof of Building 7				
H-35	48.064	48.065	+0.00	H-40	48.059	48.060	+0.00
H-36	48.044	48.047	+0.00	H-41	48.094	48.077	−0.02
H-37	48.054	48.059	+0.00	J-35	48.044	48.037	−0.01
H-38	48.064	48.050	−0.01	J-36	48.074	48.064	−0.01
H-39	48.049	48.038	−0.01	J-37	48.055	48.062	+0.00

Table B.3 — (Continued)

Survey point	Pre-Ivy elev., ft	Post-Ivy elev., ft	Net vert. displ., ft	Survey point	Pre-Ivy elev., ft	Post-Ivy elev., ft	Net vert. displ., ft
Roof of Building 7 (Continued)							
J-38	48.049	48.039	−0.01	M-37	48.064	48.071	+0.01
J-39	48.064	48.054	−0.01	M-38	48.064	48.065	+0.00
J-40	48.044	48.045	+0.00	M-39	48.079	48.075	−0.00
J-41	48.044	48.039	−0.00	M-40	48.074	48.077	+0.00
K-35	48.054	48.057	+0.00	M-41	48.039	48.043	+0.00
K-36	48.064	48.065	+0.00	N-35	48.054	48.056	+0.00
K-37	48.039	48.038	−0.00	N-36	48.064	48.067	+0.00
K-38	48.041	48.035	−0.01	N-37	48.054	48.067	+0.00
K-39	48.054	48.047	−0.01	N-38	48.044	48.051	+0.01
K-40	48.054	48.057	+0.01	N-39	48.049	48.056	+0.01
K-41	48.054	48.049	−0.00	N-40	48.064	48.069	+0.00
L-35	48.024	48.029	+0.00	N-41	48.034	48.044	+0.01
L-36	48.049	48.046	−0.00	P-35	48.089	48.100	+0.01
L-37				P-36	48.059	48.100	+0.01
L-38	48.054	48.035	−0.02	P-37	48.059	48.064	+0.00
L-39	48.079	48.066	−0.01	P-38	48.054	48.075	+0.02
L-40	48.074	48.077	+0.01	P-39	48.079	48.086	+0.01
L-41	48.054	48.045	−0.01	P-40	48.074	48.087	+0.01
M-35	48.074	48.080	+0.01	P-41	48.084	48.086	+0.00
M-36	48.074	48.075	+0.00				

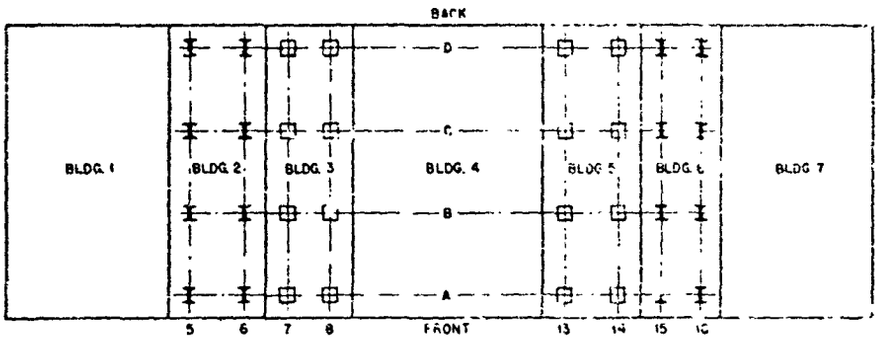

Fig. B.1 — Location of columns in Buildings 2, 3, 5, and 6.

APPENDIX C

EQUATIONS OF MOTION

C.1 GENERAL

Several general assumptions are made in the derivation of the equations of motion for Buildings 2 and 3. It is assumed that the foundation remained stationary during the response of the structure. Furthermore it is assumed that all the columns of any story act as a unit having a stiffness k. The masses concentrated at any floor level include the mass of the floor, girder, and one-half the mass of the columns above and below the floor in question. For the second floor only one-third the mass of the first-story columns is included.

The system used to describe the motion of the structure has nine independent coordinates (Fig. C.). One coordinate describes the motion of each of the three-floor masses, and one coordinate is used for the motion of each of the six front- and rear-wall panels between floors. This nine-degree-of-freedom system is used until the motion of the wall panels becomes oscillatory. A three-degree-of-freedom system is then used to describe the response of the three-floor masses for the remainder of the motion.

C.2 BUILDING 2

The V-beam sheeting of Building 2 was assumed to have no effect on the loading transmitted to the girts. The girts were assumed to act as a unit. The mass, flexural rigidity, and resistance of the girts and V-beams were distributed uniformly over the width of the structure. Since the girts were connected at the floor levels with clip angles or bolts, their shape during response was taken as that of a pin-ended beam. The detailed derivation of the equations of motion for elastic action of the front and rear faces is given below.

C.2.1 Deflected Shape

The following set of equations defines the deflected shapes for the front and rear faces, assuming that the girts remain elastic (Fig. C.1).

For the front face:

$$y_{s_1} = \frac{16y_{so_1}}{5}\left(\frac{x}{h} - \frac{2x^3}{h^3} + \frac{x^4}{h^4}\right) + \frac{x}{h}y_1 \tag{C.1}$$

$$y_{s_2} = \frac{16y_{so_2}}{5}\left(\frac{x}{h} - \frac{2x^3}{h^3} + \frac{x^4}{h^4}\right) + \frac{x}{h}(y_2 - y_1) + y_1 \tag{C.2}$$

$$y_{s_3} = \frac{16y_{so_3}}{5}\left(\frac{x}{h} - \frac{2x^3}{h^3} + \frac{x^4}{h^4}\right) + \frac{x}{h}(y_3 - y_2) + y_2 \tag{C.3}$$

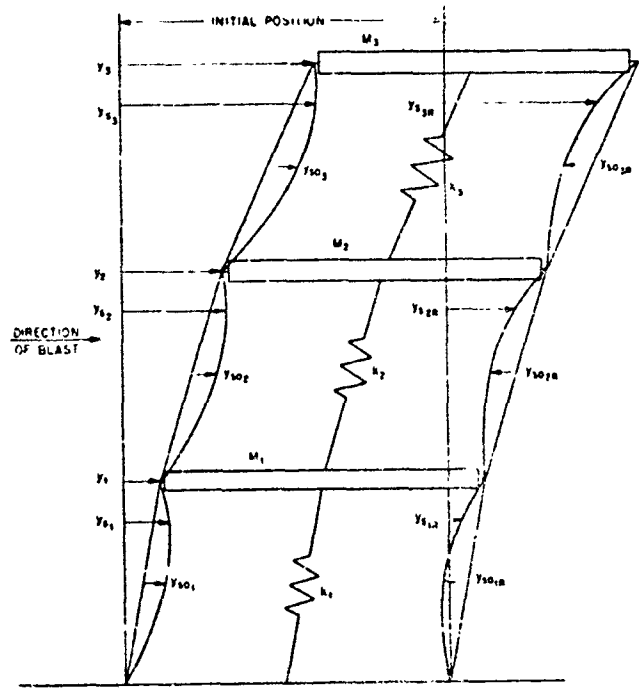

Fig. C.1—Nine-degree-of-freedom system for Buildings 2 and 3.

For the rear face:

$$y_{s_{1R}} = -\frac{16y_{so_{1R}}}{5}\left(\frac{x}{h} - \frac{2x^3}{h^3} + \frac{x^4}{h^4}\right) + \frac{x}{h}y_1 \tag{C.4}$$

$$y_{s_{2R}} = -\frac{16y_{so_{2R}}}{5}\left(\frac{x}{h} - \frac{2x^3}{h^3} + \frac{x^4}{h^4}\right) + \frac{x}{h}(y_2 - y_1) + y_1 \tag{C.5}$$

$$y_{s_{3R}} = -\frac{16y_{so_{3R}}}{5}\left(\frac{x}{h} - \frac{2x^3}{h^3} + \frac{x^4}{h^4}\right) + \frac{x}{h}(y_3 - y_2) + y_2 \tag{C.6}$$

C.2.2 Strain Energy of System

The equation by which the strain energy for the total system is evaluated is

$$PE = \frac{EI_1}{2}\int_0^{h_1}\left(\frac{\partial^2 y_{s_1}}{\partial x^2}\right)^2 dx + \frac{EI_2}{2}\int_0^{h_2}\left(\frac{\partial^2 y_{s_2}}{\partial x^2}\right)^2 dx + \frac{EI_2}{2}\int_0^{h_2}\left(\frac{\partial^2 y_{s_2}}{\partial x^2}\right) dx$$
$$+ \frac{EI_{1R}}{2}\int_0^{h_1}\left(\frac{\partial^2 y_{s_{1R}}}{\partial x^2}\right) dx + \frac{EI_{2R}}{2}\int_0^{h_2}\left(\frac{\partial^2 y_{s_{2R}}}{\partial x^2}\right) dx + \frac{EI_{3R}}{2}\int_0^{h_3}\left(\frac{\partial^2 y_{s_{3R}}}{\partial x^2}\right) dx$$
$$+ \frac{1}{2}k_1 y_1^2 + \frac{1}{2}k_2(y_2 - y_1)^2 + \frac{1}{2}k_3(y_3 - y_2)^2 \tag{C.7}$$

Substituting Eqs. C.1 to C.6 into Eq. C.7 and integrating yields

$$PE = \frac{3072EI_1}{125h_1^3} y_{so_1}^2 + \frac{3072EI_2}{125h_2^3} y_{so_2}^2 + \frac{3072EI_3}{125h_3^3} y_{so_3}^2 + \frac{3072EI_{1R}}{125h_1^3} y_{so_{1R}}^2$$
$$+ \frac{3072EI_{2R}}{125h_2^3} y_{so_{2R}}^2 + \frac{3072EI_{3R}}{125h_3^3} y_{so_{3R}}^2 + \frac{1}{2} k_1 y_1^2 + \frac{1}{2} k_2 (y_2 - y_1)^2 + \frac{1}{2} k_3 (y_3 - y_2)^2 \quad (C.8)$$

C.2.3 Kinetic Energy of System

The equation for the evaluation of the kinetic energy is as follows:

$$KE = \tfrac{1}{2} m_{s_1} \int_0^{h_1} \dot{y}_{s_1}^2 \, dx + \tfrac{1}{2} m_{s_2} \int_0^{h_2} \dot{y}_{s_2}^2 \, dx + \tfrac{1}{2} m_{s_3} \int_0^{h_3} \dot{y}_{s_3}^2 \, dx$$
$$+ \tfrac{1}{2} m_{s_{1R}} \int_0^{h_1} \dot{y}_{s_{1R}}^2 \, dx + \tfrac{1}{2} m_{s_{2R}} \int_0^{h_2} \dot{y}_{s_{2R}}^2 \, dx + \tfrac{1}{2} m_{s_{3R}} \int_0^{h_3} \dot{y}_{s_{3R}}^2 \, dx$$
$$+ \tfrac{1}{2} M_1 \dot{y}_1^2 + \tfrac{1}{2} M_2 \dot{y}_2^2 + \tfrac{1}{2} M_3 \dot{y}_3^2 \quad (C.9)$$

Substituting Eqs. C.1 to C.6 into Eq. C.9 and integrating yields

$$KE = \frac{1}{2} m_{s_1} h_1 \left(\frac{3968 \dot{y}_{so_1}^2}{7875} + \frac{16 \dot{y}_{so_1} \dot{y}_1}{25} + \frac{\dot{y}_1^2}{3} \right) + \frac{1}{2} m_{s_{1R}} h_1 \left(\frac{3968 \dot{y}_{so_{1R}}^2}{7875} - \frac{16 \dot{y}_{so_{1R}} \dot{y}_1}{25} + \frac{\dot{y}_1^2}{3} \right)$$
$$+ \frac{1}{2} m_{s_2} h_2 \left(\frac{3968 \dot{y}_{so_2}^2}{7875} + \frac{16 \dot{y}_{so_2} \dot{y}_1}{25} + \frac{16 \dot{y}_{so_2} \dot{y}_2}{25} + \frac{\dot{y}_2^2}{3} - \frac{\dot{y}_2 \dot{y}_1}{6} + \frac{5 \dot{y}_1^2}{6} \right)$$
$$+ \frac{1}{2} m_{s_{2R}} h_2 \left(\frac{3968 \dot{y}_{so_{2R}}^2}{7875} - \frac{16 \dot{y}_{so_{2R}} \dot{y}_1}{25} - \frac{16 \dot{y}_{so_{2R}} \dot{y}_2}{25} + \frac{\dot{y}_2^2}{3} - \frac{\dot{y}_2 \dot{y}_1}{6} + \frac{5 \dot{y}_1^2}{6} \right)$$
$$+ \frac{1}{2} m_{s_3} h_3 \left(\frac{3968 \dot{y}_{so_3}^2}{7875} + \frac{16 \dot{y}_{so_3} \dot{y}_2}{25} + \frac{16 \dot{y}_{so_3} \dot{y}_3}{25} + \frac{\dot{y}_3^2}{3} - \frac{\dot{y}_3 \dot{y}_2}{6} + \frac{5 \dot{y}_2^2}{6} \right)$$
$$+ \frac{1}{2} m_{s_{3R}} h_3 \left(\frac{3968 \dot{y}_{so_{3R}}^2}{7875} - \frac{16 \dot{y}_{so_{3R}} \dot{y}_2}{25} - \frac{16 \dot{y}_{so_{3R}} \dot{y}_3}{25} + \frac{\dot{y}_3^2}{3} - \frac{\dot{y}_3 \dot{y}_2}{6} + \frac{5 \dot{y}_2^2}{6} \right)$$
$$+ \frac{1}{2} M_1 \dot{y}_1^2 + \frac{1}{2} M_2 \dot{y}_2^2 + \frac{1}{2} M_3 \dot{y}_3^2 \quad (C.10)$$

C.2.4 Potential Energy of External Load

The equation for the potential energy of the external load, U_e, is

$$U_e = - w_F(t) \left(\int_0^{h_1} y_{s_1} \, dx + \int_0^{h_2} y_{s_2} \, dx + \int_0^{h_3} y_{s_3} \, dx \right)$$
$$+ w_R(t) \left(\int_0^{h_1} y_{s_{1R}} \, dx + \int_0^{h_2} y_{s_{2R}} \, dx + \int_0^{h_3} y_{s_{3R}} \, dx \right) \quad (C.11)$$

Substituting Eqs. C.1 to C.6 into Eq. C.11 and integrating yields

$$U_e = - w_F(t) \, h_1 \left(\frac{16 y_{so_1}}{25} + \frac{y_1}{2} \right) - w_R(t) \, h_1 \left(\frac{16 y_{so_{1R}}}{25} - \frac{y_1}{2} \right)$$
$$- w_F(t) \, h_2 \left(\frac{16 y_{so_2}}{25} + \frac{y_2}{2} + \frac{y_1}{2} \right) - w_R(t) \, h_2 \left(\frac{16 y_{so_{2R}}}{25} - \frac{y_2}{2} - \frac{y_1}{2} \right)$$
$$- w_F(t) \, h_3 \left(\frac{16 y_{so_3}}{25} + \frac{y_3}{2} + \frac{y_2}{2} \right) - w_R(t) \, h_3 \left(\frac{16 y_{so_{3R}}}{25} - \frac{y_3}{2} - \frac{y_2}{2} \right) \quad (C.12)$$

C.2.5 Equations of Motion

The Lagrangian form of the differential equation of motion which defines the relation between the pertinent energy quantities is

$$\frac{d}{dt}\left[\frac{\partial(KE)}{\partial \dot{y}_m}\right] - \frac{\partial(KE)}{\partial y_m} + \frac{\partial(PE)}{\partial y_m} = \frac{\partial J_e}{\partial \dot{y}_m}$$

Performing the designated differentiations with respect to each coordinate yields the following set of equations.

For the front face:

$$\frac{248m_{s_1}h_1}{315}\ddot{y}_{so_1} = w_F(t)\,h_1 - \frac{384EI_{s_1}}{5h_1^3}y_{so_1} - \frac{m_{s_1}h_1}{2}\ddot{y}_1 \tag{C.13}$$

$$\frac{248m_{s_2}h_2}{315}\ddot{y}_{so_2} = w_F(t)\,h_2 - \frac{384EI_{s_2}}{5h_2^3}y_{so_2} - \frac{m_{s_2}h_2}{2}\ddot{y}_1 - \frac{m_{s_2}h_2}{2}\ddot{y}_2 \tag{C.14}$$

$$\frac{248m_{s_3}h_3}{315}\ddot{y}_{so_3} = w_F(t)\,h_3 - \frac{384EI_{s_3}}{5h_3^3}y_{so_3} - \frac{m_{s_3}h_3}{2}\ddot{y}_2 - \frac{m_{s_3}h_3}{2}\ddot{y}_3 \tag{C.15}$$

For the rear face:

$$\frac{248m_{s_{1R}}h_1}{315}\ddot{y}_{so_{1R}} = w_R(t)\,h_1 - \frac{384EI_{s_{1R}}}{5h_1^3}y_{so_{1R}} + \frac{m_{s_{1R}}h_1}{2}\ddot{y}_1 \tag{C.16}$$

$$\frac{248m_{s_{2R}}h_2}{315}\ddot{y}_{so_{2R}} = w_R(t)\,h_2 - \frac{384EI_{s_{2R}}}{5h_2^3}y_{so_{2R}} + \frac{m_{s_{2R}}h_2}{2}\ddot{y}_1 + \frac{m_{s_{2R}}h_2}{2}\ddot{y}_2 \tag{C.17}$$

$$\frac{248m_{s_{3R}}h_3}{315}\ddot{y}_{so_{3R}} = w_R(t)\,h_3 - \frac{384EI_{s_{3R}}}{5h_3^3}y_{so_{3R}} + \frac{m_{s_{3R}}h_3}{2}\ddot{y}_2 + \frac{m_{s_{3R}}h_3}{2}\ddot{y}_3 \tag{C.18}$$

For floor levels, first floor:

$$\ddot{y}_1\left(\frac{m_{s_1}h_1}{3} + \frac{m_{s_{1R}}h_1}{3} + \frac{5m_{s_1}h_2}{6} + \frac{5m_{s_{1R}}h_2}{6} + M_1\right) = \frac{1}{2}\left[w_F(t)\,h_1 - w_R(t)\,h_1\right]$$
$$+ \frac{1}{2}\left[w_F(t)\,h_2 - w_R(t)\,h_2\right] + k_2(y_2 - y_1) - k_1y_1 + \ddot{y}_2\left(\frac{m_{s_2}h_2}{12} + \frac{m_{s_{2R}}h_2}{12}\right)$$
$$- \left(\frac{8m_{s_1}h_1}{25}\ddot{y}_{so_1} - \frac{8m_{s_{1R}}h_1}{25}\ddot{y}_{so_{1R}}\right) - \left(\frac{8m_{s_2}h_2}{25}\ddot{y}_{so_2} - \frac{8m_{s_{2R}}h_2}{25}\ddot{y}_{so_{2R}}\right) \tag{C.19}$$

Second floor:

$$\ddot{y}_2\left(\frac{m_{s_2}h_2}{3} + \frac{m_{s_{2R}}h_2}{3} + \frac{5m_{s_2}h_3}{6} + \frac{5m_{s_{2R}}h_2}{6} + M_2\right) = \frac{1}{2}\left[w_F(t)\,h_3 - w_R(t)\,h_3\right]$$
$$+ \frac{1}{2}\left[w_F(t)\,h_3 - w_R(t)\,h_3\right] + k_3(y_3 - y_2) - k_2(y_2 - y_1)$$
$$+ \ddot{y}_1\left(\frac{m_{s_2}h_2}{12} + \frac{m_{s_{2R}}h_2}{12}\right) + \ddot{y}_3\left(\frac{m_{s_3}h_3}{12} + \frac{m_{s_{3R}}h_3}{12}\right) - \left(\frac{8m_{s_2}h_2}{25}\ddot{y}_{so_2} - \frac{8m_{s_{2R}}h_2}{25}\ddot{y}_{so_{2R}}\right)$$
$$- \left(\frac{8m_{s_3}h_3}{25}\ddot{y}_{so_3} - \frac{8m_{s_{3R}}h_3}{25}\ddot{y}_{so_{3R}}\right) \tag{C.20}$$

Third floor:

$$\ddot{y}_3\left(\frac{m_{s_3}h_3}{3}+\frac{m_{s_{3R}}h_3}{3}+Mh_3\right)=\frac{1}{2}\left[w_F(t)\,h_3-w_R(t)\,h_3\right]-k_3(y_3-y_2)$$
$$+\ddot{y}_3\left(\frac{m_{s_3}h_3}{12}+\frac{m_{s_{3R}}h_3}{12}\right)-\left(\frac{8m_{s_3}h_3}{25}\ddot{y}_{so_3}-\frac{8m_{s_{3R}}h_3}{25}\ddot{y}_{so_{3R}}\right) \quad (C.21)$$

Eliminating the dynamic coupling between the front- and rear-face deflections and the floor deflections and simplifying, the equations of motion for the floor levels are as follows.

First story:

$$\ddot{y}_1\left(\frac{121m_{s_1}h_1}{930}+\frac{121m_{s_{1R}}h_1}{930}+\frac{293m_{s_1}h_2}{465}+\frac{293m_{s_{1R}}h_2}{465}+M_1\right)$$
$$=\frac{29}{310}\left[w_F(t)\,h_1-w_R(t)\,h_1\right]+\frac{29}{310}\left[w_F(t)\,h_2-w_R(t)\,h_2\right]$$
$$+\frac{126}{310}\left(\frac{384EI_{s_1}}{5h_1^3}y_{so_1}-\frac{384EI_{s_{1R}}}{5h_1^3}y_{so_{1R}}\right)+\frac{126}{310}\left(\frac{384EI_{s_2}}{5h_2^3}y_{so_2}-\frac{384EI_{s_{2R}}}{5h_2^3}y_{so_{2R}}\right)$$
$$+k_2(y_2-y_1)-k_1y_1+\ddot{y}_2\left(\frac{533m_{s_1}h_2}{1860}+\frac{533m_{s_{1R}}h_2}{1860}\right) \quad (C.22)$$

Second story:

$$\ddot{y}_2\left(\frac{121m_{s_2}h_2}{930}+\frac{121m_{s_{2R}}h_2}{930}+\frac{293m_{s_2}h_3}{465}+\frac{293m_{s_{2R}}h_3}{465}+M_2\right)=\frac{29}{310}\left[w_F(t)\,h_2-w_R(t)\,h_2\right]$$
$$+\frac{29}{310}\left[w_F(t)\,h_3-w_R(t)\,h_3\right]+\frac{126}{310}\left(\frac{384EI_{s_2}}{5h_2^3}y_{so_2}-\frac{384EI_{s_{2R}}}{5h_2^3}y_{so_{2R}}\right)$$
$$+\frac{126}{310}\left(\frac{384EI_{s_3}}{5h_3^3}y_{so_3}-\frac{384EI_{s_{3R}}}{5h_3^3}y_{so_{3R}}\right)+k_3(y_3-y_2)-k_2(y_2-y_1)$$
$$+\ddot{y}_1\left(\frac{533m_{s_1}h_2}{1860}+\frac{533m_{s_{1R}}h_2}{1860}\right)+\ddot{y}_2\left(\frac{533m_{s_2}h_3}{1860}+\frac{533m_{s_{2R}}h_3}{1860}\right) \quad (C.23)$$

Third story:

$$\ddot{y}_3\left(\frac{121m_{s_3}h_3}{930}+\frac{121m_{s_{3R}}h_3}{930}+Mh_3\right)=\frac{29}{310}\left[w_F(t)\,h_3-w_R(t)\,h_3\right]$$
$$+\frac{126}{310}\left(\frac{384EI_{s_3}}{5h_3^3}y_{so_3}-\frac{384EI_{s_{3R}}}{5h_3^3}y_{so_{3R}}\right)-k_3(y_3-y_2)+\ddot{y}_2\left(\frac{533m_{s_2}h_3}{1860}+\frac{533m_{s_{2R}}h_3}{1860}\right) \quad (C.24)$$

In order to make the numerical analysis more convenient, the terms involving the first- and third-floor accelerations are eliminated from the equation of motion of the second floor.

$$\ddot{y}_2\left[\frac{121m_{s_2}h_2}{930}+\frac{121m_{s_{2R}}h_2}{930}+\frac{293m_{s_2}h_3}{465}+\frac{293m_{s_{2R}}h_3}{465}+M_2-f_1\left(\frac{533m_{s_1}h_2}{1860}+\frac{533m_{s_{1R}}h_2}{1860}\right)\right.$$
$$\left.-f_2\left(\frac{533m_{s_2}h_3}{1860}+\frac{533m_{s_{2R}}h_3}{1860}\right)\right]=\frac{29}{310}f_1\left[w_F(t)\,h_1-w_R(t)\,h_1\right]$$
$$+\frac{29}{310}(1+f_1)\left[w_F(t)\,h_2-w_R(t)\,h_2\right]+\frac{29}{310}(1+f_2)\left[w_F(t)\,h_3-w_R(t)\,h_3\right]$$

$$+\frac{126}{310}f_1\left(\frac{384EI_{s_1}}{5h_1^3}y_{so_1}-\frac{384EI_{s_{1R}}}{5h_1^3}y_{so_{1R}}\right)$$

$$+\frac{126}{310}(1+f_1)\left(\frac{384EI_{s_2}}{5h_2^3}y_{so_2}-\frac{384EI_{s_{2R}}}{5h_2^3}y_{so_{2R}}\right)$$

$$+\frac{126}{310}(1+f_2)\left(\frac{384EI_{s_3}}{5h_3^3}y_{so_3}-\frac{384EI_{so_{3R}}}{5h_3^3}y_{so_{3R}}\right)$$

$$+k_3(1-f_2)(y_3-y_2)-k_2(1-f_1)(y_2-y_1)-k_1f_1y_1 \qquad \text{(C.25)}$$

where

$$f_1=\frac{\frac{533m_{s_1}h_2}{1860}+\frac{533m_{s_{1R}}h_2}{1860}}{\frac{121m_{s_1}h_1}{930}+\frac{121m_{s_{1R}}h_1}{930}+\frac{293m_{s_2}h_2}{465}+\frac{293m_{s_{2R}}h_2}{465}+M_1} \qquad \text{(C.26)}$$

$$f_2=\frac{\frac{533m_{s_2}h_3}{1860}+\frac{533m_{s_{2R}}h_3}{1860}}{\frac{121m_{s_2}h_2}{930}+\frac{121m_{s_{2R}}h_2}{930}+M_2} \qquad \text{(C.27)}$$

Final equations for frame.

First story:

$$\ddot{y}_1\left(\frac{121m_1h_1}{930}+\frac{121m_{1R}h_1}{930}+\frac{293m_2h_2}{465}+\frac{293m_{2R}h_2}{465}+M_1\right)=\frac{29}{310}[w_F(t)\,h_1-w_R(t)\,h_1]$$
$$+\frac{29}{310}[w_F(t)\,h_2-w_R(t)\,h_2]+\frac{126}{310}(R_{s_1}-R_{s_{1R}})+\frac{126}{310}(R_{s_2}-R_{s_{2R}})$$
$$+k_2(y_2-y_1)-k_1y_1+\ddot{y}_2\left(\frac{533m_2h_2}{1860}+\frac{533m_{2R}h_2}{1860}\right) \qquad \text{(C.28)}$$

Second story:

$$\ddot{y}_2\left[\frac{121m_{2}h_2}{930}+\frac{121m_{2R}h_2}{930}+\frac{293m_2h_2}{465}+\frac{293m_{2R}h_2}{465}+M_2-f_1\left(\frac{533m_2h_2}{1860}+\frac{533m_{2R}h_2}{1860}\right)\right.$$
$$\left.-f_2\left(\frac{533m_2h_2}{1860}+\frac{533m_{3R}h_3}{1860}\right)\right]=\frac{29}{310}f_1[w_F(t)\,h_1-w_R(t)\,h_1]+\frac{29}{310}(1+f_1)$$
$$\times[w_F(t)\,h_2-w_R(t)\,h_2]+\frac{29}{310}(1+f_2)[w_F(t)\,h_3-w_R(t)\,h_3]+\frac{126}{310}f_1(R_{s_1}-R_{s_{1R}})$$
$$+\frac{126}{310}(1+f_1)(R_{s_2}-R_{s_{2R}})+\frac{126}{310}(1+f_2)(R_{s_3}-R_{s_{3R}})$$
$$+k_3(1-f_2)(y_3-y_2)-k_2(1-f_1)(y_2-y_1)-k_1f_1y_1 \qquad \text{(C.29)}$$

Third story:

$$\ddot{y}_3\left(\frac{121m_3h_3}{930}+\frac{121m_{3R}h_3}{930}+M_3\right)=\frac{29}{310}[w_F(t)\,h_3-w_R(t)\,h_3]+\frac{126}{310}(R_{s_3}-R_{s_{3R}})$$
$$-k_3(y_3-y_2)+\ddot{y}_3\left(\frac{533m_3h_3}{1860}+\frac{533m_{3R}h_3}{1860}\right) \qquad \text{(C.30)}$$

$$f_1 = \frac{\frac{533m_1h_1}{1860} + \frac{533m_{1R}h_1}{1860}}{\frac{121m_1h_1}{930} + \frac{121m_{1R}h_1}{930} + \frac{293m_2h_2}{465} + \frac{293m_{2R}h_2}{465} + M_1} \quad \text{(C.26)}$$

$$f_2 = \frac{\frac{533m_2h_2}{1860} + \frac{533m_{2R}h_2}{1860}}{\frac{121m_2h_2}{930} + \frac{121m_{2R}h_2}{930} + M_2} \quad \text{(C.27)}$$

Final equations for from and rear walls.

Front face, first story:

$$\frac{248m_1h_1}{315}\ddot{y}_{so_1} = w_F(t)\,h_1 - \frac{384EI_1}{5h_1^3}y_{so_1} - \frac{m_1h_1}{2}\ddot{y}_1 \quad \text{(C.13)}$$

Second story:

$$\frac{248m_2h_2}{315}\ddot{y}_{so_2} = w_F(t)\,h_2 - \frac{384EI_2}{5h_2^3}y_{so_2} - \frac{m_1h_1}{2}\ddot{y}_1 - \frac{m_2h_2}{2}\ddot{y}_2 \quad \text{(C.14)}$$

Third story:

$$\frac{248m_3h_3}{315}\ddot{y}_{so_3} = w_F(t,\,h_3 - \frac{384EI_3}{5h_3^3}y_{so_3} - \frac{m_2h_2}{2}\ddot{y}_2 - \frac{m_3h_3}{2}\ddot{y}_3 \quad \text{(C.15)}$$

Rear face, first story:

$$\frac{248m_{1R}h_1}{315}\ddot{y}_{so_{1R}} = w_R(t)\,h_1 - \frac{384EI_{1R}}{5h_1^3}y_{so_{1R}} + \frac{m_{1R}h_1}{2}\ddot{y}_1 \quad \text{(C.16)}$$

Second story:

$$\frac{248m_{2R}h_2}{315}\ddot{y}_{so_{2R}} = w_R(t,\,h_2 - \frac{384EI_{2R}}{5h_2^3}y_{so_{2R}} + \frac{m_{1R}h_1}{2}\ddot{y}_1 + \frac{m_{2R}h_2}{2}\ddot{y}_2 \quad \text{(C.17)}$$

Third story:

$$\frac{248m_{3R}h_3}{315}\ddot{y}_{so_{3R}} = w_R(t)\,h_3 - \frac{384EI_{3R}}{5h_3^3}y_{so_{3R}} + \frac{m_{1R}h_1}{2}\ddot{y}_1 + \frac{m_{2R}h_2}{2}\ddot{y}_2 + \frac{m_{3R}h_3}{2}\ddot{y}_3 \quad \text{(C.18)}$$

Final equations evaluated for the particular constants of Building 2, Structure 1.1, from Appendix D are:

$h_1 = h_2 = h_3 = 12$ ft

$m_{s_1}h_1 = m_{s_2}h_2 = m_{s_3}h_3 = 0.15892$ kip*-sec^2/ft

$m_{s_{1R}}h_1 = m_{s_{2R}}h_2 = m_{s_{3R}}h_3 = 0.05304$ kip-sec^2/ft

$M_1 = 2.6764$ kip-sec^2/ft $\quad M_2 = 2.5416$ kip-sec^2/ft $\quad M_3 = 1.7298$ kip-sec^2/ft

*Kip represents 1000 lb.

$k_1 = 13{,}820$ kips/ft $\quad k_2 = 5090$ kips/ft $\quad k_3 = 2940$ kips/ft

$w_F(t)\ h = 16.485P_{front}$ kips $\quad w_R(t)\ h = 16.485P_{back}$ kips

$\frac{384EI_{s_{1,2,3}}}{5h^3} = 40{,}300$ kips/ft $\quad \frac{384EI_{s_{1,2,3R}}}{5h^3} = 9310$ kips/ft

Front face:

$$0.12516\ddot{y}_{so_1} = 16.485P_{front} - 40{,}300y_{so_1} - 0.07946\ddot{y}_1 \tag{C.31}$$

$$0.12516\ddot{y}_{so_2} = 16.485P_{front} - 40{,}300y_{so_2} - 0.07946\ddot{y}_1 - 0.07946\ddot{y}_2 \tag{C.32}$$

$$0.12516\ddot{y}_{so_3} = 16.485P_{front} - 40{,}300y_{so_3} - 0.07946\ddot{y}_2 - 0.07946\ddot{y}_3 \tag{C.33}$$

Rear face:

$$0.04648\ddot{y}_{so_{1R}} = 16.485P_{back} - 9310y_{so_{1R}} + 0.02952\ddot{y}_1 \tag{C.34}$$

$$0.04648\ddot{y}_{so_{2R}} = 16.485P_{back} - 9310y_{so_{2R}} + 0.02952\ddot{y}_1 + 0.02952\ddot{y}_2 \tag{C.35}$$

$$0.04648\ddot{y}_{so_{3R}} = 16.485P_{back} - 9310y_{so_{3R}} + 0.02952\ddot{y}_2 + 0.02952\ddot{y}_3 \tag{C.36}$$

Floor levels including the effect of vertical load.

First story:

$$2.8421\ddot{y}_1 = 2.8972(P_F - P_B) + 0.406(40{,}300y_{so_1} - 9310y_{so_{1R}}) + 0.406(40{,}300y_{so_2} - 9310y_{so_{2R}}) + 5090(y_2 - y_1) - 13{,}820y_1 + 0.06246\ddot{y}_1 + \frac{\Sigma P_1}{h_1}\,y_1 \tag{C.37}$$

Second story:

$$2.7037\ddot{y}_2 = 2.2046(P_F - P_B) + 0.009(40{,}300y_{so_1} - 9310y_{so_{1R}}) + 0.415(40{,}300y_{so_2} - 9310y_{so_{2R}}) + 0.421(40{,}300y_{so_3} - 9310y_{so_{3R}}) + 0.964(2940)\,(y_3 - y_2) - 0.979(5090)\,(y_2 - y_1) - 0.021(13{,}820)y_1 + \frac{\Sigma P_2}{h_2}\,(y_2 - y_1) \tag{C.38}$$

Third story:

$$1.7582\ddot{y}_3 = 1.8423(P_F - P_B) + 0.406(40{,}300y_{so_3} - 9310y_{so_{3R}}) - 2940(y_3 - y_2) + 0.06246\ddot{y}_2 + \frac{\Sigma P_3}{h_3}\,(y_3 - y_2) \tag{C.39}$$

Equations of motion for three floor levels using the average applied load for wall reactions.

First story:

$$2.8421\ddot{y}_1 = 16.485(P_F - P_B) + 5090(y_2 - y_1) - 13{,}820y_1 + 0.06246\ddot{y}_1 + \frac{\Sigma P_1}{h_1}\,y_1 \tag{C.40}$$

Second story:

$$2.7037\ddot{y}_2 = 17.128(P_F - P_B) + 0.964(2940)\,(y_3 - y_2) - 0.979(5090)\,(y_2 - y_1) - 0.021(13{,}820)\,y_1 + \frac{\Sigma P_2}{h_2}\,(y_2 - y_1) \tag{C.41}$$

Third story:

$$1.7583\ddot{y}_3 - 8.243(P_F - P_B) - 2940(y_3 - y_2) + 0.06246\ddot{y}_3 + \frac{\Sigma P_3}{h_3}(y_3 - y_2) \qquad \text{(C.42)}$$

C.3 BUILDING 3

The reinforced-concrete walls of Building 3 were continuous over the entire height of the structure. The assumed deflected shape for the walls was that of a three-span continuous beam fixed at both the foundation and the roof slab. The detailed derivation of the equations of motion for elastic motion of the front and rear faces is given below.

C.3.1 Deflected Shape

The following set of equations defines the assumed deflected shapes for the front and rear walls of Building 3. These equations assume elastic behavior of the wall elements.

For front face:

$$y_{s_1} = \frac{y_1}{5}\left(-9\frac{x^3}{h^3} + 14\frac{x^2}{h^2}\right) + \frac{y_2}{5}\left(4\frac{x^3}{h^3} - 4\frac{x^2}{h^2}\right) + \frac{y_3}{5}\left(-\frac{x^3}{h^3} + \frac{x^2}{h^2}\right) + 16y_{so_1}\left(\frac{x^4}{h^4} - 2\frac{x^3}{h^3} + \frac{x^2}{h^2}\right) \qquad \text{(C.43)}$$

$$y_{s_2} = \frac{y_1}{5}\left(7\frac{x^3}{h^3} - 13\frac{x^2}{h^2} + \frac{x}{h} + 5\right) + \frac{y_2}{5}\left(-7\frac{x^3}{h^3} + 8\frac{x^2}{h^2} + 4\frac{x}{h}\right)$$
$$+ \frac{y_3}{5}\left(3\frac{x^3}{h^3} - 2\frac{x^2}{h^2} - \frac{x}{h}\right) + 16y_{so_2}\left(\frac{x^4}{h^4} - 3\frac{x^3}{h^3} + \frac{x^2}{h^2}\right) \qquad \text{(C.44)}$$

$$y_{s_3} = \frac{y_1}{5}\left(-4\frac{x^3}{h^3} + 8\frac{x^2}{h^2} - 4\frac{x}{h}\right) + \frac{y_2}{5}\left(9\frac{x^3}{h^3} - 13\frac{x^2}{h^2} - \frac{x}{h} + 5\right)$$
$$+ \frac{y_3}{5}\left(-8\frac{x^3}{h^3} + 7\frac{x^2}{h^2} + 4\frac{x}{h}\right) + 16y_{so_3}\left(\frac{x^4}{h^4} - 2\frac{x^3}{h^3} + \frac{x^2}{h^2}\right) \qquad \text{(C.45)}$$

For rear face:

$$y_{s_{1R}} = \frac{y_1}{5}\left(-9\frac{x^3}{h^3} + 14\frac{x^2}{h^2}\right) + \frac{y_2}{5}\left(4\frac{x^3}{h^3} - 4\frac{x^2}{h^2}\right) + \frac{y_3}{5}\left(-\frac{x^3}{h^3} + \frac{x^2}{h^2}\right) - 16y_{so_{1R}}\left(\frac{x^4}{h^4} - 2\frac{x^3}{h^3} + \frac{x^2}{h^2}\right) \qquad \text{(C.46)}$$

$$y_{s_{2R}} = \frac{y_1}{5}\left(7\frac{x^3}{h^3} - 13\frac{x^2}{h^2} + \frac{x}{h} + 5\right) + \frac{y_2}{5}\left(-7\frac{x^3}{h^3} + 8\frac{x^2}{h^2} + 4\frac{x}{h}\right)$$
$$+ \frac{y_3}{5}\left(3\frac{x^3}{h^3} - 2\frac{x^2}{h^2} - \frac{x}{h}\right) - 16y_{so_{2R}}\left(\frac{x^4}{h^4} - 3\frac{x^3}{h^3} + \frac{x^2}{h^2}\right) \qquad \text{(C.47)}$$

$$y_{s_{3R}} = \frac{y_1}{5}\left(-4\frac{x^3}{h^3} + 8\frac{x^2}{h^2} - 4\frac{x}{h}\right) + \frac{y_2}{5}\left(9\frac{x^3}{h^3} - 13\frac{x^2}{h^2} - \frac{x}{h} + 5\right)$$
$$+ \frac{y_3}{5}\left(-8\frac{x^3}{h^3} + 7\frac{x^2}{h^2} + 4\frac{x}{h}\right) - 16y_{so_{3R}}\left(\frac{x^4}{h^4} - 2\frac{x^3}{h^3} + \frac{x^2}{h^2}\right) \qquad \text{(C.48)}$$

C.3.2 Strain Energy of System

The equation by which the strain energy of the total system is evaluated is given below:

$$PE = \frac{EI_1}{2}\int_0^{h_1}\left(\frac{\partial^2 y_{s_1}}{\partial x^2}\right)^2 dx + \frac{EI_2}{2}\int_0^{h_2}\left(\frac{\partial^2 y_{s_2}}{\partial x^2}\right)^2 dx + \frac{EI_3}{2}\int_0^{h_3}\left(\frac{\partial^2 y_{s_3}}{\partial x^2}\right)^2 dx$$

$$+\frac{EI_{1R}}{2}\int_0^{h_1}\left(\frac{\partial^2 y_{s_{1R}}}{\partial x^2}\right)^2 dx+\frac{EI_{2R}}{2}\int_0^{h_2}\left(\frac{\partial^2 y_{s_{2R}}}{\partial x^2}\right)^2 dx+\frac{EI_{3R}}{2}\int_0^{h_3}\left(\frac{\partial^2 y_{s_{3R}}}{\partial x^2}\right)^2 dx$$

$$+\frac{1}{2}k_1y_1^2+\frac{1}{2}k_2(y_2-y_1)^2+\frac{1}{2}k_3(y_3-y_2)^2 \qquad (C.49)$$

where $I_1 = I_2 = I_3 = I_{1R} = I_{2R} = I_{3R} = I_s$.

Substituting Eqs. C.43 to C.48 into Eq. C.49 and integrating yields

$$PE=\frac{EI_s}{h^3}\left(\frac{512y_{s0_1}^2}{5}+\frac{512y_{s0_2}^2}{5}+\frac{512y_{s0_3}^2}{5}+\frac{512y_{s0_{1R}}^2}{5}+\frac{512y_{s0_{2R}}^2}{5}+\frac{512y_{s0_{3R}}^2}{5}\right.$$

$$\left.+\frac{96y_1^2}{5}+\frac{96y_2^2}{5}+\frac{96y_3^2}{5}-\frac{132y_1y_2}{5}+\frac{48y_1y_3}{5}-\frac{108y_2y_3}{5}\right)$$

$$+\frac{1}{2}k_1y_1^2+\frac{1}{2}k_2(y_2-y_1)^2+\frac{1}{2}k_3(y_3-y_2)^2 \qquad (C.50)$$

C.3.3 Kinetic Energy of System

The equation for the evaluation of the kinetic energy is as follows:

$$KE=\tfrac{1}{2}m_{s_1}\int_0^{h_1}\dot{y}_{s_1}^2\,dx+\tfrac{1}{2}m_{s_2}\int_0^{h_2}\dot{y}_{s_2}^2\,dx+\tfrac{1}{2}m_{s_3}\int_0^{h_3}\dot{y}_{s_3}^2\,dx$$

$$+\tfrac{1}{2}m_{s_{1R}}\int_0^{h_1}\dot{y}_{s_{1R}}^2dx+\tfrac{1}{2}m_{s_{2R}}\int_0^{h_2}\dot{y}_{s_{2R}}^2\,dx+\tfrac{1}{2}m_{s_{3R}}\int_0^{h_3}\dot{y}_{s_{3R}}^2dx$$

$$+\tfrac{1}{2}M_1\dot{y}_1^2+\tfrac{1}{2}M_2\dot{y}_2^2+\tfrac{1}{2}M_3\dot{y}_3^2 \qquad (C.51)$$

Substituting Eqs. C.43 to C.48 into Eq. C.51 and integrating yields (noting that $m_{s_1} = m_{s_2} = m_{s_3} = m_{s_{1R}} = m_{s_{2R}} = m_{s_{3R}} = m_s$):

$$KE=\frac{1}{2}m_sh\left[\frac{128\dot{y}_{s0_1}^2}{315}+\frac{128\dot{y}_{s0_2}^2}{315}+\frac{128\dot{y}_{s0_3}^2}{315}+\frac{128\dot{y}_{s0_{1R}}^2}{315}+\frac{128\dot{y}_{s0_{2R}}^2}{315}+\frac{128\dot{y}_{s0_{3R}}^2}{315}\right.$$

$$+\dot{y}_{s0_1}\left(\frac{268\dot{y}_1}{525}-\frac{32\dot{y}_2}{350}+\frac{4\dot{y}_3}{175}\right)-\dot{y}_{s0_{1R}}\left(\frac{268\dot{y}_1}{525}-\frac{32\dot{y}_2}{350}+\frac{4\dot{y}_3}{175}\right)$$

$$+\dot{y}_{s0_2}\left(\frac{68\dot{y}_1}{105}+\frac{68\dot{y}_2}{105}-\frac{4\dot{y}_3}{35}\right)-\dot{y}_{s0_{2R}}\left(\frac{68\dot{y}_1}{105}+\frac{68\dot{y}_2}{105}-\frac{4\dot{y}_3}{35}\right)$$

$$+\dot{y}_{s0_3}\left(-\frac{16\dot{y}_1}{175}+\frac{268\dot{y}_2}{525}+\frac{328\dot{y}_3}{525}\right)-\dot{y}_{s0_{3R}}\left(-\frac{16\dot{y}_1}{175}+\frac{268\dot{y}_2}{525}+\frac{328\dot{y}_3}{525}\right)$$

$$\left.+\frac{4240\dot{y}_1^2}{2625}+\frac{4240\dot{y}_2^2}{2625}+\frac{2290\dot{y}_3^2}{2625}+\frac{838\dot{y}_1\dot{y}_2}{1050}-\frac{136\dot{y}_1\dot{y}_3}{525}+\frac{592\dot{y}_2\dot{y}_3}{1050}\right]$$

$$+\frac{1}{2}M_1\dot{y}_1^2+\frac{1}{2}M_2\dot{y}_2^2+\frac{1}{2}M_3\dot{y}_3^2 \qquad (C.52)$$

C.3.4 Potential Energy of External Load

The equation for the potential energy of the external load, U_e, is

$$U_e=-w_F(t)\left(\int_0^{h_1}y_{s_1}\,dx+\int_0^{h_2}y_{s_2}\,dx+\int_0^{h_3}y_{s_3}\,dx\right.$$

$$\left.+w_R(t)\int_0^{h_1}y_{s_{1R}}\,dx+\int_0^{h_2}y_{s_{2R}}\,dx+\int_0^{h_3}y_{s_{3R}}\,dx\right) \qquad (C.53)$$

Substituting Eqs. C.43 to C.48 into Eq. C.53 and integrating (noting that $h_1 = h_2 = h_3 = h$) yields:

$$U_e = -w_F(t)\,h\left(\frac{8y_{so_1}}{15} + \frac{8y_{so_2}}{15} + \frac{8y_{so_3}}{15} + y_1 + y_2 + \frac{y_3}{2}\right)$$
$$+ w_R(t)\,h\left(\frac{8y_{so_{1R}}}{15} - \frac{8y_{so_{2R}}}{15} - \frac{8y_{so_{3R}}}{15} + y_1 + y_2 - \frac{y_3}{2}\right) \quad (C.54)$$

C.3.3 Equations of Motion

The Lagrangian form of the differential equation of motion which defines the relation between the pertinent energy quantities is

$$\frac{d}{dt}\left[\frac{\partial(KE)}{\partial \dot{y}_m}\right] - \frac{\partial(KE)}{\partial y_m} + \frac{\partial(PE)}{\partial y_m} = -\frac{\partial U_e}{\partial y_m}$$

Performing the designated differentiations with respect to each coordinate yields the following set of equations.

For front face:

$$\frac{16m_s h}{21}\ddot{y}_{so_1} = w_F(t)\,h - \frac{384EI_s}{h^3}y_{so_1} - \frac{67m_s h}{140}\ddot{y}_1 + \frac{6mh}{70}\ddot{y}_2 - \frac{3mh}{140}\ddot{y}_3 \quad (C.55)$$

$$\frac{16m_s h}{21}\ddot{y}_{so_2} = w_F(t)\,h - \frac{384EI_s}{h^3}y_{so_2} - \frac{17m_s h}{28}\ddot{y}_1 - \frac{17m_s h}{28}\ddot{y}_2 + \frac{3m_s h}{28}\ddot{y}_3 \quad (C.56)$$

$$\frac{16m_s h}{21}\ddot{y}_{so_3} = w_F(t)\,h - \frac{384EI_s}{h^3}y_{so_3} + \frac{3m_s h}{35}\ddot{y}_1 - \frac{67m_s h}{140}\ddot{y}_2 - \frac{41m_s h}{70}\ddot{y}_3 \quad (C.57)$$

For rear face:

$$\frac{16m_s h}{21}\ddot{y}_{so_{1R}} = w_R(t)\,h - \frac{384EI_s}{h^3}y_{so_{1R}} + \frac{67m_s h}{140}\ddot{y}_1 - \frac{3m_s h}{35}\ddot{y}_2 + \frac{3m_s h}{140}\ddot{y}_3 \quad (C.58)$$

$$\frac{16m_s h}{21}\ddot{y}_{so_{2R}} = w_R(t)\,h - \frac{384EI_s}{h^3}y_{so_{2R}} + \frac{17m_s h}{28}\ddot{y}_1 + \frac{17m_s h}{28}\ddot{y}_2 - \frac{3m_s h}{28}\ddot{y}_3 \quad (C.59)$$

$$\frac{16m_s h}{21}\ddot{y}_{so_{3R}} = w_R(t)\,h - \frac{384EI_s}{h^3}y_{so_{3R}} - \frac{3m_s h}{35}\ddot{y}_1 + \frac{67m_s h}{140}\ddot{y}_2 + \frac{41m_s h}{70}\ddot{y}_3 \quad (C.60)$$

For floor levels, second floor:

$$\left(\frac{4240m_s h}{2625} + M_1\right)\ddot{y}_1 + \frac{310m_s h}{1050}\ddot{y}_2 - \frac{68m_s h}{525}\ddot{y}_3 + \frac{134m_s h}{525}(\ddot{y}_{so_1} - \ddot{y}_{so_{1R}}) + \frac{34m_s h}{105}(\ddot{y}_{so_2} - \ddot{y}_{so_{2R}})$$
$$- \frac{8m_s h}{175}(\ddot{y}_{so_3} - \ddot{y}_{so_{3R}}) = w_F(t)\,h - w_R(t)\,h - \frac{EI_s}{h^3}\left(\frac{192y_1}{5} - \frac{132y_2}{5} + \frac{48y_3}{5}\right) + k_1(y_2 - y_1) - b_1\dot{y}_1 \quad (C.61)$$

Third floor:

$$\frac{310m_s h}{1050}\ddot{y}_1 + \left(\frac{4240m_s h}{2625} + M_2\right)\ddot{y}_2 + \frac{221m_s h}{1050}\ddot{y}_3 - \frac{8m_s h}{175}(\ddot{y}_{so_1} - \ddot{y}_{so_{1R}}) + \frac{34m_s h}{105}(\ddot{y}_{so_2} - \ddot{y}_{so_{2R}})$$

$$+\frac{134m_s h}{525}(\ddot{y}_{ao_3}-\ddot{y}_{ao_{32}})=w_F(t)\,h-w_R(t)\,h-\frac{EI_s}{h^3}\left(-\frac{132y_1}{5}+\frac{192y_2}{5}-\frac{108y_3}{5}\right)$$
$$+k_3(y_3-y_2)-k_2(y_2-y_1) \qquad (C.62)$$

Roof:

$$-\frac{68m_s h}{525}\ddot{y}_1+\frac{221m_s h}{1050}\ddot{y}_2+\left(\frac{22v0m_s h}{2625}+M_3\right)\ddot{y}_3+\frac{2m_s h}{175}(\ddot{y}_{ao_3}-\ddot{y}_{ao_{32}})-\frac{2\pi_s h}{35}(\ddot{y}_{ao_2}-\ddot{y}_{ao_{21}})$$
$$+\frac{164m_s h}{525}(\ddot{y}_{ao_3}-\ddot{y}_{ao_{32}})=\frac{1}{2}[w_F(t)\,h-w_R(t)\,h]-\frac{EI_s}{h^3}\left(\frac{46y_1}{5}-\frac{108y_2}{5}+\frac{72y_3}{5}\right)-k_3(y_3-y_2) \qquad (C.63)$$

Eliminating the dynamic coupling between the front- and rear-face coordinates and the floor coordinates and simplifying, the equations of motion for the floor levels are as follows.

Second floor:

$$\left(\frac{16,133m_s h}{21,000}+M_1\right)\ddot{y}_1-\frac{4091m_s h}{42,000}\ddot{y}_2+\frac{367m_s h}{21,000}\ddot{y}_3+\frac{3}{10}\left[w_F(t)\,h-w_R(t)\,h\right]$$
$$+\frac{67}{200}\left[\frac{384EI_s}{h^3}(y_{ao_3}-y_{ao_{32}})\right]+\frac{17}{40}\left[\frac{384EI_s}{h^3}(y_{ao_3}-y_{ao_{32}})\right]-\frac{3}{50}\left[\frac{384EI_s}{h^3}(y_{ao_2}-y_{ao_{21}})\right]$$
$$-\frac{108EI_s}{5h^3}y_1+\frac{84EI_s}{5h^3}(y_2-y_1)-\frac{48EI_s}{5h^3}(y_3-y_2)+k_3(y_3-y_2)-k_2y_1 \qquad (C.64)$$

Third floor:

$$\frac{4091m_s h}{42,000}\ddot{y}_1+\left(\frac{16,133m_s h}{21,000}+M_2\right)\ddot{y}_2-\frac{8591m_s h}{42,000}\ddot{y}_3+\frac{3}{10}\left[w_F(t)\,h-w_R(t)\,h\right]$$
$$-\frac{3}{50}\left[\frac{384EI_s}{h^3}(y_{ao_3}-y_{ao_{32}})\right]+\frac{17}{40}\left[\frac{384EI_s}{h^3}(y_{ao_3}-y_{ao_{32}})\right]-\frac{67}{200}\left[\frac{384EI_s}{h^3}(y_{ao_2}-y_{ao_{21}})\right]$$
$$+\frac{48EI_s}{5h^3}y_1-\frac{84EI_s}{5h^3}(y_2-y_1)+\frac{108EI_s}{5h^3}(y_3-y_2)+k_3(y_3-y_2)-k_2(y_2-y_1) \qquad (C.65)$$

Roof:

$$\frac{367m_s h}{21,000}\ddot{y}_1+\frac{8253m_s h}{42,000}\ddot{y}_2+\left(M_3+\frac{7883m_s h}{21,000}\right)\ddot{y}_3+\left[\frac{3}{20}w_F(t)\,h-w_R(t\,h\right]$$
$$-\frac{3}{200}\left[\frac{384EI_s}{h^3}(y_{ao_3}-y_{ao_{32}})\right]-\frac{3}{40}\left[\frac{384EI_s}{h^3}(y_{ao_3}-y_{ao_{32}})\right]+\frac{67}{400}\left[\frac{384EI_s}{h^3}(y_{ao_2}-y_{ao_{21}})\right]$$
$$-\frac{12EI_s}{5h^3}y_1+\frac{36EI_s}{5h^3}(y_2-y_1)-\frac{72EI_s}{5h^3}(y_3-y_2)-k_3(y_3-y_2) \qquad (C.66)$$

In order to make the numerical analysis more convenient, the terms involving the second- and third-floor accelerations are eliminated from the equation of motion of the roof. The term involving the acceleration of the second floor is eliminated from the equation of motion of the third floor. The resulting set of final equations is given below.

For second floor:

$$\left(\frac{16,133m_s h}{21,000}+M_1\right)\ddot{y}_1+\frac{3}{10}\left[w_F(t)\,h-w_R(t)\,h\right]+\frac{67}{200}\left[\frac{384EI_s}{h^3}(y_{ao_3}-y_{ao_{32}})\right]$$

$$+\frac{17}{40}\left[\frac{384EI_s}{h^3}(y_{so_2}-y_{so_{2R}})\right]-\frac{3}{50}\left[\frac{384EI_s}{h^3}(y_{so_3}-y_{so_{3R}})\right]-\frac{108EI_s}{5h^3}y_1+\frac{84EI_c}{5h^3}(y_2-y_1)$$

$$-\frac{48EI_s}{5h^3}(y_3-y_2)+k_2(y_2-y_1)-k_1y_1+\frac{4091m_sh}{42,000}\ddot{y}_2-\frac{367m_sh}{21,000}\ddot{y}_3+\frac{\Sigma P_1}{h_1}y_1 \qquad (C.67)$$

For third floor:

$$\left(\frac{16,133m_sh}{21,000}+\frac{4091m_sh}{42,000}f_1+M_2\right)\ddot{y}_2=\frac{3}{10}(1-f_1)\left[w_F(t)\,h-w_R(t)\,h\right]$$

$$-\left(\frac{3}{50}+\frac{67}{200}f_1\right)\left[\frac{384EI_s}{h^3}(y_{so_1}-y_{so_{1R}})\right]+\frac{17}{40}(1-f_1)\left[\frac{384EI_s}{h^3}(y_{so_2}-y_{so_{2R}})\right]$$

$$+\left(\frac{67}{200}+\frac{3}{50}f_1\right)\left[\frac{384EI_s}{h^3}(y_{so_3}-y_{so_{3R}})\right]+\left(\frac{48}{5}+\frac{108}{5}f_1\right)\frac{EI_s}{h^3}y_1-(1+f_1)\frac{84EI_c}{5h^3}(y_2-y_1)$$

$$+\left(\frac{108}{5}+\frac{48}{5}f_1\right)\frac{EI_s}{h^3}(y_3-y_2)+k_2(y_3-y_2)-(1+f_1)\,k_2(y_2-y_1)+f_1k_1y_1$$

$$+\left(\frac{8591m_sh}{42,000}+\frac{367m_sh}{21,000}f_1\right)y_2+\frac{\Sigma P_2}{h_2}(y_2-y_1) \qquad (C.68)$$

where

$$f_1=\frac{\frac{4091m_sh}{42,000}}{\frac{16,133m_sh}{21,000}+M_2} \qquad (C.69)$$

Roof:

$$\left[M_3+\frac{7883m_sh}{21,000}-\frac{367m_sh}{21,000}f_2+\left(\frac{8591m_sh}{42,000}+\frac{367m_sh}{21,000}f_1\right)f_2\right]\ddot{y}_3=\left[\frac{3}{20}-\frac{3}{10}f_2-\frac{3}{50}(1-f_1)f_2\right]$$

$$\times\left[w_F(t)\,h-w_R(t)\,h\right]+\left[\frac{3}{200}-\frac{67}{200}f_2+\left(\frac{3}{50}+\frac{67}{200}f_1\right)f_2\right]\left[\frac{384EI_s}{h^3}(y_{so_1}-y_{so_{1R}})\right]$$

$$-\left[\frac{3}{40}+\frac{17}{40}f_2+\frac{17}{40}(1-f_1)f_2\right]\left[\frac{384EI_s}{h^3}(y_{so_2}-y_{so_{2R}})\right]+\left[\frac{21}{100}+\frac{3}{50}f_2-\left(\frac{67}{200}-\frac{3}{50}f_1\right)f_2\right]$$

$$\times\left[\frac{384EI_s}{h^3}(y_{so_3}-y_{so_{3R}})\right]-\left[\frac{12}{5}-\frac{108}{5}f_2+\left(\frac{48}{5}+\frac{108}{5}f_1\right)f_2\right]\frac{EI_s}{h^3}y_1$$

$$\cdot\left[\frac{36}{5}-\frac{84}{5}f_2+\frac{84}{5}(1+f_1)f_2\right]\frac{EI_s}{h^3}(y_2-y_1)-\left[\frac{72}{5}-\frac{48}{5}f_2+\left(\frac{108}{5}-\frac{48}{5}f_1\right)f_2\right]\frac{EI_s}{h^3}(y_3-y_2)$$

$$+(f_2-f_1f_2)\,k_1y_1-\left[f_2-(1+f_1)\,f_2\right]k_2(y_2-y_1)-(1+f_2)\,k_3(y_3-y_2)+\frac{\Sigma P_3}{h_3}(y_3-y_2) \qquad (C.70)$$

where

$$f_1=\frac{\frac{4091m_sh}{42,000}}{\frac{16,133m_sh}{21,000}+M_1} \qquad (C.69)$$

$$f_2=\frac{\frac{367m_sh}{21,000}}{\frac{16,133m_sh}{21,000}+M_1} \qquad (C.71)$$

$$f_3 = \frac{\frac{6353m_8h}{42,000} + \frac{4091m_8h}{42,000} f_2}{\frac{16,133m_8h}{21,000} + M_3 + \frac{4091m_8h}{42,000} f_1} \qquad (C.72)$$

Final equations evaluated for the particular constants of Building 3 of Structure 3.1.1.

$m_8h = 0.53339$ kip-sec^2/ft

$M_1 = 3.55387$ kip-sec^2/ft $\quad M_2 = 3.28043$ kip-sec^2/ft $\quad M_3 = 2.59925$ kip-sec^2/ft

$k_1 = 11,370$ kips/ft $\quad k_2 = 3810$ kips/ft $\quad k_3 = 1760$ kips/ft

$w_F(t)\,h = 16.485P_F \quad w_B(t)\,h = 16.485P_B$

$\frac{EI_8}{h^3} = 198.4$ kips/ft

Front face:

$$0.40639\ddot{y}_{so_1} = 16.485P_F - 76,200y_{so_1} - 0.25527y_1 + 0.04572\ddot{y}_2 - 0.01143\ddot{y}_3 \qquad (C.73)$$

$$0.40639\ddot{y}_{so_2} = 16.485P_F - 76,200y_{so_2} - 0.32384\ddot{y}_1 - 0.32384\ddot{y}_2 + 0.05715\ddot{y}_3 \qquad (C.74)$$

$$0.40639\ddot{y}_{so_3} = 16.485P_F - 76,200y_{so_3} + 0.04572\ddot{y}_1 - 0.25527\ddot{y}_2 - 0.31241\ddot{y}_3 \qquad (C.75)$$

Rear face:

$$0.40639\ddot{y}_{so_{1R}} = 16.485P_B - 76,200y_{so_{1R}} + 0.25527\ddot{y}_1 - 0.04572\ddot{y}_2 + 0.01143\ddot{y}_3 \qquad (C.76)$$

$$0.40639\ddot{y}_{so_{2R}} = 16.485P_B - 76,200y_{so_{2R}} + 0.32384\ddot{y}_1 + 0.32384\ddot{y}_2 - 0.05715\ddot{y}_3 \qquad (C.77)$$

$$0.40639\ddot{y}_{so_{3R}} = 16.485P_B - 76,200y_{so_{3R}} - 0.04572\ddot{y}_1 + 0.25527\ddot{y}_2 + 0.31241\ddot{y}_3 \qquad (C.78)$$

For second floor:

$$3.9636\ddot{y}_1 = 0.3(16.485)(P_F - P_B) + 0.335\left[\frac{384EI_8}{h^3}(y_{so_1} - y_{so_{1R}})\right] + 0.455\left[\frac{384EI_8}{h^3}(y_{so_2} - y_{so_{2R}})\right]$$
$$- 0.060\left[\frac{384EI_8}{h^3}(y_{so_3} - y_{so_{3R}})\right] - 4280y_1 + 3330(y_2 - y_1) - 1900(y_3 - y_2)$$
$$+ 3810(y_2 - y_1) - 11,370v_1 + 0.05195\ddot{y}_2 - 0.00932\ddot{y}_3 + \frac{\Sigma P_1}{h_1}y_1 \qquad (C.79)$$

For third floor:

$$3.7909\ddot{y}_2 = 0.296(16.485)(P_F - P_B) - 0.064\left[\frac{384EI_8}{h^3}(y_{so_1} - y_{so_{1R}})\right]$$
$$+ 0.419\left[\frac{384EI_8}{h^3}(y_{so_2} - y_{so_{2R}})\right] + 0.336\left[\frac{384EI_8}{h^3}(y_{so_3} - y_{so_{3R}})\right] + 1900v_1$$
$$- 3380(y_2 - y_1) + 4310(y_3 - y_2) + 1760(y_3 - y_2) - 1.013(3810)(v_2 - y_2)$$
$$+ 0.013(11,370)y_1 + 0.10922\ddot{y}_3 + \frac{\Sigma P_2}{h_2}(y_2 - y_1) \qquad (C.80)$$

For roof:

$$2.8018\ddot{y}_3 = 0.143(16.485)\,(P_F - P_B) + 0.0156\left[\frac{384EI_s}{h^3}\,(y_{so_3} - y_{so_{3R}})\right]$$
$$- 0.085\left[\frac{384EI_s}{h^3}\,(y_{so_2} - y_{so_{2R}})\right] + 0.403\left[\frac{384EI_s}{h^3}\,(y_{so_3} - y_{so_{3R}})\right]$$
$$- 510y_1 + 1490(y_2 - y_1) - 2940(y_3 - y_2) + 0.00207(11,370)y_1$$
$$+ 0.01924(3810)(y_2 - y_1) - 1.02131(1760)(y_3 - y_2) + \frac{\Sigma P_3}{h_3}(y_3 - y_2) \qquad (C.81)$$

A simplified set of equations is presented below for the motion of the floors after the response of the wall slabs has become oscillatory.

Second floor:

$$\left(M_1 + \frac{16,133m_sh}{21,000}\right)\ddot{y}_1 = [w_F(t)\,h - w_R(t)\,h] - R_{w_1} + k_2(y_2 - y_1) - k_1y_1 + \frac{4091m_sh}{42,000}\ddot{y}_2$$
$$- \frac{367m_sh}{21,000}\ddot{y}_3 + \frac{\Sigma P_1}{h_1}y_1 \qquad (C.82)$$

Third floor:

$$\left(M_2 + \frac{16,133m_sh}{21,000} + \frac{4091m_sh}{42,000}f_1\right)\ddot{y}_2 = (1 - f_1)\,[w_F(t)\,h - w_R(t)\,h] - R_{w_2} + f_1R_{w_1} + k_2(y_2 - y_2)$$
$$- (1 + f_1)\,k_2(y_2 - y_1) + f_1k_1y_1 + \left(\frac{8591m_sh}{42,000} + \frac{367m_sh}{21,000}f_1\right)\ddot{y}_3 + \frac{\Sigma P_2}{h_2}(y_2 - y_1) \qquad (C.83)$$

Roof:

$$\left[M_3 + \frac{7883m_sh}{21,000} - \frac{367m_sh}{21,000}f_2 + \left(\frac{8591m_sh}{42,000} + \frac{367m_sh}{21,000}f_1\right)f_1\right]\ddot{y}_3 = \left[\frac{1}{2} - f_2 - f_3(1 - f_2)\right]$$
$$\times [w_F(t)\,h - w_R(t)\,h] - R_{w_3} + (f_2 + f_3)\,R_{w_2} - f_1(f_2 + f_3)R_{w_1} - (1 + f_2)\,k_3(y_3 - y_2)$$
$$- [f_2 - (1 + f_1)f_3]\,k_2(y_2 - y_1) + (f_2 - f_1f_3)\,k_1y_1 + \frac{\Sigma P_3}{h_3}(y_3 - y_2) \qquad (C.84)$$

where R_{w_1}, R_{w_2}, and R_{w_3} are the resisting shears of the front and rear walls developed at the second floor, third floor, and roof, respectively, due to the deflection of the various floors only.

APPENDIX D

STRUCTURAL PROPERTIES

D.1 BUILDING 2

Refer to the detailed plans of Building 2 in Figs. 2.39 to 2.41.

D.1.1 Columns

The strength properties of the rolled column sections are based on the relations of reference 3. Figure D.1 shows a typical P vs M curve for WF shape, where

$$P_p = f_{dy} A \tag{D.1}$$

$$P_1 = \frac{f_{dy}}{d}\left(2bt_f^2 + \frac{t_w d^2}{2} - 2t_w t_f^2\right) \tag{D.2}$$

$$M_1 = \frac{f_{dy}}{3d}\left[4t_w\left(\frac{d}{2} - t_f\right)^3 + bt_f\left(3d^2 - 6dt_f + 4t_f^2\right)\right] \tag{D.3}$$

$$M_p = \frac{M_y + M_p'}{2} \tag{D.4}$$

$$M_y = f_{dy} S \tag{D.5}$$

$$M_p' = f_{dy} Z \tag{D.6}$$

and where f_{dy} is the dynamic yield stress.

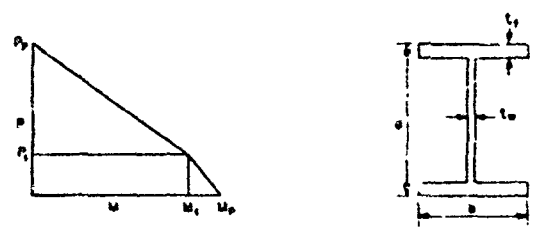

Fig. D.1—Typical P vs M curve for WF shape.

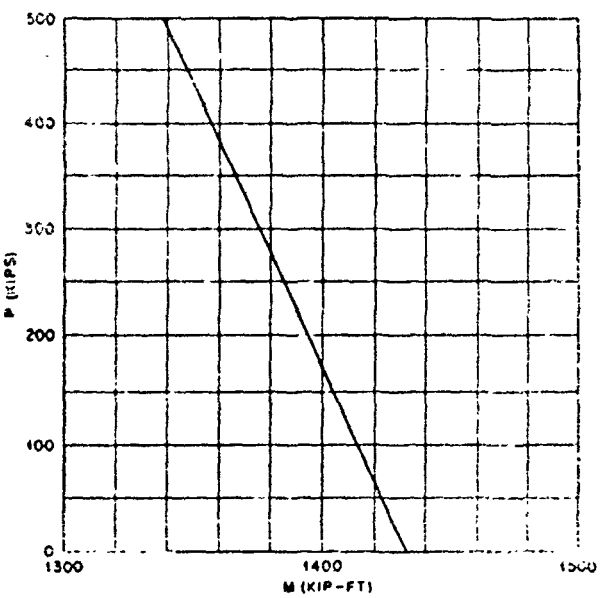

Fig. D.2—Column-capacity interaction curve for [illegible] first-story interior column

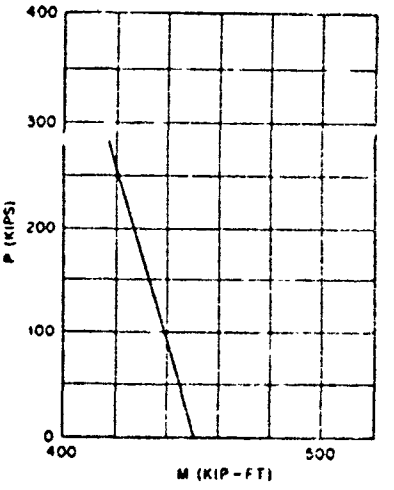

Fig. D.3—Column-capacity interaction curve for 10 WF 112 first- and second-story exterior columns.

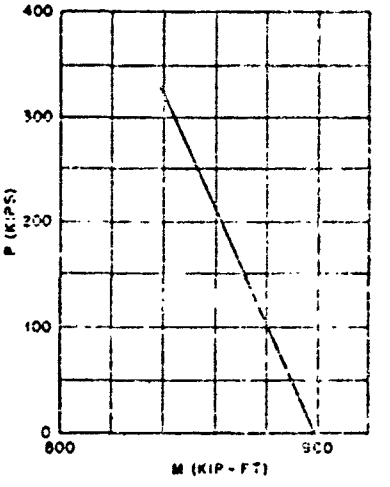

Fig. D.4—Column-capacity interaction curve for 14 WF 158 second-story interior column.

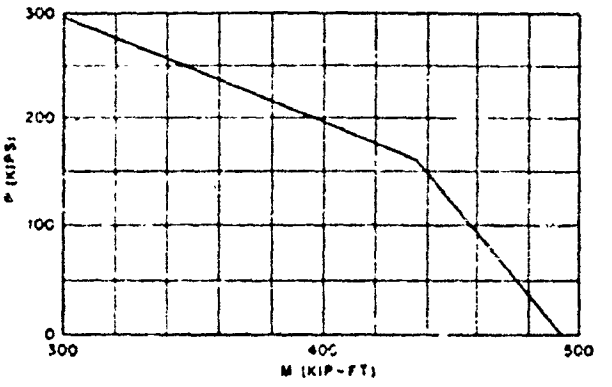

Fig. D.5—Column-capacity interaction curve for 14 WF 74 third-story interior column.

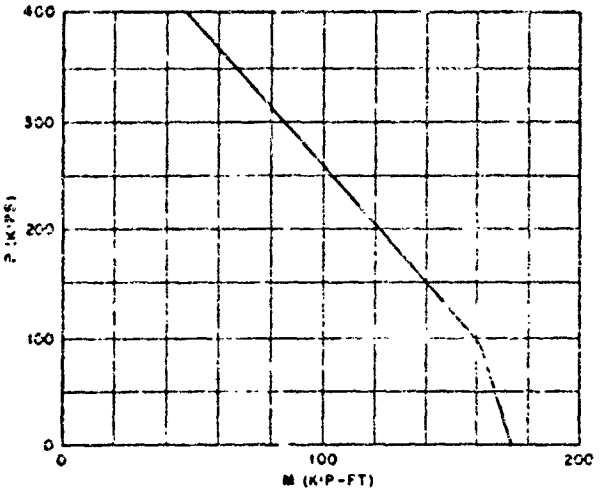

Fig. D.6—Column-capacity interaction curve for 10 WF 45 third-story exterior column.

Interaction curves of P vs M for the appropriate column sections are presented in Figs. D.2 to D.6. These curves are based on a static yield stress. The increase due to a rapid rate of strain is determined by the particular analysis and is applied to the static values listed in the table of axial load and moment for each load.

The basic properties of the column sections are taken from the AISC Manual.

D.1.2 Girders

Since the girders were designed for elastic action, their capacity is not checked in this report.

The actual variation in moment of inertia for the girders is a function of the type of loading. This condition is due to the fact that the reinforced-concrete floor or roof slab will influence the girder section considerably when the top flange is in compression but only slightly when the bottom flange is in compression. To avoid the complexity of evaluating the true variation in I, the moment of inertia was assumed uniform over the span, and the value taken was that at the center of the span assuming composite action. Figure D.7 gives the values of moment of inertia used for the various girders.

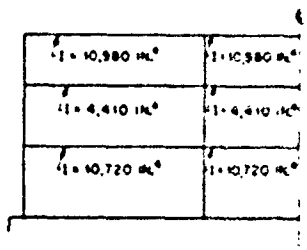

Fig. D.7 — Girder moment-of-inertia values for Building 2.

D.1.3 Stiffness

The calculation of stiffness factors for each story of Building 2 is based on the methods formulated in reference 6. The relation for the stiffness of any story including the effect of girder flexibility is given below.

$$k = \frac{\sum M_p \, 12E \sum I}{h^3 \left(\sum M_p\right) + 6Eh^2 \sum I\theta} \qquad (D.7)$$

where ΣM_p = the sum of the plastic hinge moments for both ends of every column in a story
ΣI = the sum of moments of inertia for all columns in a story
$\Sigma I\theta$ = the sum of all the $I\theta$ products for each end of all columns in a story
θ = joint rotation under full plastic moment from both the column above and below the joint

The stiffness values for the various stories were computed on the basis of an average set of M_p values. Although the values of M_p vary with time and loading conditions, a separate evaluation of stiffness for each analysis was considered unwarranted. The values of stiffness used in all analyses are as presented below. A more complete discussion of stiffness in multistory frames is presented in reference 6. Figure D.8 gives evaluated joint rotations for girders of Building 2.

First story: k_1 = 13,820 kips ft h_1 = 10.64 ft
Second story: k_2 = 5090 kips ft h_2 = 12.5 ft
Third story: k_3 = 2940 kips ft h_3 = 11.33 ft

Note that the height of column is based on the distance between center lines of girders.

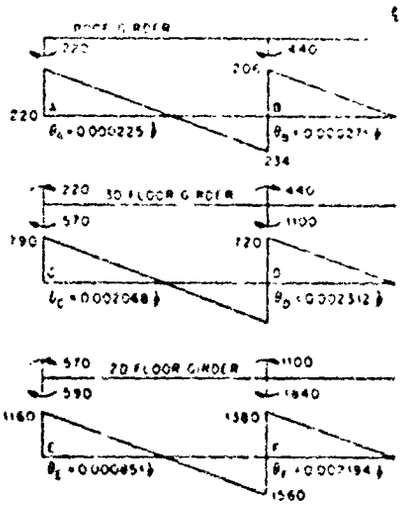

Fig D.8—Joint rotations evaluated for girders of Building 2.

D.1.4 V-beam Siding

The properties of V-beam siding are tabulated below. These values were obtained from the manufacturer's pamphlet.

W_T = 3.4 lbs./ft² S = 0.368 in.³/ft
I = 0.346 in.⁴/ft Z = 0.445 in.³/ft

Assuming fixed end conditions,

$$k = \frac{384EI}{L^3} = 5080 \text{ kips/ft for 1 ft 8 in. span}$$

$$m = 0.000176 \text{ kip-sec}^2/\text{ft}$$

$$K_{LM} = 0.762$$

$$T_n = 2\pi\sqrt{\frac{m}{kK_{LM}}} = 2\pi\sqrt{\frac{0.000176}{5080(0.762)}} = 0.0012$$

Owing to the short period of this sheathing, the effect of the V-beam response on the frame is small and was neglected.

D.1.5 Girts

The blast load is assumed to act directly on the girts, which are considered to act as a unit. The computations as prescribed deal with the quantities for a single frame.

Front face (one 14 WF 150, four 14 WF 61 per frame):

$$\sum I = 4353 \text{ in.}^4 \qquad \sum S = 609 \text{ in.}^3 \qquad \sum Z = 680 \text{ in.}^3$$

$$M_p = f_d \frac{\sum S + \sum Z}{2} = 53.7 f_d \text{ kip-ft}$$

$$R_m = \frac{8M_p}{L} = 35.8 f_d \text{ kips, where } L = 12 \text{ ft}$$

$$k = \frac{384E}{5L^3} \sum I = 40,300 \text{ kips/ft}$$

Rear face (one 12 WF 72, two 12 WF 27 per frame):

$$\sum I = 1006 \text{ in.}^4 \qquad \sum S = 165.7 \text{ in.}^3 \qquad \sum Z = 194 \text{ in.}^3$$

$$M_p = f_d \frac{\sum S + \sum Z}{2} = 14.6 f_d \text{ kip-ft}$$

$$R_m = \frac{8M_p}{L} = 9.7 f_d \text{ kips}$$

$$k = \frac{384E}{5L^3} \sum I = 9310 \text{ kips/ft}$$

D.1.6 Mass

The values of mass used for the particular elements are listed in **Table D.1.** These values are associated with a single frame.

Table D.1 --MASS OF PARTICULAR ELEMENTS*

	First story	Second story	Third story
Columns	0.23170	0.18[illegible]	0.09180
Girders	0.42556	0.[illegible]42	0.16472
Floor or roof	0.82337	0.82337	1.45806
V-beam, front or rear	0.01209	0.01209	0.01209
Girts, front	0.14683	0.14683	0.14683
Girts, rear	0.04695	0.04695	0.04695
Sand live load	1.45174	1.45174	0
Edge beams	0	0	0.06[illegible]1

*All values in kip-sec^2/ft.

D.1.7 Dead Loads

The average value of dead load for each column is listed in Table D.2. These values are based on the tributary area for each column as illustrated in Fig. D.9.

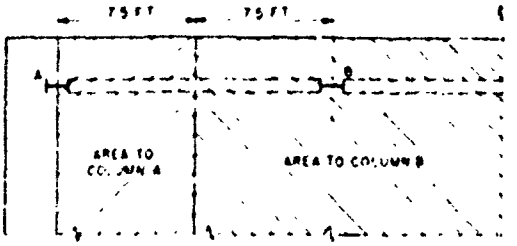

Fig. D.9 — Loaded areas for columns of Building 2

Table D.2 — COLUMN DEAD LOADS*

	External column	Internal column
Third story	8.2	17.3
Second story	20.9	43.9
First story	34.5	72.4

*All values in kips.

D.2 BUILDING 3

Refer to the detailed plans of Building 3 in Figs. 2.42 to 2.44.

D.2.1 Columns

The strength properties of the columns are based on the ultimate strength theory as presented in reference 3. The basic relations used are given by Fig. D.10 and Eqs. D.8 to D.11

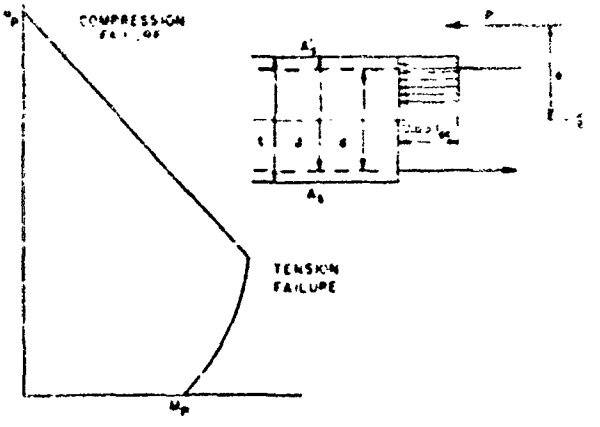

Fig. D.10 — Typical P vs M curve for reinforced-concrete column